

Reviewer #1

Section 3.1: In the discussion of cloud cover, as indicated by satellites, the authors should provide the exact details of the cloud data (parameter value, time of data, and spatial area of data obtained relative to the sample site) and discuss the satellite retrieval(s) used.

The presence of clouds was determined by examining satellite pictures provided by Sat24. We used the view over Europe at 11:00 LT. The text has been updated to indicate this and Lines 219-222 now read as “Cloud cover, as indicated from satellite measurements, showed that the days preceding Period A were generally cloud free whereas clouds developed west of the ground sites preceding Periods B, C, and D (not shown). The presence of clouds was determined by examining satellite pictures set to the view of Europe at 11:00 LT provided by Sat24 (<http://en.sat24.com/en/eu>).”

Section 3.1: In addition to the previous comment, were there reports of precipitation in Period B to the west or anywhere near the measurement site? In other words, was wet scavenging important in explaining any aspect of the data?

Wet scavenging was not likely important as very little precipitation was observed during the study period. There was little evidence of precipitation west of the site and measurable precipitation was recorded at SPC only on the afternoons of 23 June and 6 July. The text has been updated to reflect this and Lines 223-225 now read as “Also, wet scavenging was not likely important as there was very little precipitation at SPC or west of the site during the entire study period. Only two cases of light rain lasting ~30 min, which occurred on the afternoons of 23 June and 6 July, were recorded at SPC.”

Section 3.1, Lines 11-25 on pg 35493: the discussion about correlation coefficients is useful, but I am not sure what rationale went into these three categories (>0.7 , $0.4-0.7$, <0.3). How do these relate to statistical significance on a standard students t-test table for the respective degrees of freedom used to generate the best fit lines? More discussion is required about the choice of these three categories.

We feel R^2 values are more informative for looking at the data since a R^2 value tells the fraction of variance in the y variable explained by the x variable. The three bins of R^2 values, therefore, are intended to quantify broad ranges of explained variance. p-values can also be useful for examining the statistical significance of a relationship, but even relationships where little variance is explained can be significant and thus not terribly interesting to discuss. For example, performing a t-test on both WSOC vs. OOA-4 for Period A (now Figure 10g) and Period C (now Figure 10h) would suggest their relationships were significant (Period A WSOC - OOA-4 = 3.07 $>$ t-test = 0.89 and Period C WSOC - OOA-4 = 0.75 $>$ t-test = 0.35). However, the R^2 value for Period A is 0.04 and Period C is 0.64, respectively. Therefore, while the t-test shows both relationships are statistically significant, the R^2 values are telling us more about the importance of the relationship between WSOC and OOA-4. Lines 238-248 now read as “We first will compare all four periods to examine for evidence of aqSOA. Then we will provide a further examination of aqueous aerosol tracers and WSOC for the two periods with similar air flow

(Periods A and C). Our analysis will largely be based on least square regression correlation analysis to examine the relationship between various species and provide a general approach to examine for evidence of aqSOA. We have chosen to examine R^2 values as opposed to p-values since R^2 values can provide a useful tool for explaining the amount of observed variance in a dependent variable that is explained by variation in an independent variable. p-values merely indicate whether a relationship is statistically significant without information about the amount of variance explained. To help categorize the fraction of variance explained, we consider a high correlation as R^2 values greater than 0.7, a moderate correlation as R^2 values between 0.3 to 0.7, and a low correlation as R^2 values less than 0.3.”

Figure 2: for Period B there seems to be a gap in the ALW data. Why is that? Also, why aren't data used (in the context of Figures 3-5) for the next couple of days when large changes in ALW are observed?

The gap in the ALW data is due to missing PILS-IC data. The caption of Figure 2 (now Figure 3) has been updated to indicate this and it now reads as “**Figure 3.** Times series of hourly averaged measured (a) WSOC, (b) calculated ALW, (c) RH, and (d) Temperature at SPC. Any gaps in ALW are due to missing PILS-IC data. The dashed vertical lines indicate midnight local time (UTC+2). Periods A, B, C, and D are also indicated.”

As suggested by the reviewer, we have also expanded the analysis to cover the periods before and after the original Period B. The original Period B is now called Period C. The new Period B covers 30 June, 1-2 July and Period D covers 6-7 July. The new Period B has moderate ALW and Period D has the highest ALW observed during the study. This allows comparison of different scenarios to help strengthen our results. Figures 3-5 (now Figures 4-6 and Figures S8-S9) have been updated to include all four Periods. The discussion about these figures in Section 3.2 has been updated and Lines 251-281 now read as “WSOC is shown as a function of RH for the times of RH increasing (Fig. 4a and 4b) and decreasing (Fig. 4c and 4d) during Periods A, B, C, and D. For Periods B, C, and D, WSOC had no relationship with RH. Only during the times of increasing RH did Period A have a relationship of increasing WSOC with RH, consistent with local aqSOA formation. This can further be illustrated by examining the correlation of WSOC vs. organic aerosol (OA), aerosol liquid water (ALW), and RH for Periods A, B, C, and D during the times of RH increasing (Fig. 5 and S8). In general, WSOC had a strong relationship with OA, but only Period A additionally had a moderate correlation of the WSOC with both ALW (Period A $R^2 = 0.65$ vs. Period B $R^2 = 0.15$, Period C $R^2 = 0.29$, and Period D $R^2 = 0.01$) and RH (Period A $R^2 = 0.39$ vs. Period B $R^2 = 0.01$, Period C $R^2 = 0.12$, and Period D $R^2 = 0.07$). The good correlation between WSOC and ALW is in agreement with a previous smog chamber study that found that ALW is a key determinant of SOA yield [Zhou *et al.*, 2011]. This also supports a recent study that observed ambient aqSOA formation during the nighttime as evident by the increased partitioning of gas-phase WSOC to the particle-phase with increasing RH [El-Sayed *et al.*, 2015]. The study by El-Sayed *et al.* [2015] found the increase in the fraction of total WSOC in the particle phase (F_p) at the two highest RH levels (70-80%, >80%) to be statistically significant compared to the F_p values at RH < 60%. The main focus of their work was to investigate if the uptake of gas-phase WSOC to aerosol water occurs through reversible or

irreversible pathways. The data suggested the aqSOA was formed irreversibly. We investigate this with our data in section 3.3.2.

Figures 6 and S9 show the correlation of WSOC vs. nitrate, oxalate, and sulfate for the times of RH increasing. Nitrate and WSOC are strongly correlated only during the times of RH increasing for Period A. Early morning nitrate peaks were observed at SPC during the first part of the study, but were absent at the upwind Bologna site (Fig. 7). The occurrence of these peaks overlaps with Period A. (Note, the nitrate event observed on 6 and 7 July during Period D will be discussed in Sect. 3.4.) This additionally suggested that the nitrate formation or the ammonium-nitrate-ammonia-nitric acid equilibrium at SPC was locally controlled since the back trajectory analysis indicated both the SPC and Bologna sites were sampling similar upwind air masses to each other in each period (Fig. 2). Therefore, the correlation with locally formed particulate nitrate suggests local formation of WSOC. (Note, increased nitrate also results in higher ALW at the same RH.) This argues that aqSOA formation was predominately local during Period A.”

It should also be noted that we updated the overview section to explain the expanded analysis and Lines 206-218 now read as “Therefore, our analysis will focus on comparing these two different halves of the study. Given our interest in examining for evidence of aqSOA we picked four periods with varying levels of WSOC and ALW. We also picked cases with both sites sampling similar air masses on a given day. Period A represents the first half of the study and covers 19-21 June. Period A has elevated WSOC and moderate ALW. As indicated by the difference in the length of the back trajectories [*Draxler and Rolph, 2013; Rolph, 2013*] shown in Fig. 2, Period A occurred during the end of a stagnation. Period B (30 June, 1-2 July), Period C (3-5 July), and Period D (6-7 July) represent three different cases in the second half of the study. Period B has moderate ALW, Period C has low ALW, and Period D has the highest ALW observed during the study. As indicated by Fig. 2, all three of these periods represent typical background conditions influenced by regional transport, but with slightly different flow patterns. The flows of Periods A and C are most similar. Due to changes in the WSOC concentrations and a non-consistent flow pattern on a daily basis, no periods between 23-29 June were examined.”

Figure 2: Avoid having numbers overlap on the y-axis for the two panels.

The y-axis has been fixed. The updated figure is shown below.

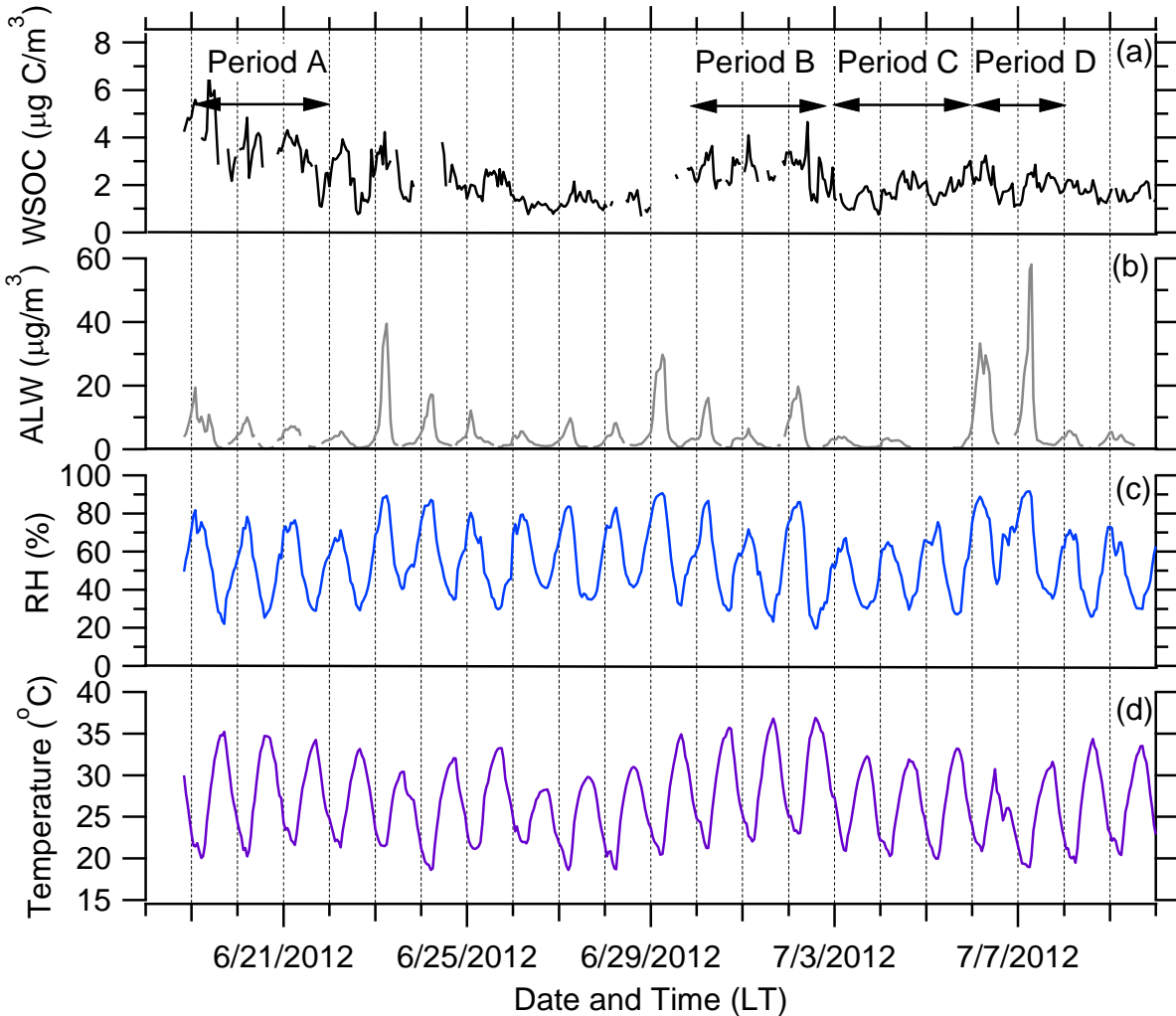
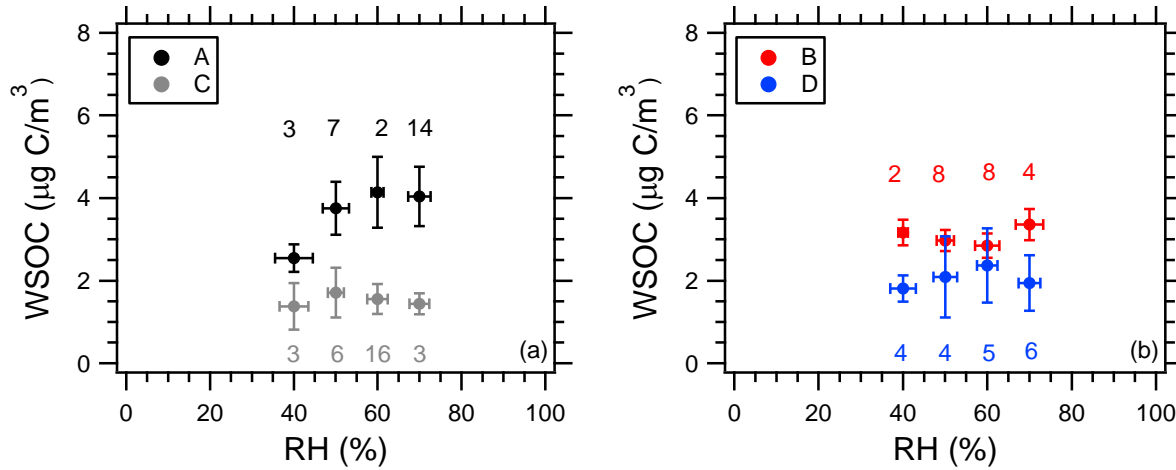


Figure 3: add error bars in the RH axis too for each marker. Also, it would be useful to report the number of points used for each marker in the two panels. For example, is the 80% RH point in panel A based on very few points compared to the other markers? And why isn't there a point at 80% RH for the bottom panel for Period A. The decrease in RH should start at 80% if the increase in RH ended near 80%. It seems as though if the RH increased to 80% that one can be picky as to which panel that marker is placed in and obviously it looks much better in the top panel to make the case for the reported conclusions. This is an issue that needs to be discussed in a revision.

Errors bars on the RH axis have been added to the figure as suggested. The number of points used in each RH bin has also been included in the figure. The updated Figure 3 (now Figure 4) is shown below. The 80% point in Period A was due to only one point, which is why it was included in only the RH increasing figure. However, this point does not drive the observations. Therefore, to show how robust the results are we have redone the analysis going from 40% to 70% RH and then from 70% to 40% RH. All relevant figures and text in the paper have been updated accordingly for this reanalysis.

RH Increasing



RH Decreasing

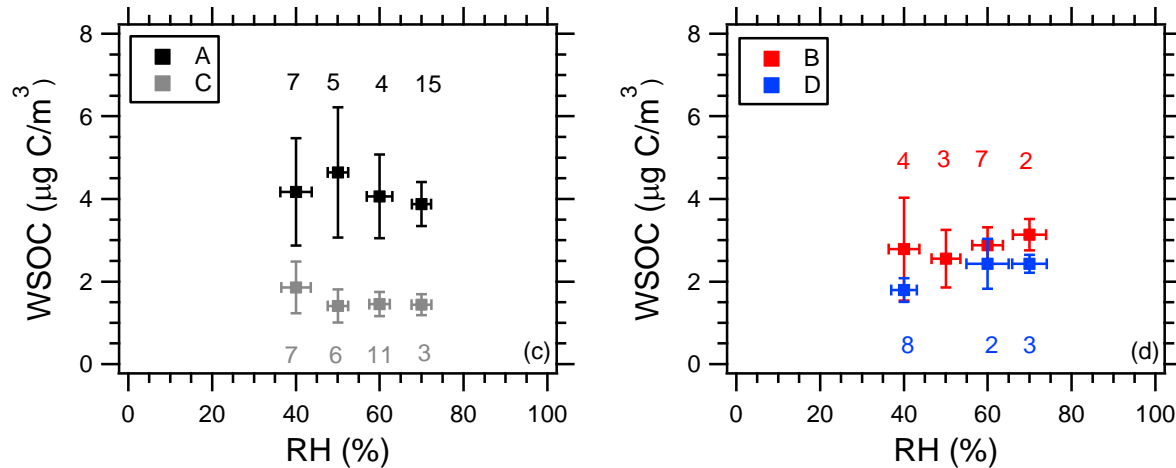


Figure 8C: what would the correlation be if the outlier point farthest to the left is omitted and are there any special characteristics associated with that datapoint? In the absence of that point it could be argued that a somewhat similar relationship exists as compared to panel D.

We believe this is in reference to Figure 5c (now Figure 6c) as Figure 8 is a time series. The outlier point does not dramatically change the correlation. If the outlier point is not included in the fit the R^2 value remains low, changing from 0.16 to 0.32. The point itself does not appear to have any special characteristics. It looks like the oxalate concentration could possibly be a bit lower than would be expected at its WSOC concentration, but we double checked even the chromatogram and it appears to be correct. Therefore, the point is still included.

Figure 8A-B: it seems that the same general positive trend exists in both panels. The issue in panel B could be that there is a bit more noise and it has (what appears to be) fewer data points.

We believe this is also in reference to Figures 5a and 5b (now Figures 6a and 6b). We agree that due to the differences in the axes the same general trend does appear in both plots. There is a bit less data in Figure 5b due to the missing anion data during the original Period B. Therefore, we have supplemented AMS nitrate and sulfate data into the new Figures 6b and 6f. However, this does not change the lack of relationship between WSOC and nitrate, the R^2 value changes from 0.18 to 0.01 when including the AMS data.

Figure 9: Panel B shows the presence of 2 outlier points to the middle-right that reduce its correlation. Having more datapoints would help in this case as it is unclear as to what explained those outlier points. The same applies to Panel B; note also that the right value on the x-axis of panel d is cut off.

The two outliers appear to be an artifact from the PMF analysis. However, they do not significantly change the correlation. If those two points are removed then the R^2 value for WSOC vs. OOA-1 (Figure 9b, now 10b) changes from 0.02 to 0.09 and the R^2 value for WSOC vs. OOA-2 (Figure 9d, now 10d) changes from 0.03 to 0.14. Also, the x-axis on Figure 9d (now 10d) has been fixed.

Table 2/3: These tables seem somewhat distracting in my view and I am not sure how important they are to the discussion in the paper. The authors should strongly consider incorporating discussion of those tables to a larger extent if they think they should be kept.

We have removed Table 2. However, since Table 3 includes the results from the two different fits used to perform the multilinear regression to determine the contribution of each AMS ME-2 factor to the WSOC, we have moved Table 3 to the supporting information (now Table S2).

-It would be useful to know exactly the times corresponding to when RH was increasing and decreasing for the plots shown in Figures 3/4/5. Some discussion about what other factors varying during those two periods of time would be helpful to show that the authors have considered all possibilities affecting their organic aerosol data and why their stated conclusions are the most obvious reason as to why different results exist.

We have added a table to the supporting information (Table S1) that now lists the exact dates and times used to create the times of RH increasing and decreasing in each Period. A copy is shown below. We also have expanded Table 1, which provides the concentrations of the various aerosol and gas-phase species measured in each period. The updated table is shown below. We also added some text in the overview section to point out that the only differences across all of Period A and the other periods are elevated OA, WSOC, and NO_x concentrations. Lines 225-228 now read as “Table 1 provides a comparison of the various concentrations and parameters observed during all four periods. With the exception of WSOC mentioned above, only the OA and NO_x (nitric oxides) concentrations across all of Period A are noticeably elevated compared to Periods B, C, and D.”

Table S1. Dates and times for the times of RH increasing and decreasing during Periods A, B, C, and D.

Period	RH Increasing	RH Decreasing
A	18 June at 20:00 – 19 June at 01:00, 19 June at 20:00 – 20 June at 06:00, 20 June at 21:00 – 21 June at 07:00	19 June at 02:00 – 19 June at 12:00, 20 June at 03:00 – 20 June at 11:00, 21 June at 00:00 – 21 June at 12:00
B	29 June at 19:00 – 30 June at 06:00, 30 June at 19:00 – 1 July at 06:00, 1 July at 21:00 – 2 July at 07:00	30 June at 04:00 – 1 July at 12:00, 1 July at 01:00 – 1 July at 08:00, 2 July at 02:00 – 2 July at 10:00
C	2 July at 21:00 – 3 July at 07:00, 3 July at 23:00 – 4 July at 06:00, 4 July at 20:00 – 5 July at 07:00	3 July at 03:00 – 3 July at 11:00, 4 July at 01:00 – 4 July at 12:00, 5 July at 05:00 – 5 July at 11:00
D	5 July at 19:00 – 6 July at 07:00, 6 July at 16:00 – 7 July at 03:00	6 July at 01:00 – 6 July at 15:00, 7 July at 07:00 – 7 July at 14:00

Table 1. Average concentrations of aerosol and gas-phase species along with various meteorological parameters observed during the times of RH increasing and decreasing during Periods A, B, C, and D. NA = not available

	OA ($\mu\text{g}/\text{m}^3$)	WSOC ($\mu\text{g}/\text{C}/\text{m}^3$)	Glycolate ($\mu\text{g}/\text{m}^3$)	Acetate ($\mu\text{g}/\text{m}^3$)	Formate ($\mu\text{g}/\text{m}^3$)	Chloride ($\mu\text{g}/\text{m}^3$)	Sulfate ($\mu\text{g}/\text{m}^3$)	Oxalate ($\mu\text{g}/\text{m}^3$)	Nitrate ($\mu\text{g}/\text{m}^3$)	Sodium ($\mu\text{g}/\text{m}^3$)	Ammonium ($\mu\text{g}/\text{m}^3$)	Potassium ($\mu\text{g}/\text{m}^3$)	Magnesium ($\mu\text{g}/\text{m}^3$)	Calcium ($\mu\text{g}/\text{m}^3$)	ALW ($\mu\text{g}/\text{m}^3$)
Period A RH Increasing	8.93	4.73	0.28	0.40	0.43	0.13	3.49	0.24	2.91	NA	NA	NA	NA	NA	6.81
Period A RH Decreasing	9.63	5.09	0.30	0.33	0.47	0.17	3.23	0.23	5.61	NA	NA	NA	NA	NA	7.29
Period B RH Increasing	4.06	2.87	0.22	0.24	0.24	0.09	3.22	0.12	1.67	0.01	1.04	0.43	0.10	0.37	4.21
Period B RH Decreasing	3.78	2.89	0.22	0.24	0.23	0.09	2.69	0.11	1.56	0.01	1.04	0.48	0.09	0.13	4.34
Period C RH Increasing	2.05	1.55	0.24	0.28	0.23	0.11	2.80	0.13	1.18	0.04	0.92	0.51	0.11	0.26	2.89
Period C RH Decreasing	2.01	1.54	0.22	0.32	0.23	0.10	2.75	0.12	1.28	0.04	0.94	0.54	0.09	0.06	2.64
Period D RH Increasing	2.89	1.92	0.17	0.18	0.21	0.11	3.38	0.12	1.31	0.02	1.07	0.48	0.10	0.32	4.10
Period D RH Decreasing	3.02	1.99	0.19	0.19	0.24	0.14	4.89	0.13	3.56	0.03	2.00	0.55	0.10	0.20	7.90

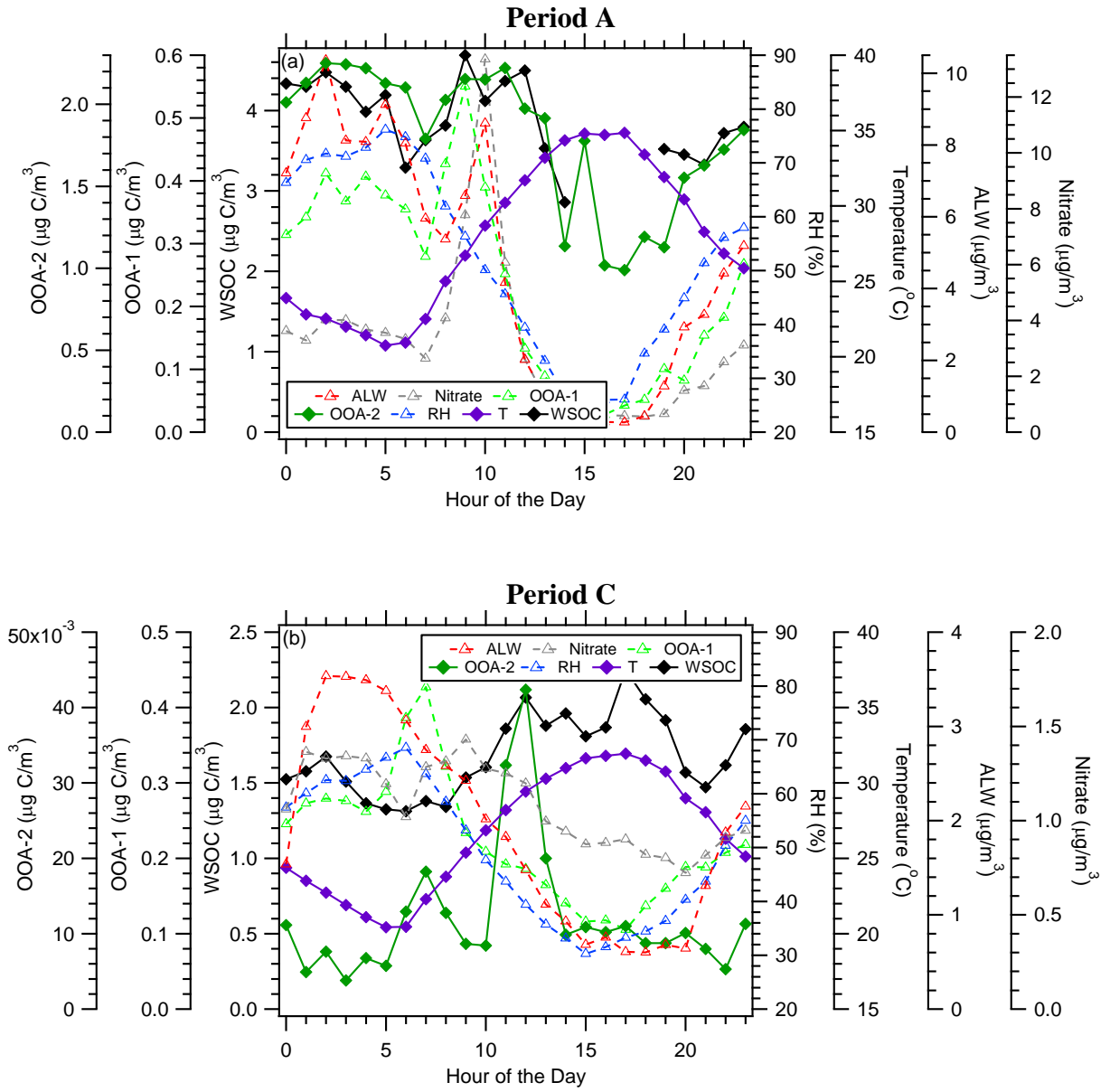
	Ozone ($\mu\text{g}/\text{m}^3$)	NO _x ($\mu\text{g}/\text{m}^3$)	SO ₂ (ppb)	Benzene ($\mu\text{g}/\text{m}^3$)	Toluene ($\mu\text{g}/\text{m}^3$)	Xylene ($\mu\text{g}/\text{m}^3$)	Glyoxal (ppb)	T (°C)	RH (%)
Period A RH Increasing	47.42	28.90	0.65	0.21	1.21	0.26	0.05	24.47	64.49
Period A RH Decreasing	63.70	17.75	1.14	0.27	1.78	0.34	0.09	26.09	57.66
Period B RH Increasing	76.6	10.94	0.68	0.19	0.83	0.53	0.06	26.74	60.87
Period B RH Decreasing	51.6	9.30	0.69	0.29	1.43	0.66	0.07	26.2	61.20
Period C RH Increasing	61.29	9.72	0.40	0.17	1.18	0.40	0.05	23.31	60.60
Period C RH Decreasing	75.40	8.08	0.51	0.17	1.11	0.44	0.07	25.02	53.88
Period D RH Increasing	87.21	8.93	0.30	0.12	0.52	0.23	0.05	25.63	63.45
Period D RH Decreasing	93.73	5.12	0.38	0.15	0.85	0.28	0.07	27.32	54.92

Reviewer #2

p. 35497 lines 3-19: This argument distinguishing between OOA-1 and OOA-2 needs to be clarified, and requires more data to be shown in support of the distinction. The authors state in line 12 that OOA-1 correlates with WSOC during increasing RH in period A, but not period B, as shown in Figure 9. This also appears to be the case for OOA-2. Furthermore, the authors state in line 5 that both OOA-1 and OOA-2 increase with RH and WSOC throughout period A, but do not show this data. They state in line 10 that OOA-1 drops in late morning when the RH declines (perhaps visible in Figure 8a?), and use this to argue for reversible aqueous formation of OOA-1. Then, the authors “illustrate” this, reversibility by appealing to increasing RH data. They state that OOA-1, but not OOA-2, correlates with RH during times of increasing RH during period A, but fail to show this data, either. These observations are then used to make inferences about the different natures of OOA-1 and OOA-2, but too little data distinguishing the two (beyond the O/C ratio) has been shown to make the argument convincing.

In order to better explain and illustrate the differences between OOA-1 and OOA-2 we have added diurnal profiles of WSOC, OOA-1, OOA-2, RH, temperature, ALW, and nitrate for Periods A and B (now Period C). This figure, shown below, helps to better show the relationship and timing of when OOA-1, OOA-2, RH, and ALW decrease. The discussion has also been updated and Lines 344-356 now read as “The multilinear regression analysis performed on the Period A measurements suggests that the largest water-soluble fractions are exhibited by OOA-1 and OOA-2, whose concentrations were observed to increase along with RH and WSOC for all the days in this period of the campaign. Due to the very different absolute average concentrations, the second factor (OOA-2) provided the largest contribution to WSOC, accounting for more than one third of the total water-soluble organic carbon concentration. Interestingly, the diurnal trend of OOA-1 indicated that its partitioning to the aerosol phase was largely reversible, and its concentrations declined steeply in the late morning hours when RH and ALW decreased (Fig. 12a). In the same hours of the day, the OOA-2 concentrations were largely unaffected by RH indicating (a) that OOA-2 mainly accounted for oxidized compounds stable in the aerosol phase and (b) that boundary layer growth is not the reason for the decrease in OOA-1 as this should have affected all factors. OOA-1 and OOA-2 can therefore be hypothesized as two aging stages of aqSOA formation during Period A.”

Figure 12



It would be appropriate to reference the paper by Jian Yu et al. (2005), who identified the correlation between aerosol oxalate and sulfate, either in the last paragraph of the introduction or with the Sorooshian reference at the bottom of p. 35494.

The *Yu et al.* [2005] paper has been added. Lines 127-130 now read as “We also look at the relationship of oxalate with sulfate and gas-phase glyoxal; oxalate and sulfate are both produced by cloud processing and glyoxal is a known precursor to aqSOA formation [*Yu et al.*, 2005; *Tan et al.*, 2009; *Ervens and Volkamer*, 2010; *Lim et al.*, 2010; *Sorooshian et al.*, 2010].” and Lines 286-288 as “Oxalate and sulfate are known tracers for aerosol formation through cloud processing [*Yu et al.*, 2005; *Sorooshian et al.*, 2010], although sulfate does also have a substantial, albeit slower, gas-phase formation pathway [*Seinfeld and Pandis*, 2006].”

This reviewer would like to see more connection or comparison made between the results of this study and the closely related work of El-Sayed (2015), briefly references in line 12 of p 35494.

A discussion about the *El-Sayed et al.* [2015] paper has been added. Lines 262-269 now read as “This also supports a recent study that observed ambient aqSOA formation during the nighttime as evident by the increased partitioning of gas-phase WSOC to the particle-phase with increasing RH [*El-Sayed et al.*, 2015]. The study by *El-Sayed et al.* [2015] found the increase in the fraction of total WSOC in the particle phase (F_p) at the two highest RH levels (70-80%, >80%) to be statistically significant compared to the F_p values at RH < 60%. The main focus of their work was to investigate if the uptake of gas-phase WSOC to aerosol water occurs through reversible or irreversible pathways. The data suggested the aqSOA was formed irreversibly. We investigate this with our data in section 3.3.2.”

Reviewer #3

1. Page 35488, line 16-21: Lee et al. (2012) experimentally demonstrated formation of aqueous SOA through photo-oxidation of real cloud water samples. It is recommended to include this reference here.

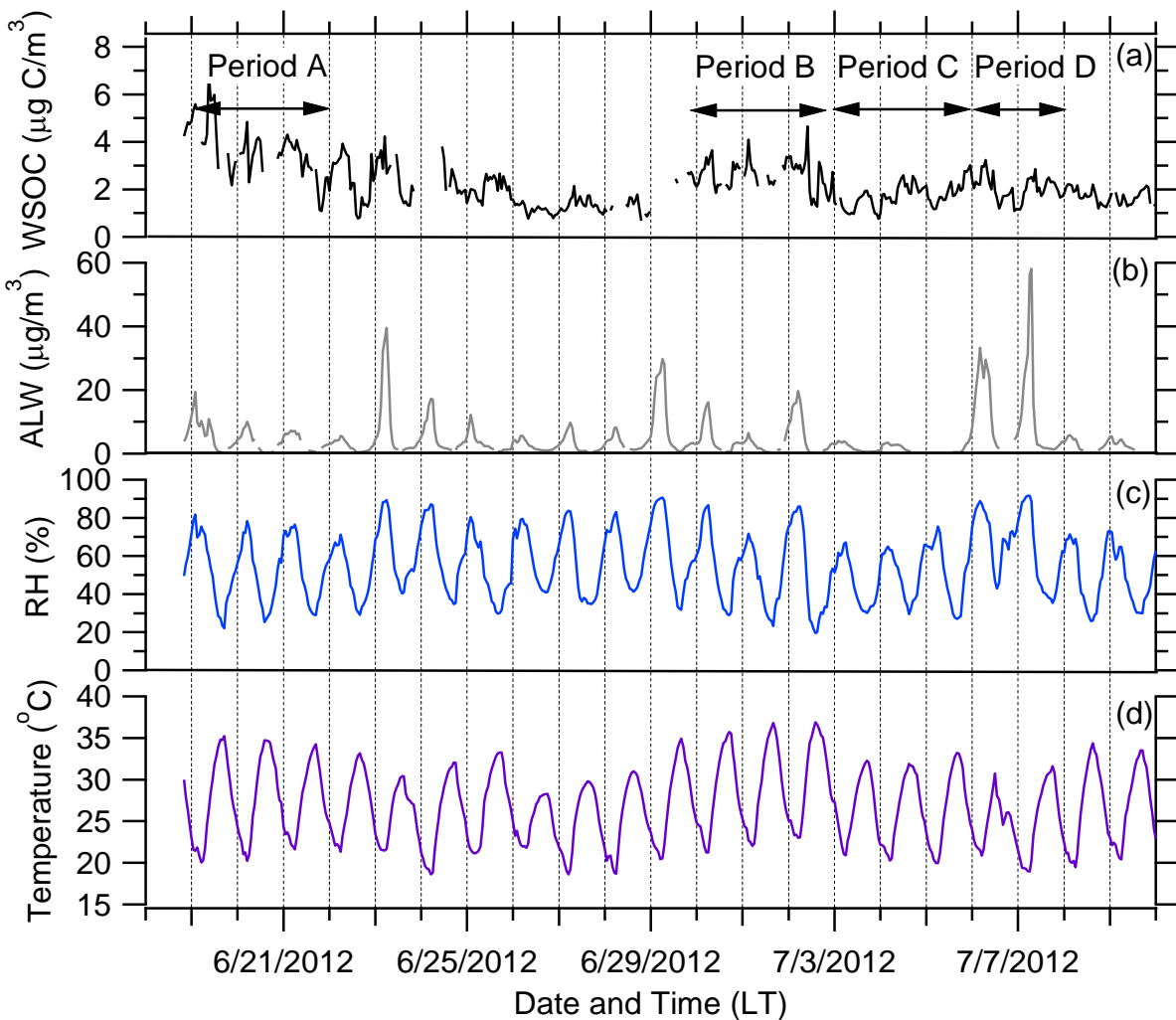
The *Lee et al.* [2012] reference has been added. Lines 99-103 now read as “These products can remain in the particle phase after water evaporation, forming what is termed aqueous secondary organic aerosol (aqSOA) (e.g. [*Blando et al.*, 2000; *Altieri et al.*, 2006; *Carlton et al.*, 2007; *de Haan et al.*, 2009; *Galloway et al.*, 2009; *Ervens and Volkamer*, 2010; *Sun et al.*, 2010; *Lee et al.*, 2012; *Monges et al.*, 2012; *Nguyen et al.*, 2012; *Tan et al.*, 2012; *Gaston et al.*, 2014]).”

2. Page 35492, line 17-25: The justification of using Period A and B to represent the first and second halves of the study, respectively, is unclear. Are the two selected periods defined based on meteorological conditions and/or aerosol chemical compositions? In particular, the mass loading of nitrate and ALW content in Period B are very different to those observed in the rest of second half. Furthermore, the authors mention that Periods A and B had similar air mass origins in general (line 20-22), which is somewhat contradict to the following sentence highlighting that Period A occurred during the end of a stagnation event and Period B represents typical background conditions influenced by regional transport (line 23-25).

The two periods were originally picked because they have similar transport patterns. In response to reviewer comments, we have now updated our analysis to include two more periods. The original Period B is now called Period C. The new Period B covers 30 June, 1-2 July and Period D covers 6-7 July. The new Period B has moderate ALW and Period D has the highest ALW observed during the study. We have also tried to clarify our meaning of similar air mass origins by instead talking about the flow direction. Lines 206-218 now read as “Therefore, our analysis will focus on comparing these two different halves of the study. Given our interest in examining for evidence of aqSOA we picked four periods with varying levels of WSOC and ALW. We also picked cases with both sites sampling similar air masses on a given day. Period A represents the first half of the study and covers 19-21 June. Period A has elevated WSOC and moderate ALW. As indicated by the difference in the length of the back trajectories [*Draxler and Rolph*, 2013; *Rolph*, 2013] shown in Fig. 2, Period A occurred during the end of a stagnation. Period B (30 June, 1-2 July), Period C (3-5 July), and Period D (6-7 July) represent three different cases in the second half of the study. Period B has moderate ALW, Period C has low ALW, and Period D has the highest ALW observed during the study. As indicated by Fig. 2, all three of these periods represent typical background conditions influenced by regional transport, but with slightly different flow patterns. The flows of Periods A and C are most similar. Due to changes in the WSOC concentrations and a non-consistent flow pattern on a daily basis, no periods between 23-29 June were examined.”

3. Page 35493, line 8-10 and Figure 2: Please add time series of ambient temperature and RH in Figure 2 for better illustration. Please also briefly explain how the RH variations can be used to diminish the influence of dilution and mixing. I wonder if the RH increasing period represents the period with a stable nocturnal layer.

Figure 2 (now Figure 3) has been updated to include temperature and RH. The new version of the figure is shown below. Also, our idea behind looking at the RH increasing vs. decreasing period is exactly as suggested, that the RH increasing period would represent a time with a stable nocturnal boundary layer. Lines 229-236 have been updated and read as “Each period will be examined in terms of the times when RH increased from 40 to 70% (times of RH increasing) and then when the RH decreased from 70 back to 40% (times of RH decreasing). This was done to try to diminish the influence of dilution and mixing on SOA concentrations and measurements of other key variables, since measurements of a conserved tracer were not available. The idea being that the times of RH increasing would represent a time with a stable nocturnal boundary layer. The switch in regimes on average occurs at 05:00 LT, but varied from 03:00 to 08:00 LT. Therefore, the times of RH increasing primarily occurred in the dark. “



4. Page 35494, second paragraph: It is recommended to discuss the potential formation mechanism of particle nitrate. In particular, NO_x concentration in Period A was higher than that observed in Period B. It is well known that NO_x can be lost at night to form N_2O_5 , which can

further react with water on aerosol surfaces to yield nitric acid. Increasing ambient RH may actually increase nitrate concentrations in particle-phase through N₂O₅ hydrolysis, that subsequently enhances ALW content for aqSOA production. In addition, it is possible that some nitrate can be formed in the residual layer at night and then convectively mixed after boundary layer break up, resulting in strong nitrate peaks (with relative low ALW probably because of the low RH after mixing) observed at around 9-11am.

The question of how the nitrate forms overnight is very interesting. We had a similar hypothesis that the elevated NO_x in Period A is contributing to the nitrate peak observed around midnight. Likely the second peak in nitrate observed in morning around 07:00 LT is due to mixing from aloft as the boundary layer breaks up. However, we prefer not to add any discussion to the text about this as we don't have any additional data to convincingly support these hypotheses.

5. Page 35495, line 6-17: I agree with the authors that oxalate is not a unique marker for aqSOA. As highlighted in the manuscript, previous laboratory studies have shown that photo-oxidation of glyoxal generates oligomers as major products through radical-radical reactions in aerosol water when OH radical concentrations is one the order of 10⁻¹²M. However, oxalate can be largely produced in aerosol water at a lower OH radical concentration (10⁻¹³M) likely due to insufficient organic radicals concentration for oligomers formation (Lee et al., 2011). Considering the uncertainty of OH radical concentrations in aerosol water, it is inappropriate to rule out the possibility of oxalate production in aqueous aerosol particles.

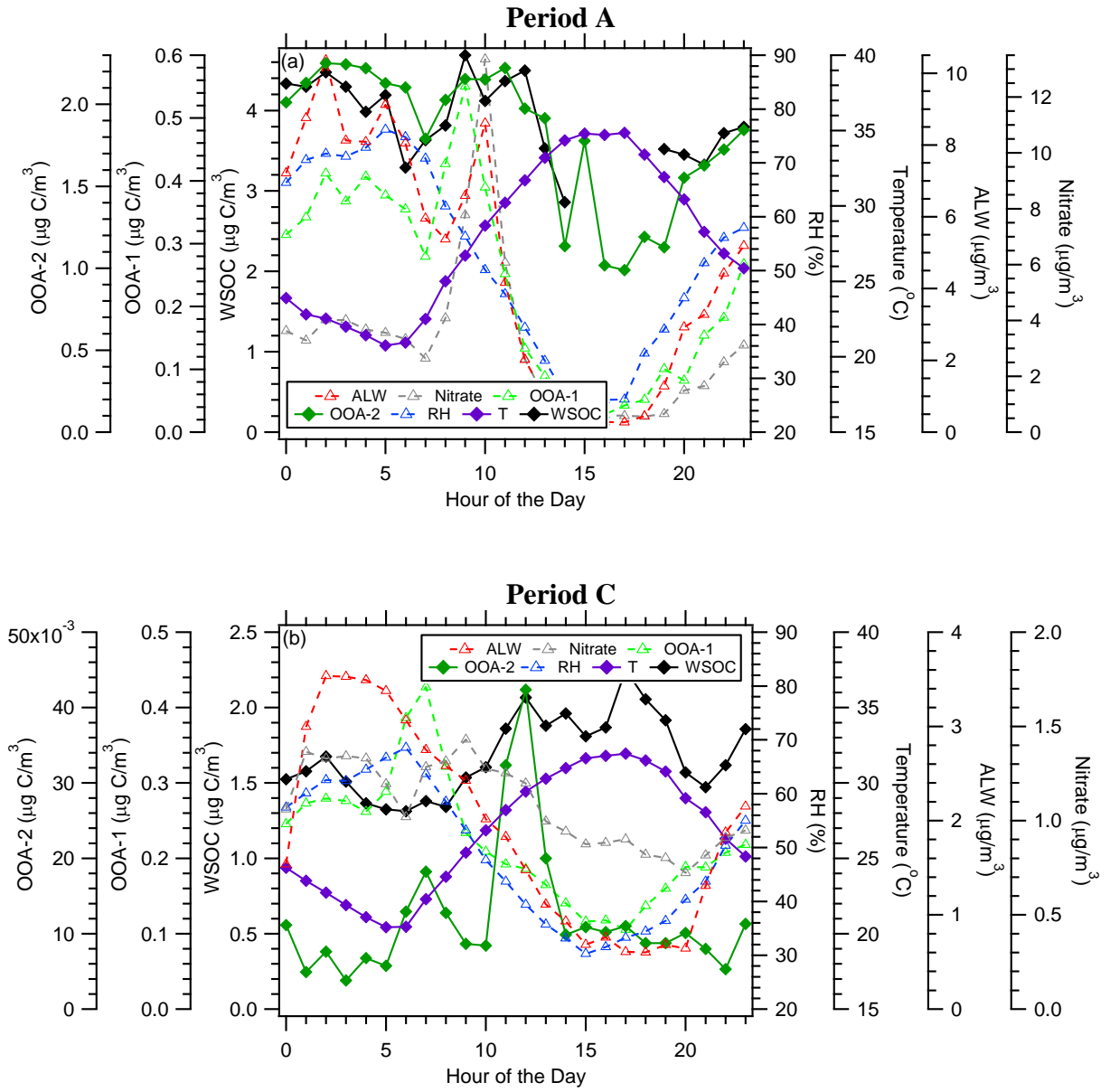
We have updated the discussion about oxalate to include the *Lee et al.* [2011] reference. We also now just mention that oxalate is not a universal marker for aqSOA, but do not go further to discuss it being a tracer for chemistry in clouds vs. wet aerosols. Lines 288-305 now read as “As shown in Fig. 8a and 8b for Periods A and C, during both the times of RH increasing and decreasing, there is a positive linear relationship between oxalate and sulfate (R^2 ranged from 0.39 to 0.68). The association between oxalate and sulfate but not oxalate and WSOC in Period A suggests that the local aqSOA formed in wet aerosols during Period A has little effect on oxalate. This result supports the supposition that oxalate is not a universal marker for aqSOA. This is further illustrated in our data by examining the correlation of oxalate vs. gas-phase glyoxal, a known precursor for aqSOA [*Tan et al.*, 2009; *Ervens and Volkamer*, 2010; *Lim et al.*, 2010], and ALW (Fig. 8c-f). Laboratory experiments suggest a relationship between oxalate and gas-phase glyoxal when there is in-cloud processing as oligomers have been proposed to be the dominant products from processing in aerosol water when hydroxyl radical concentrations are on the order of 10⁻¹² M [*Lim et al.*, 2010; *Tan et al.*, 2010]. Oxalate could be produced in aerosol water at lower hydroxyl radical concentrations, such as 10⁻¹³ M, due to insufficient organic radical concentrations for oligomer formation [*Lee et al.*, 2011]. Although the hydroxyl radical concentrations are unknown, there is only a relationship between oxalate and gas-phase glyoxal for Period C during times of RH decreasing ($R^2 = 0.44$), which is when clouds were observed west of the site. In addition, there is no important relationship observed between oxalate and ALW for either period (all $R^2 < 0.17$).”

6. Page 35497, line 9-14: Please explain the connection between Fig. 9a (i.e., correlation of WSOC with OOA-1 during the times of RH increasing for only Period A) and the argument in

line 9-11 (i.e., OOA-1 reversibility and its concentrations declined steeply in the late morning hours when RH and ALW decreased). Similar to comment 3, It is difficult to follow the description here without a timer series of ambient RH and temperature in Figure 8.

In order to better explain and illustrate this we have added diurnal profiles of WSOC, OOA-1, OOA-2, RH, temperature, ALW, and nitrate for Periods A and C (Figures 12), which are shown below. These help to better show the relationship than our previous explanation, which has been removed. Lines 344-356 now read as “The multilinear regression analysis performed on the Period A measurements suggests that the largest water-soluble fractions are exhibited by OOA-1 and OOA-2, whose concentrations were observed to increase along with RH and WSOC for all the days in this period of the campaign. Due to the very different absolute average concentrations, the second factor (OOA-2) provided the largest contribution to WSOC, accounting for more than one third of the total water-soluble organic carbon concentration. Interestingly, the diurnal trend of OOA-1 indicated that its partitioning to the aerosol phase was largely reversible, and its concentrations declined steeply in the late morning hours when RH and ALW decreased (Fig. 12a). In the same hours of the day, the OOA-2 concentrations were largely unaffected by RH indicating (a) that OOA-2 mainly accounted for oxidized compounds stable in the aerosol phase and (b) that boundary layer growth is not the reason for the decrease in OOA-1 as this should have affected all factors. OOA-1 and OOA-2 can therefore be hypothesized as two aging stages of aqSOA formation during Period A.”

Figure 12

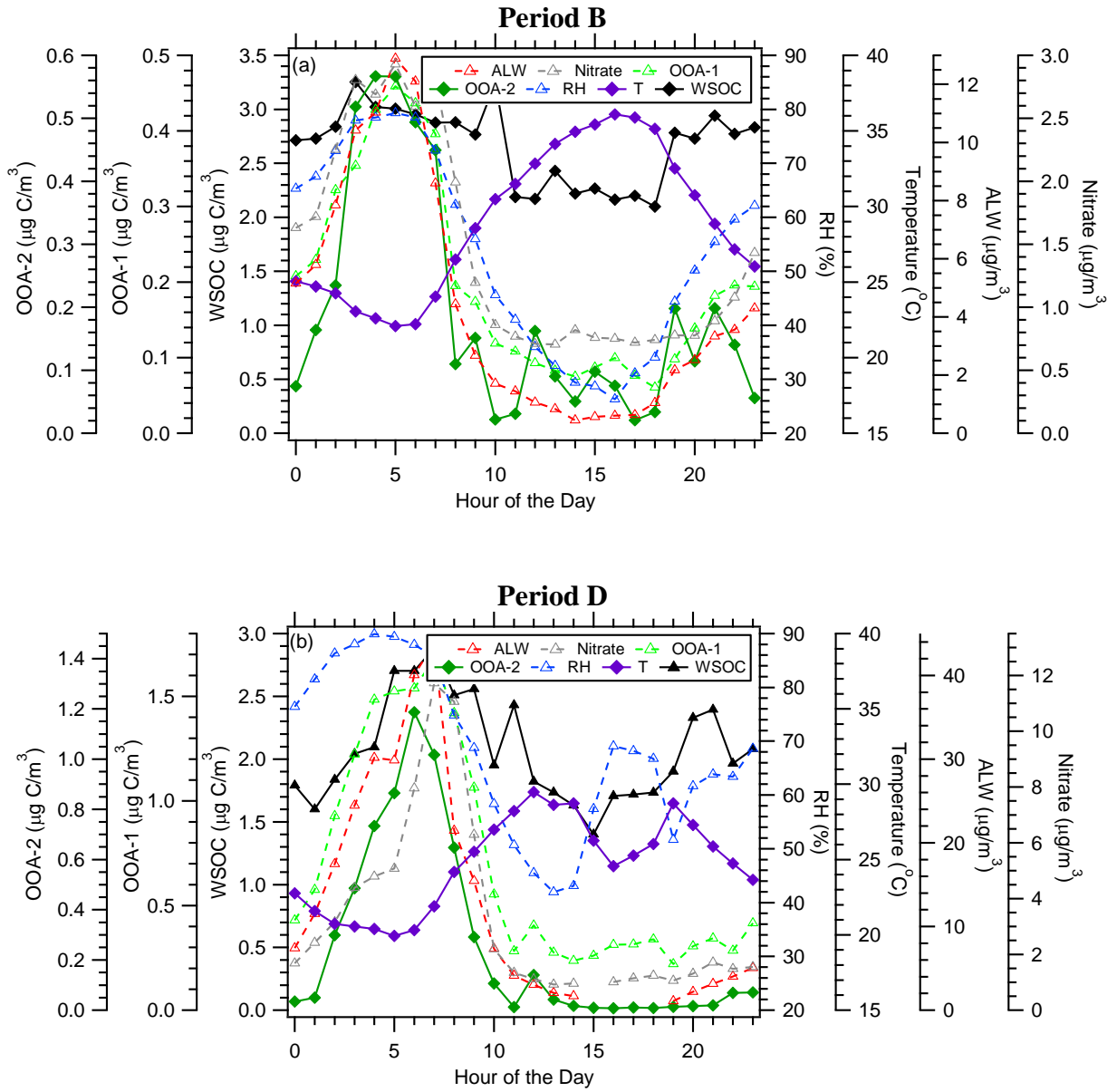


7. Page 35498, Section 3.4: It is recommended to add some discussion regarding OOA-1 and OOA-2 formation outside of Period A and B. In particular, significant amounts of OOA-1 and OOA-2 were produced during July 6-7, which are comparable to those observed in Period A. Therefore, the weak correlations between WSOC and nitrate (also OOA-1 and OOA-2) are probably due to the large contribution of background organic aerosol. In addition, the temporal variations of OOA-1 and OOA-2 looks very different. OOA-1 was formed and correlated well with nitrate throughout the whole sampling period. If OOA-1 and OOA-2 represent volatile/semi-volatile aqSOA and stable aqSOA respectively, can the authors comments on the atmospheric conditions that can produce OOA-1 but not OOA-2?

We have added discussion about the formation of OOA-1 and OOA-2 outside of Period B. This is done in conjunction with the addition of the analysis of two more Periods. The original Period B is now called Period C. The new Period B covers 30 June, 1-2 July and Period D covers 6-7 July. Diurnal profiles of WSOC, OOA-1, OOA-2, RH, temperature, ALW, and nitrate for these two new periods are included in the supporting information (Figure S10, shown below). Lines 357-363 now read as “Interestingly, some OOA-2 is also produced in Periods B and D. Although the concentrations levels of OOA-2 observed are similar between Periods A and D, OOA-2 concentrations are much more sustained across the day in Period A. In addition, as illustrated in the diurnal profiles for these periods (Fig. S10) the OOA-2 follows along more closely with OOA-1, RH, and ALW in Periods B and D, likely due to the differences in meteorology and/or chemistry of these periods compared to Period A. Regardless of these differences the observations all still point to the strong relationship between OOA-1, OOA-2, and ALW.”

We also added text to point out that the original Period B is an example of a case where OOA-1 is produced, but not OOA-2. Lines 370-373 now read as “Similar to Period A, here again the times when RH and ALW were high showed relatively high concentrations of OOA-1 (Fig. 12b), which represented an additional (though small compared to OOA-4) contribution to WSOC. Period C provides a case where significant OOA-1 is formed, but not OOA-2.”

Figure S10



1 **Evidence for Ambient Dark Aqueous SOA Formation in the Po Valley, Italy**
2
3
4

5 A.P. Sullivan¹, N. Hodas², B.J. Turpin³, K Skog⁴, F.N. Keutsch^{4,5}, S. Gilardoni⁶, M. Paglione⁶,
6 M. Rinaldi⁶, S. Decesari⁶, M.C. Facchini⁶, L. Poulain⁷, H. Herrmann⁷, A. Wiedensohler⁷, E.
7 Nemitz⁸, M.M. Twigg⁸, and J.L. Collett, Jr.¹
8
9
10

11 ¹Colorado State University, Department of Atmospheric Science, Fort Collins, Colorado 80523,
12 USA

13 ²California Institute of Technology, Division of Chemical Engineering, Pasadena, California
14 91125, USA

15 ³Rutgers University, Department of Environmental Sciences, New Brunswick, New Jersey
16 08901, USA

17 ⁴University of Wisconsin – Madison, Department of Chemistry, Madison, Wisconsin 53706,
18 USA

19 ⁵Harvard University, Department of Chemistry and Chemical Biology, Cambridge,
20 Massachusetts 02138, USA

21 ⁶Istituto di Scienze dell' Atmosfera e del Clima, Consiglio Nazionale delle Ricerche, 40129
22 Bologna, Italy

23 ⁷Leibniz Institute for Tropospheric Research, 04318 Leipzig, Germany

24 ⁸Centre for Ecology and Hydrology, Bush Estate, Penicuik, EH26QB, United Kingdom
25
26
27
28
29
30
31
32
33
34
35
36
37
38
39
40
41
42
43
44
45

46 **Abstract**

47 Laboratory experiments suggest that water-soluble products from the gas-phase oxidation
48 of volatile organic compounds can partition into atmospheric waters where they are further
49 oxidized to form low volatility products, providing an alternative route for oxidation in addition
50 to further oxidation in the gas-phase. These products can remain in the particle phase after water
51 evaporation forming what is termed as aqueous secondary organic aerosol (aqSOA). However,
52 few studies have attempted to observe ambient aqSOA. Therefore, a suite of measurements,
53 including near real-time WSOC (water-soluble organic carbon), inorganic anions/cations,
54 organic acids, and gas-phase glyoxal, were made during the PEGASOS (Pan-European Gas-
55 AeroSols-climate interaction Study) 2012 campaign in the Po Valley, Italy to search for evidence
56 of aqSOA. Our analysis focused on ~~two-four specific~~ periods: Period A on 19-21 June, ~~and~~
57 ~~Period B on 30 June, 1-2 July,~~ Period ~~CB~~ on 3-5 July, ~~and Period D on 6-7 July~~ to represent the
58 first (Period A) and second halves (Periods B, C, and D) of the study, ~~respectively~~. ~~These~~
59 ~~periods were picked to cover varying levels of WSOC and aerosol liquid water. The large scale~~
60 ~~circulation was predominately from the west in both periods.~~ Plus back trajectory analysis
61 suggested all sites sampled similar air masses ~~on a given day during both periods allowing for~~
62 ~~comparison of Periods A and B~~. The data collected during both periods were divided into times
63 of increasing relative humidity (RH) and decreasing RH with the aim of diminishing the
64 influence of dilution and mixing on SOA concentrations and other measured variables. Evidence
65 for local aqSOA formation was only observed during Period A. When this occurred, there was a
66 correlation of WSOC with organic aerosol ($R^2 = 0.846$), aerosol liquid water ($R^2 = 0.659$), RH
67 ($R^2 = 0.3945$), and aerosol nitrate ($R^2 = 0.6674$). Additionally, this was only observed during
68 times of increasing RH, which coincided with dark conditions. Comparisons of WSOC with
69 oxygenated organic aerosol (OOA) factors determined from application of positive matrix
70 factorization analysis on the aerosol mass spectrometer observations of the submicron non-
71 refractory organic particle composition suggested that the WSOC ~~in Periods A and B~~ differed ~~in~~
72 ~~the two halves of the study~~ (Period A WSOC vs. OOA-2 $R^2 = 0.835$ and OOA-4 $R^2 = 0.043$
73 whereas Period ~~BC~~ WSOC vs. OOA-2 $R^2 = 0.03$ and OOA-4 $R^2 = 0.64$). OOA-2 had a high O/C
74 (oxygen/carbon) ratio of 0.77, providing evidence that aqueous processing was occurring during
75 Period A. Key factors for local aqSOA production during Period A appear to include: air mass
76 stagnation, which allows aqSOA precursors to accumulate in the region; the formation of
77 substantial local particulate nitrate during the overnight hours, which enhances water uptake by
78 the aerosol; and the presence of significant amounts of ammonia, which may contribute to
79 ammonium nitrate formation and subsequent water uptake and/or play a more direct role in the
80 aqSOA chemistry.

81
82
83
84
85
86
87
88
89
90

91
92
93
94
95
96
97
98
99
100
101
102
103
104
105
106
107
108
109
110
111
112
113
114
115
116
117
118
119
120
121
122
123
124
125
126
127
128
129
130
131
132
133
134
135

1. Introduction

The formation of secondary organic aerosol (SOA) remains a major source of uncertainty in predicting organic aerosol concentrations and properties that affect visibility, health, and climate [Kanakidou *et al.*, 2005]. SOA can form through gas-to-particle partitioning of semi-volatile organic compounds formed from gas-phase oxidation of VOCs (volatile organic compounds) [Seinfeld and Pankow, 2003]. However, laboratory experiments and predictions suggest that water-soluble products from the gas-phase oxidation of VOCs can also partition into atmospheric waters (i.e., clouds, fogs, and aerosol water) and react to form low volatility products. These products can remain in the particle phase after water evaporation, forming what is termed aqueous secondary organic aerosol (aqSOA) (e.g. [Blando *et al.*, 2000; Altieri *et al.*, 2006; Carlton *et al.*, 2007; de Haan *et al.*, 2009; Galloway *et al.*, 2009; Ervens and Volkamer, 2010; Sun *et al.*, 2010; *Lee et al., 2012; Monges et al., 2012; Nguyen et al., 2012; Tan et al., 2012; Gaston et al., 2014*]).

Formatted: Font: Italic

Evidence that aqSOA may be a contributor to ambient SOA includes a gap between observed SOA and SOA predicted by models that only include SOA formed via gas-phase oxidation and gas-particle partitioning [de Gouw *et al.*, 2005; Heald *et al.*, 2005]. In addition, there is a tendency for smog chamber experiments (generally conducted under dry conditions) to form SOA that is less oxygenated and hygroscopic than ambient SOA, suggesting a missing source of SOA [Aiken *et al.*, 2008]. In some locations, SOA surrogates have been shown to be more strongly correlated with liquid water than organic aerosol [Hennigan *et al.*, 2008; Zhang *et al.*, 2012], contrary to partitioning theory. Lastly, the abundance of ambient oxalate, an important product of aqSOA mechanisms [Carlton *et al.*, 2007; Ervens *et al.*, 2011], cannot be explained solely by gas-phase chemistry.

While it is important to study aqSOA, there have been few studies designed to observe aqSOA formation in the ambient atmosphere. Therefore, a suite of near real-time measurements was assembled with the goal of identifying evidence of aqSOA formation in the Po Valley of Italy during the summer of 2012. A key measurement for this analysis was water-soluble organic carbon (WSOC), which previous research has suggested is a good proxy for SOA (e.g., [Sullivan *et al.*, 2004; Miyazaki *et al.*, 2006; Kondo *et al.*, 2007]). Fog measurements in the Po Valley have been well documented (e.g., [Facchini *et al.*, 1999; Fuzzi *et al.*, 2002]). Fog is unlikely to occur in the summer. But even in summer, the region does have high relative humidity (60% to 80%) and is polluted, providing favorable conditions for aqSOA formation in wet aerosols.

Herein, we present an approach for the investigation of aqSOA formation in the ambient atmosphere and provide results from such analyses. We examine WSOC as a function of known parameters likely to be associated with aqSOA, such as relative humidity (RH), aerosol liquid water (ALW), and organic aerosol (OA) concentration. We also look at the relationship of oxalate with sulfate and gas-phase glyoxal; oxalate and sulfate are both produced by cloud processing and glyoxal is a known precursor to aqSOA formation [*Yu et al., 2005; Tan et al., 2009; Ervens and Volkamer, 2010; Lim et al., 2010; Sorooshian et al., 2010*]. This study aims to identify conditions conducive to aqSOA formation in this region.

Formatted: Font: Italic

136 **2. Methods**

137 Measurements were conducted within the Italian field campaign of the European Project
138 PEGASOS (Pan-European Gas-AeroSOLs-climate interaction Study) in June and July 2012,
139 focusing on the Po Valley. PEGASOS was a European wide study to address regional to global
140 feedbacks between atmospheric chemistry and climate in different locations as well as in the
141 laboratory. The observations included airborne measurements using a Zeppelin and multiple
142 ground sites to study surface-atmosphere exchange, assess the vertical structure of the
143 atmosphere, and study boundary layer photochemistry. An auxiliary site was located in Bologna.
144 Our measurements were made at the main ground site in San Pietro Capofiume (SPC, Fig. 1 [and](#)
145 [2](#)). The SPC field station is located approximately 40 km northeast of Bologna and 30 km south
146 of the Po River in flat terrain of agricultural fields (Fig. 1 ~~e~~ ~~and~~ ~~d~~).

147 Our measurements included running a Particle-into-Liquid Sampler – Ion
148 Chromatography (PILS-IC) [Orsini *et al.*, 2003] system for inorganic cations, inorganic anions,
149 and light organic acids and a Particle-into-Liquid Sampler – Total Organic Carbon (PILS-TOC)
150 system [Sullivan *et al.*, 2004] for particle-phase WSOC. A PILS collects the ambient particles
151 into purified water, providing the liquid sample for analysis. Both systems operated at 15 LPM
152 with a 2.5 µm size-cut cyclone. Two annular denuders coated with sodium carbonate and
153 phosphorous acid to remove inorganic gases were placed upstream of the PILS-IC and for the
154 PILS-TOC an upstream activated carbon parallel plate denuder [Eatough *et al.*, 1993] was used
155 to remove organic gases. In addition, for the PILS-TOC, a normally open actuated valve
156 controlled by an external timer was periodically closed every 2 hours for 30 min forcing the
157 airflow through a Teflon filter before entering the PILS. This was to allow for a real background
158 measurement to be determined. Ambient PM_{2.5} WSOC concentrations were calculated as the
159 difference between the filtered and non-filtered measurements. The background was assumed to
160 be constant between consecutive background measurements. Based on comparison with
161 integrated quartz filter WSOC measurements, it appears the difference between filtered and non-
162 filtered measurements was being overestimated by ~20% before the carbon denuder was
163 switched out on June 25. Therefore, the WSOC concentrations before this date have been
164 corrected for this.

165 For the PILS-IC, the liquid sample from the PILS was split between two Dionex ICS-
166 1500 ion chromatographs. These systems include an isocratic pump, self-regenerating anion or
167 cation SRS-ULTRA suppressor, and conductivity detector. The cations were separated using a
168 Dionex IonPac CS12A analytical (4 x250 mm) column with eluent of 18 mM methanesulfonic
169 acid at a flowrate of 1.0 ml/min. A Dionex IonPac AS15 analytical (4 x 250 mm) column
170 employing an eluent of 38 mM sodium hydroxide at a flowrate of 1.5 ml/min was used for the
171 anion analysis. A new chromatogram was obtained every 30 min with a sample loop fill time of
172 8 min. The limit of detection (LOD) for the various anions and cations was approximately 0.02
173 µg/m³. These inorganic PILS data were also used to determine ALW from the Extended Aerosol
174 Inorganics Model (E-AIM, [Wexler and Clegg, 2002]) run in a metastable state. More
175 information on the ALW calculations can be found in Hodas *et al.* [2014].

176 In the PILS-TOC, the liquid sample obtained from the PILS was pushed through a 0.2
177 µm PTFE liquid filter by a set of syringe pumps to ensure any insoluble particles were removed.
178 The flow was then directed into a Sievers Model 800 Turbo TOC (Total Organic Carbon)
179 Analyzer. This analyzer works by converting the organic carbon in the liquid sample to carbon
180 dioxide through chemical oxidation involving ammonium persulfate and ultraviolet light. The

181 conductivity of the dissolved carbon dioxide formed is determined. The amount of organic
182 carbon in the liquid sample is proportional to the measured increase in conductivity. The
183 analyzer was run in on-line mode providing a 6 min integrated measurement of WSOC with a
184 LOD of 0.1 $\mu\text{g C/m}^3$.

185 Other measurements presented here include 2.5 min integrated organic aerosol (OA)
186 concentrations determined by a High Resolution - Time-of-Flight Aerosol Mass Spectrometer
187 (HR-ToF-AMS) [Drewnick *et al.*, 2005; DeCarlo *et al.*, 2006; Canagaratna *et al.*, 2007].
188 Positive matrix factorization (PMF) analysis of the AMS OA data was performed using the
189 Multilinear Engine algorithm (ME-2) [Paatero, 1999] implemented within the toolkit Solution
190 Finder (SoFi) developed by Canonaco *et al.* [2013]. More details on the AMS ME-2 analysis
191 can be found in the supplement [text and Fig. S1-S7](#). Gas-phase glyoxal was determined by the
192 Madison Laser-Induced Phosphorescence (Mad-LIP) instrument [Huisman *et al.*, 2008] at a time
193 resolution of 51 s, hourly integrated ammonia was determined by a Monitor for AeRosols and
194 Gases (MARGA) [ten Brink *et al.*, 2007] in SPC and 30 min ammonia was determined by
195 AiRRmonia [Erisman *et al.*, 2001] in Bologna, and relative humidity was collected at an 1 min
196 time resolution from a Vaisala weather transmitter WXT510. All data presented throughout is
197 hourly averaged starting at the top of the hour.

199 3. Results and Discussion

200 3.1. Overview

201 As previously mentioned, WSOC is key to our analysis, since in the absence of biomass
202 burning (see supplement for more details on the source apportionment of the AMS OA), the
203 main contributor to WSOC has been found to be SOA [Sullivan *et al.*, 2006]. Figure [2a-3](#) shows
204 the time series for WSOC during the entire study at SPC. Overall, the WSOC concentration was
205 higher in the first half of the study (before 25 June) compared with the second half. The WSOC
206 concentration peaked on 19 June then steadily decreased through 22 June. During this time the
207 concentration ranged from about 1 to 7 $\mu\text{g C/m}^3$. During July, the WSOC was relatively
208 constant at around 2 $\mu\text{g C/m}^3$.

209 ~~Therefore, our analysis will focus on two time periods (Periods A and B) to represent the~~
210 ~~two different halves of the study. Period A covers 19-21 June and Period B covers 3-5 July (Fig.~~
211 ~~2). The large scale circulation indicated flow predominately from the west, typical for this~~
212 ~~region. Back trajectory analysis [Draxler and Rolph, 2013; Rolph, 2013] suggested both periods~~
213 ~~had generally similar air mass origins, but more importantly that both sites sampled similar air~~
214 ~~masses on a given day (Fig. 1). As indicated by the difference in the length of the back~~
215 ~~trajectories, Period A occurred during the end of a stagnation event and Period B represents~~
216 ~~typical background conditions influenced by regional transport. In addition, cloud cover, as~~
217 ~~indicated from satellite measurements, showed that the days preceding Period A were generally~~
218 ~~cloud free whereas clouds developed west of the ground sites preceding Period B (not shown).~~
219 ~~Table 1 provides a comparison of the various concentrations and parameters observed during~~
220 ~~both periods.~~

221 Therefore, our analysis will focus on comparing these two different halves of the study.
222 Given our interest in examining for evidence of aqSOA we picked four periods with varying
223 levels of WSOC and ALW. We also picked cases with both sites sampling similar air masses on
224 a given day. Period A represents the first half of the study and covers 19-21 June. Period A has
225 elevated WSOC and moderate ALW. As indicated by the difference in the length of the back

226 trajectories [Draxler and Rolph, 2013; Rolph, 2013] shown in Fig. 2, Period A occurred during
227 the end of a stagnation. Period B (30 June, 1-2 July), Period C (3-5 July), and Period D (6-7
228 July) represent three different cases in the second half of the study. Period B has moderate
229 ALW, Period C has low ALW, and Period D has the highest ALW observed during the study.
230 As indicated by Fig. 2, all three of these periods represent typical background conditions
231 influenced by regional transport, but with slightly different flow patterns. The flows of Periods
232 A and C are most similar. Due to changes in the WSOC concentrations and a non-consistent
233 flow pattern on a daily basis, no periods between 23-29 June were examined.

234 Cloud cover, as indicated from satellite measurements, showed that the days preceding
235 Period A were generally cloud free whereas clouds developed west of the ground sites preceding
236 Periods B, C, and D (not shown). The presence of clouds was determined by examining satellite
237 pictures set to the view of Europe at 11:00 LT provided by Sat24 (<http://en.sat24.com/en/eu>).
238 Also, wet scavenging was not likely important as there was very little precipitation at SPC or
239 west of the site during the entire study period. Only two cases of light rain lasting ~30 min,
240 which occurred on the afternoons of 23 June and 6 July, were recorded at SPC. Table 1 provides
241 a comparison of the various concentrations and parameters observed during all four periods.
242 With the exception of WSOC mentioned above, only the OA and NO_x (nitric oxides)

243 Each period will be examined in terms of the times when RH increased from 40 to
244 80-70% (times of RH increasing) and then when the RH decreased from 80-70 back to 40%
245 (times of RH decreasing). This was done to try to diminish the influence of dilution and mixing
246 on SOA concentrations and measurements of other key variables, since measurements of a
247 conserved tracer were not available. The idea being that the times of RH increasing would
248 represent a time with a stable nocturnal boundary layer. The switch in regimes on average
249 occurs at 05:00 LT, but could vary from 03:00 to 08:00 LT. Therefore, the times of RH
250 increasing primarily occurred in the dark. Table S1 provides a list of the exact times used for the
251 times of RH increasing and decreasing in each period.

252 Our analysis will largely be based on least square regression correlation analysis to
253 examine the relationship between various species and provide a general approach to examine for
254 evidence of aqSOA. We have chosen to examine R² values as opposed to p-values since R²
255 values can provide a more useful tool for understanding the influence of the x variable on the y
256 variable. A R² value tells you the fraction of variance in the y variable explained by the x
257 variable, whereas a p-value tells you if a relationship is significant. However, a relationship can
258 be statistically significant regardless of the relationship between the x and y variables. In other
259 words, the x variable could explain only a very small fraction of the variability in the y variable
260 even when a small p-value was obtained. Therefore, the use of R² values would be more
261 meaningful for our analysis. We consider a high correlation as a R² value greater than 0.7, a
262 moderate correlation as a R² value between 0.4 to 0.7, and a low or poor correlation as a R² value
263 less than 0.3. For clarity only the R² values are shown in the figures, but the equations for the
264 least square regressions can be found in Table 2 for each individual correlation plot.

265 We first will compare all four periods to examine for evidence of aqSOA. Then we will
266 provide a further examination of aqueous aerosol tracers and WSOC for the two periods with
267 similar air flow (Periods A and C). Our analysis will largely be based on least square regression
268 correlation analysis to examine the relationship between various species and provide a general
269 approach to examine for evidence of aqSOA. We have chosen to examine R² values as opposed
270 to p-values since R² values can provide a useful tool for explaining the amount of observed

271 variance in a dependent variable that is explained by variation in an independent variable. p-
272 values merely indicate whether a relationship is statistically significant without information
273 about the amount of variance explained. To help categorize the fraction of variance explained,
274 we consider a high correlation as R^2 values greater than 0.7, a moderate correlation as R^2 values
275 between 0.3 to 0.7, and a low correlation as R^2 values less than 0.3.

276 277 **3.2. Evidence for aqSOA**

278 WSOC is shown as a function of RH for the times of RH increasing (Fig. ~~3a4a~~ 4a and 4b)
279 and decreasing (Fig. ~~3b4c~~ 4c and 4d) during both Periods ~~A, and B, C, and D.~~ For Periods B, C,
280 and D, WSOC had no relationship with RH. Only during the times of increasing RH did Period
281 A have a relationship of increasing WSOC with RH, consistent with local aqSOA formation.
282 This can further be illustrated by examining the correlation of WSOC vs. organic aerosol (OA),
283 aerosol liquid water (ALW), and RH for Periods ~~A, and B, C, and D~~ during the times of RH
284 increasing (Fig. 45 and S8). ~~In both periods during the time of RH increasing~~ In general, WSOC
285 had a strong relationship with OA (~~Period A $R^2 = 0.86$ and Period B $R^2 = 0.66$~~), but only Period
286 A additionally had a moderate correlation of the WSOC with both ALW (Period A $R^2 = 0.65$ vs.
287 Period B $R^2 = 0.15$, Period C $R^2 = 0.29$, and Period D $R^2 = 0.01$) and RH (Period A $R^2 = 0.39$ vs.
288 Period B $R^2 = 0.01$, Period C $R^2 = 0.12$, and Period D $R^2 = 0.07$). The good correlation between
289 WSOC and ALW is in agreement with a previous smog chamber study that found that ALW is a
290 key determinant of SOA yield [Zhou *et al.*, 2011]. This also supports a recent study that
291 observed ambient aqSOA formation during the nighttime as evident by the increased partitioning
292 of gas-phase WSOC to the particle-phase with increasing RH [El-Sayed *et al.*, 2015]. The study
293 by El-Sayed *et al.* [2015] found the increase in the fraction of total WSOC in the particle phase
294 (F_p) at the two highest RH levels (70-80%, >80%) to be statistically significant compared to the
295 F_p values at RH < 60%. The main focus of their work was to investigate if the uptake of gas-
296 phase WSOC to aerosol water occurs through reversible or irreversible pathways. The data
297 suggested the aqSOA was formed irreversibly. We investigate this with our data in section 3.3.2.

298 Figures 56 and S9 shows the correlation of WSOC vs. nitrate, oxalate, and sulfate for the
299 times of RH increasing. Nitrate and WSOC are strongly correlated only during the times of RH
300 increasing for Period A (~~Period A $R^2 = 0.71$ vs. Period B $R^2 = 0.18$~~). ~~This likely reflects the~~
301 ~~difference in ALW in the two periods as well since nitrate drives ALW concentrations [Hodas *et*~~
302 ~~*al.*, 2014].~~ Early morning nitrate peaks were observed at SPC during the first part of the study,
303 but were absent at the upwind Bologna site (Fig. 67). The occurrence of these peaks overlaps
304 with Period A. (Note, the nitrate event observed on 6 and 7 July during Period D will be
305 discussed in Sect. 3.4.) This additionally suggested that the nitrate formation or the ammonium-
306 nitrate-ammonia-nitric acid equilibrium at SPC was locally controlled since the back trajectory
307 analysis indicated both the SPC and Bologna sites were sampling similar upwind air masses to
308 each other in each period (Fig. 42). Therefore, the correlation with locally formed particulate
309 nitrate suggests local formation of WSOC. (Note, increased nitrate also results in higher ALW at
310 the same RH.) This argues that aqSOA formation was predominately local during Period A.

311 312 **3.3. Further Examination of Oxalate, Sulfate, and WSOC During Periods A and C**

313 **3.3.1. Oxalate and Sulfate**

314 To help better understand the potential for aqSOA formation, correlations with oxalate
315 and sulfate can be examined. Oxalate and sulfate are known tracers for aerosol formation

Formatted: Indent: First line: 0"

316 | through cloud processing [*Yu et al., 2005; Sorooshian et al., 2010*], although sulfate does also
317 | have a substantial, albeit slower, gas-phase formation pathway [*Seinfeld and Pandis, 2006*]. As
318 | shown in Fig. ~~7a-8a~~ and ~~7b-8b~~ for Periods A and **BC**, during both the times of RH increasing and
319 | decreasing, there is a positive linear relationship between oxalate and sulfate (R^2 ranged from
320 | 0.39 to 0.68). The association between oxalate and sulfate but not oxalate and WSOC in Period
321 | A suggests that the local aqSOA formed in wet aerosols during Period A has little effect on
322 | oxalate. This result supports the supposition that oxalate is not a universal marker for aqSOA; ~~it~~
323 | ~~is a tracer for chemistry in clouds rather than in wet aerosols [*Lim et al., 2010*]~~. This is further
324 | illustrated in our data by examining the correlation of oxalate vs. gas-phase glyoxal, a known
325 | precursor for aqSOA [*Tan et al., 2009; Ervens and Volkamer, 2010; Lim et al., 2010*], and ALW
326 | (Fig. ~~7e8c-f~~). Laboratory experiments suggest a relationship between oxalate and gas-phase
327 | glyoxal only when there is in-cloud processing as oligomers have been proposed to be the
328 | dominant products from processing in aerosol water when hydroxyl radical concentrations are on
329 | the order of 10^{-12} M [*Lim et al., 2010; Tan et al., 2010*]. Oxalate could be produced in aerosol
330 | water at lower hydroxyl radical concentrations, such as 10^{-13} M, due to insufficient organic
331 | radical concentrations for oligomer formation [*Lee et al., 2011*]. Although the hydroxyl radical
332 | concentrations are unknown, ~~there~~ there is only a relationship between oxalate and gas-phase glyoxal
333 | for Period **BC** during times of RH decreasing ($R^2 = 0.44$), which is when clouds were observed
334 | west of the site. In addition, ~~there~~ there is no important relationship observed between oxalate and
335 | ALW for either period (all $R^2 < 0.17$), ~~consistent with the expectation that the oxalate forms in~~
336 | ~~clouds, not in aerosol water.~~

Formatted: Font: Italic

Formatted: Superscript

Formatted: Superscript

Formatted: Font: Italic

337 | ~~3.3. Further Examination of WSOC During Periods A and B~~ **3.3.2. WSOC**

339 | The above analysis suggests that the majority of the WSOC observed during the first half
340 | of the study, as illustrated by Period A, is formed locally via chemistry in aerosol liquid water.
341 | Clearly, WSOC in the second half of the measurements appears to be different and to derive
342 | from different sources. As illustrated by Period **BC**, the WSOC during this time is likely more
343 | regional with contributions from gas-to-particle partitioning and possibly in-cloud aqSOA.

344 | To further explore this idea of different types of WSOC, the WSOC observations were
345 | compared to positive matrix factorization (PMF) analysis of the AMS OA data collected at SPC.
346 | Five factors, one HOA (hydrocarbon-like OA) and four OOA (oxygenated OA), were found.
347 | The four OOA factors include one semi-volatile type (OOA-1) and three low volatility types
348 | (OOA-2, OOA-3, and OOA-4). More details on the AMS ME-2 analysis can be found in the
349 | supporting information.

350 | As shown in Fig. ~~89~~, the measured WSOC from the first half of the study is dominated by
351 | OOA-2 and the second half by OOA-4. This can be further illustrated by looking at the
352 | correlation of WSOC vs. OOA-2 and OOA-4 during the times of RH increasing for Periods A
353 | and **BC** (Fig. ~~910~~). The WSOC in Period A is most strongly correlated with OOA-2 ($R^2 =$
354 | ~~0.8583~~) and in Period **BC** with OOA-4 ($R^2 = 0.64$).

355 | To estimate how each AMS ME-2 factor contributed to WSOC and what fraction of each
356 | factor was water-soluble, a multilinear regression analysis was tentatively performed using the
357 | method proposed by *Timonen et al.* [2013]. The results are shown in Table ~~3-S2~~ and Fig. ~~1011~~.
358 | This approach seeks to reproduce the total WSOC as a linear combination of the different
359 | factors, whilst minimizing the residuals and, unlike in *Timonen et al.* [2013], capping the
360 | individual factor contributions at 1 to allow conservation of the carbon mass. The regression

361 analysis was carried out with a zero intercept like in *Timonen et al.* [2013], as well as with a non-
362 zero intercept to account for possible instrumental biases between the AMS and PILS methods.
363 Only the four OOA factors were considered, while HOA was assumed to be completely
364 insoluble. All concentrations are in carbon mass units, which for the AMS factors were derived
365 from organic mass concentrations through factor-specific OM/OC ratios. The results of the
366 regression are reported for the whole PILS measurement period and also for Periods A and ~~B-C~~
367 separately.

368 The results for the whole measurement period indicate that the largest contributions to the
369 WSOC must be attributed to the OOA types which were simply the most abundant (OOA-3 and
370 OOA-4), but the water-soluble fractions as reflected in the regression coefficients were greatest
371 for OOA-2 and OOA-4 in agreement with their high correlation coefficients with WSOC.
372 Interestingly, OOA-2 and OOA-4 are also the factors possessing the highest O/C ratios (0.77 and
373 0.76, respectively), with respect to the other two (O/C = 0.48 for OOA-1 and 0.36 for OOA-3).
374 Therefore, in this study the factor-specific WSOC fractions seem related to the oxygen contents
375 measured by the AMS.

376 The multilinear regression analysis performed on the Period A measurements suggests
377 that the largest water-soluble fractions are exhibited by OOA-1 and OOA-2, whose
378 concentrations were observed to increase along with RH and WSOC for all the days in this
379 period of the campaign. Due to the very different absolute average concentrations, the second
380 factor (OOA-2) provided the largest contribution to WSOC, accounting for more than one third
381 of the total water-soluble organic carbon concentration. Interestingly, the diurnal trend of OOA-
382 1 indicated that its partitioning to the aerosol phase was largely reversible, and its concentrations
383 declined steeply in the late morning hours when RH and ALW decreased (Fig. 12a). ~~This can be
384 illustrated by the additional correlation of WSOC with OOA-1 during the times of RH increasing
385 for only Period A (Fig. 9a, $R^2 = 0.50$). This is not surprising given the high correlation between
386 OOA-1 and nitrate, which drives ALW in this region, during the whole measurement period (R^2
387 = 0.64).~~ In the same hours of the day, the OOA-2 concentrations were largely unaffected by RH
388 indicating (a) that OOA-2 mainly accounted for oxidized compounds stable in the aerosol phase
389 and (b) that boundary layer growth is not the reason for the decrease in OOA-1 as this should
390 have affected all factors. OOA-1 and OOA-2 can therefore be interpreted-hypothesized as two
391 aging stages of aqSOA formation during Period A.

392 Interestingly, some OOA-2 is also produced in Periods B and D. Although the
393 concentrations levels of OOA-2 observed are similar between Periods A and D, OOA-2
394 concentrations are much more sustained across the day in Period A. In addition, as illustrated in
395 the diurnal profiles for these periods (Fig. S10) the OOA-2 follows along more closely with
396 OOA-1, RH, and ALW in Periods B and D, likely due to the differences in meteorology and/or
397 chemistry of these periods compared to Period A. Regardless of these differences the
398 observations all still point to the strong relationship between OOA-1, OOA-2, and ALW.

399 The results obtained for Period ~~B-C~~ show again that the greatest coefficients (hence the
400 largest water-soluble fractions) were found for OOA-2 and OOA-4. However, due to its very
401 small concentrations in this period, OOA-2 provided a negligible contribution to WSOC (1%),
402 while OOA-4 was estimated to account for more than half of the WSOC carbon content. The
403 examination of time trends indicates that OOA-4 is mainly a background component of the
404 aerosol, showing no appreciable increase at the time when RH increased for a few hours on the
405 mornings of 5 and 6 July. Similar to Period A, here again the times when RH and ALW were

406 | high showed relatively high concentrations of OOA-1 (Fig. 12b), which represented an
407 | additional (though small compared to OOA-4) contribution to WSOC. Period C provides a case
408 | where significant OOA-1 is formed, but not OOA-2.

409 | Overall, whilst not without uncertainty, the above findings support the idea that two
410 | different types of WSOC occurred during these two different periods. They also support the idea
411 | that aqueous processing is dominating during the times of RH increasing during Period A and
412 | OOA-2 represented the most important component. The high O/C ratio of OOA-2 is expected
413 | for SOA formed through aqueous-phase reactions, because precursors are water-soluble and thus
414 | have low carbon numbers and high O/C ratios. Average O/C ratios of ~0.7 to 1.1 have been
415 | observed in the oligomeric products formed from laboratory experiments involving hydroxyl
416 | radical oxidation and/or aqueous photolysis of methylglyoxal, glycolaldehyde, and phenolic
417 | compounds [Altieri *et al.*, 2008; Tan *et al.*, 2009; Perri *et al.*, 2010; Sun *et al.*, 2010]. The high
418 | O/C ratios observed for the other main WSOC component, OOA-4, which dominates Period B,
419 | could be explained by extensive aging of non-aqueous SOA [Lambe *et al.*, 2011]. However, in-
420 | cloud aqueous-phase reactions could have occurred upwind of the Po Valley, as indicated by the
421 | occurrence of oxalate and clouds previously discussed. Our measurements are fully consistent,
422 | in indicating that OOA-4 was mainly transported to the site and was not a product of the local
423 | aqueous-phase heterogeneous chemistry in the Po Valley atmospheric surface layer.

424

425 | 3.4. Conditions for local aqSOA

426 | What leads to strong local aqSOA formation during Period A at SPC? High ALW was
427 | present throughout the study (Fig. 2b3b). It was observed that the days with the highest ALW
428 | also had the highest aerosol loading in the lowest layers of the atmosphere. However, no other
429 | day outside of Period A, except for 23 June, had a relationship of WSOC with RH during the
430 | times of RH increasing. This suggests that high ALW or aerosol loading alone are not sufficient
431 | for local aqSOA formation.

432 | As previously mentioned, during Period A early morning nitrate peaks were observed
433 | only at the SPC ground site and not at the urban site. However, just the presence of high nitrate
434 | (above 2 $\mu\text{g}/\text{m}^3$) does not seem to lead to aqSOA as no relationship of WSOC as a function of
435 | RH was observed on 6 and 7 July (Period D) when nitrate in concentrations similar to those of
436 | Period A were observed at SPC. Interestingly, the nitrate observed on these days was also
437 | observed in Bologna (Fig. 67). The timing of the peak nitrate concentration also differed from
438 | Period A; it occurred later in the morning, around 07:00 LT, whereas during Period A nitrate
439 | peaked around midnight or 01:00 LT and then again around 07:00 LT. This suggests that the
440 | presence and timing of elevated nitrate, which is a strong determinant of ALW, may be
441 | important for local aqSOA production and resulting WSOC aerosol concentrations in this region.

442 | As previously mentioned, An examination of possible gas-phase precursors (e.g.,
443 | aromatic VOCs and glyoxal, Table 1) shows no noticeable decline in concentration from the first
444 | to second half of the measurement period. Therefore, a possible explanation for the difference
445 | between Period A and Period B-the other period is meteorology. Period A featured an
446 | anticyclonic condition that led to air stagnation; Period B-the other periods featured stronger
447 | transport and ventilation. Therefore, during Periods B, C, and D intermediate products needed to
448 | form appreciable concentrations of aqSOA are less likely to quickly accumulate in the local
449 | boundary layer.

450 It is possible that another key ingredient in the chemistry is ammonia. Recent studies
451 have suggested possible aqSOA formation processes mediated by ammonia and other
452 atmospheric bases [Galloway *et al.*, 2009; Nozière *et al.*, 2009; Ortiz-Montalvo *et al.*, 2014; Yu *et*
453 *al.*, 2011]. Ammonia is prevalent in the Po Valley due to agricultural activities. During Period
454 A, high ammonia concentrations (greater than $\sim 30 \mu\text{g}/\text{m}^3$) were observed only at SPC (Fig.
455 [H13a](#)).

456 Overall, the data suggest that local aqSOA production during the stagnation of Period A
457 is not due to cloud processing. Our results also suggest that this aqueous chemistry occurs in the
458 dark, which likely provides the favorable low temperatures and high RH for nitrate aerosol and
459 ALW [Hodas *et al.*, 2014]. Based on other measurements at SPC, the stagnation conditions and
460 elevated nitrate around midnight occurred each day from 14 June through 23 June, suggesting
461 that the local aqSOA formation actually commenced five days earlier. When all these conditions
462 were met, each day $\sim 1 \mu\text{g C}/\text{m}^3$ of new WSOC (determined as the change in WSOC
463 concentration during the times of RH increasing) can be attributed to this process.
464

465 4. Summary

466 Measurements were conducted during the PEGASOS Study in the Po Valley of Italy
467 during June and July 2012 in San Pietro Capofiume (SPC). The goal was to look for evidence of
468 aqSOA in the ambient atmosphere. Measurements included near real-time WSOC (a good proxy
469 for SOA), inorganic anions/cations, and organic acids. The data were analyzed in terms of the
470 times when RH increased from 40 to ~~80~~70% (times of RH increasing) and then when the RH
471 decreased from ~~80-70~~ back to 40% (times of RH decreasing) in order to diminish influences from
472 dilution and mixing on ambient measurements. The analysis focused on ~~two-four~~ periods: Period
473 A on 19-21 June, ~~and~~ Period B on 30 June, 1-2 July, Period C on 3-5 July, and Period D on 6-7
474 July.

475 Evidence for local aqSOA formation in wet aerosols was observed during Period A.
476 When this occurred there was a correlation of WSOC with OA, ALW, RH, and nitrate.
477 Additionally, this was only observed during times of RH increasing, suggesting the aqSOA was
478 formed in the dark. The aqSOA formation is thought to be local because elevated nitrate, the
479 driver for aerosol water, was only observed at the main ground site in SPC even though the
480 auxiliary site in Bologna was sampling similar upwind air masses at the time.

481 A comparison of Periods A and C suggested Period ~~CB~~ differed from Period A. The
482 WSOC during Period ~~B-C~~ was likely formed regionally. Interestingly, during Period ~~B-C~~ as well
483 as Period A a correlation was found between oxalate and sulfate. This suggests that oxalate
484 concentrations were not strongly affected by local aqSOA formation. More importantly, it
485 indicates that oxalate is not a good universal marker for aqSOA. ~~It is probably better for~~
486 ~~observing aqSOA produced in clouds, which were present west of SPC only in Period B.~~

487 A comparison of WSOC with the AMS PMF OOA factors showed that Period A featured
488 high O/C ratios, consistent with aqSOA formation. However, they also reinforce the conclusion
489 that the composition of the WSOC differed between ~~Periods A and B~~ the two halves of the study.
490 Periods A and ~~B-C~~ were dominated by two different OOA factors, OOA-2 (locally produced)
491 and OOA-4 (long-range transported), respectively.

492 Overall, by examining the conditions observed in Period A, the data suggest that the local
493 aqSOA formation observed is not due to cloud processing and occurs in the dark. The timing of
494 elevated nitrate concentrations is critical (around midnight local time) to provide the liquid water

495 reservoir needed for aqueous chemistry. Approximately $1 \mu\text{g C/m}^3$ of new WSOC was formed
496 through this process each day these conditions were met, indicating the importance of aqSOA as
497 a source of ambient OA in this region.

498

499 **Acknowledgements**

500 We acknowledge funding from the National Science Foundation under Projects AGS-1050052,
501 AGS-1052611, and AGS-1051338. Measurements at SPC were also funded by the European
502 Union FP7 project PEGASOS (FP7-ENV-2010/265148) and by the Regione Emilia Romagna
503 (project SUPERSITO DRG n. 428/10). The authors thank the European Union FP7 ÉCLAIRE
504 (FP7-ENV-2011/282910) project for funding the ammonia measurements in Bologna, the
505 Energy Research Centre of the Netherlands (ECN) for providing the MARGA instrument at
506 SPC, and C. DiMarco, M. Blom, S. Leeson, T. Hutchings, C. Braban, and L. Giulianelli for
507 supporting the ammonia measurements. The authors gratefully acknowledge the NOAA Air
508 Resources Laboratory (ARL) for the provision of the HYSPLIT transport and dispersion model
509 and/or READY website (<http://www.arl.noaa.gov/ready.html>) used in this publication.

510

511

512

513

514

515

516

517

518

519

520

521

522

523

524

525

526

527

528

529

530

531

532

533

534

535

536

537

538

539

540 **References**

- 541 Aiken, A.C., DeCarlo, P.F., Kroll, J.H., Worsnop, D.R., Huffman, J.A., Docherty, K.S., Ulbrich,
542 I.M., Mohr, C., Kimmel, J.R., Sueper, D., Sun, Y., Zhang, Q., Trimborn, A., Northway,
543 M., Ziemann, P.J., Canagaratna, M.R., Onasch, T.B., Alfarra, M.R., Prévôt, A.S.,
544 Dommen, J., Duplissy, J., Metzger, A., Baltensperger, U., and Jimenez, J.L.: O/C and
545 OM/OC ratios of primary, secondary, and ambient organic aerosols with high-resolution
546 time-of-flight aerosol mass spectrometry, *Environ. Sci. Technol.*, *42*, 4478-4485, 2008.
547
- 548 Altieri, K.E., A.G. Carlton, H.-J. Lim, B.J. Turpin, and S.P. Seitzinger, Evidence for oligomer
549 formation in clouds: Reactions of isoprene oxidation products, *Environ. Sci. Technol.*, *40*,
550 4956-4960, 2006.
551
- 552 Altieri, K., S.P. Seitzinger, A.G. Carlton, B.J. Turpin, G.C. Klein, and A.G. Marshall, Oligomers
553 formed through in-cloud methylglyoxal reactions: Chemical composition, properties, and
554 mechanisms investigated by ultra-high resolution FT-ICR Mass Spectrometry, *Atmos.*
555 *Environ.*, *42*, 1476-1490, 2008.
556
- 557 Blando, J.D. and B.J. Turpin, Secondary Organic Aerosol Formation in Cloud and Fog Droplets:
558 A Literature Evaluation of Plausibility, *Atmos. Environ.*, *34*, 1623-1632, 2000.
559
- 560 Canagaratna, M.R., J.T. Jayne, J.L. Jimenez, J.D. Allan, M.R. Alfarra, Q. Zhang, T.B. Onasch, F.
561 Drewnick, H. Coe, A. Middlebrook, A. Delia, L.R. Williams, A.M. Trimborn, M.J.
562 Northway, P.F. DeCarlo, C.E. Kolb, P. Davidovits, and D.R. Worsnop, Chemical and
563 Microphysical Characterization of Ambient Aerosols with the Aerodyne Aerosol Mass
564 Spectrometer, *Mass Spectrometry Reviews*, *26*, 185-222, 2007.
565
- 566 Canonaco, F., M. Crippa, J.G. Slowik, U. Baltensperger, and A.S.H. Prévôt, SoFi, an Igor-based
567 interface for the efficient use of the generalized multilinear engine (ME-2) for the source
568 apportionment: ME-2 application to aerosol mass spectrometer data, *Atmos. Meas. Tech.*,
569 *6*, 3649-3661, doi:10.5194/amt-6-3649-2013, 2013.
570
- 571 Carlton, A.G., B.J. Turpin, K.E. Altieri, A. Reff, S. Seitzinger, H. Lim, and B. Ervens,
572 Atmospheric oxalic acid and SOA production from glyoxal: Results of aqueous
573 photooxidation experiments, *Atmos. Environ.*, *41*, 7588-7602, 2007.
574
- 575 DeCarlo, P.F., J.R. Kimmel, A. Trimborn, M.J. Northway, J.T. Jayne, A.C. Aiken, M. Gonin, K.
576 Fuhrer, T. Horvath, K.S. Docherty, D.R. Worsnop, and J.L. Jimenez, Field-Deployable,
577 High-Resolution, Time-of-Flight Aerosol Mass Spectrometer, *Anal. Chem.*, *78*, 8281-
578 8289, 2006.
579
- 580 de Gouw, J.A., Middlebrook, A.M., Warneke, C., Goldan, P.D., Kuster, W.C., Roberts, J.M.,
581 Fehsenfeld, F.C., Worsnop, D.R., Canagaratna, M.R., Pszenny, A.A.P., Keene, W.C.,
582 Marchewka, M., Bertman, S.B., and Bates, T.S.: Budget of organic carbon in a polluted
583 atmosphere: Results from the New England Air Quality Study in 2002, *J. Geophys. Res.*,
584 *110*, D16305, doi:10.1029/2004JD005623, 2005.

585
586 de Haan, D.O., A.L. Corrigan, M.A. Tolbert, J.L. Jimenez, S.E. Wood, and J.J. Turley,
587 Secondary organic aerosol formation by self-reaction of methylglyoxal and glyoxal in
588 evaporating droplets, *Environ. Sci. Technol.*, *43*, 8184 -8190, 2009.
589
590 Draxler, R.R. and G.D. Rolph, HYSPLIT (HYbrid Single-Particle Lagrangian Integrated
591 Trajectory) Model access via NOAA ARL READY Website, available at:
592 <http://www.arl.noaa.gov/ready/hysplit4.html> (last access: 5 August 2013), NOAA Air
593 Resources Laboratory, Silver Spring, MD, 2013.
594
595 Drewnick, F., S.S. Hings, P. DeCarlo, J.T. Jayne, M. Gonin, K. Fuhrer, S. Weimer, J.L. Jimenez,
596 K.L. Demerjian, S. Borrmann, and D.R. Worsnop, A New Time-of-Flight Aerosol Mass
597 Spectrometer (TOF-AMS) – Instrument Description and First Field Deployment, *Aerosol*
598 *Sci. Technol.*, *39*, 637-658, 2005.
599
600 Eatough, D.J., A. Wadsworth, D.A. Eatough, J.W. Crawford, L.D. Hansen, and E.A. Lewis, A
601 multiple system, multi-channel diffusion denuder sampler for the determination of fine-
602 particulate organic material in the atmosphere, *Atmos. Environ. A-Gen.*, *27*, 1213-1219,
603 1993.
604
605 El-Sayed, M.M.H., Y. Wang, and C.J. Hennigan, Direct atmospheric evidence for the
606 irreversible formation of aqueous secondary organic aerosol, *Geophys. Res. Lett.*, *42*,
607 doi:10.1002/2015GL064556, 2015.
608
609 Ersiman, J.W., R. Otjes, A. Hensen, P. Jongejan, P. van den Bulk, A. Khlystov, H. Möls, and S.
610 Slanina, Instrument development and application in studies and monitoring of ambient
611 ammonia, *Atmos. Environ.*, *35*, 1913-1922, 2001.
612
613 Ervens, B., B.J. Turpin, and R.J. Weber, Secondary organic aerosol formation in cloud droplets
614 and aqueous particles (aqSOA): a review of laboratory, field and model studies, *Atmos.*
615 *Chem. Phys.*, *11*, 11069-11102, doi:10.5194/acp-11-11069-2011, 2011.
616
617 Ervens, B. and R. Volkamer, Glyoxal processing by aerosol multiphase chemistry: towards a
618 kinetic modeling framework of secondary formation in aqueous particles, *Atmos. Chem.*
619 *Phys.*, *10*, 8219-8244, doi:10.5194/acp-10-8219-2010, 2010.
620
621 Facchini, M.C., S. Fuzzi, S. Zappoli, A. Andracchio, A. Gelencsér, G. Kiss, Z. Krivácsy, E.
622 Mészáros, H.C. Hansson, T. Alsberg, and Y. Zebühr, Partitioning of the organic aerosol
623 component between fog droplets and interstitial aerosol, *J. Geophys. Res.*, *104*, 26821-
624 26832, 1999.
625
626 Fuzzi, S., M.C. Facchini, S. Decesari, E. Matta, and M. Mircea, Soluble organic compounds in
627 fog and cloud droplets: What have we learned over the past few years?. *Atmos. Res.*, *64*,
628 89-98, 2002.
629

630 Galloway, M.M., P.S. Chhabra, A.W.H. Chan, J.D. Surratt, R.C. Flagan, J.H. Seinfeld, and F.N.
631 Keutsch, Glyoxal uptake on ammonium sulphate seed aerosol: Reaction products and
632 reversibility of uptake under dark and irradiated conditions, *Atmos. Chem. Phys.*, *9*, 3331-
633 3345, 2009.

634
635 Gaston, C.J., T.P. Riedel, Z. Zhang, A. Gold, J.D. Surratt, and J.A. Thornton, Reactive Uptake of
636 an Isoprene-Derived Epoxydiol to Submicron Aerosol Particles, *Environ. Sci. Technol.*,
637 *48*, 11178-11186, 2014.

638
639 Heald, C.L., D.J. Jacob, R.J. Park, L.M. Russell, B.J. Huebert, J.H. Seinfeld, H. Liao, and R.J.
640 Weber, A large organic aerosol source in the free troposphere missing from current
641 models, *Geophys. Res. Lett.*, *32*, L18809, doi:10.1029/2005GL023831, 2005.

642
643 Hennigan, C.J., M.H. Bergin, J.E. Dibb, and R.J. Weber, Enhanced secondary organic aerosol
644 formation due to water uptake by fine particles, *Geophys. Res. Lett.*, *35*, L18801,
645 doi:10.1029/2008GL035046, 2008.

646
647 Hodas, N., A.P. Sullivan, K. Skog, F.N. Keutsch, J.L. Collett, Jr., S. Decesari, M.C. Facchini,
648 A.G. Carlton, A. Laaksonen, and B.J. Turpin, Aerosol liquid water driven by
649 anthropogenic nitrate: implications for lifetimes of water-soluble organic gases and
650 potential for secondary aerosol formation, *Environ. Sci. Technol.*, *48*, 11127-11136,
651 2014.

652
653 Huisman, A.J., J.R. Hottle, K.L. Coens, J.P. DiGangi, M.M. Galloway, A. Kammrath, and F.N.
654 Keutsch, Laser-Induced Phosphorescence for the in Situ Detection of Glyoxal at Part per
655 Trillion Mixing Ratios, *Anal. Chem.*, *80*, 5884-5891, 2008.

656
657 Kanakidou, M., et al., Organic aerosol and global climate modelling: a review, *Atmos. Chem.*
658 *Phys.*, *5*, 1053-1123, doi:10.5194/acp-5-1053-2005, 2005.

659
660 Kondo, Y., Y. Miyazaki, N. Takegawa, T. Miyakawa, R.J. Weber, J.L. Jimenez, Q. Zhang, and
661 D.R. Worsnop, Oxygenated and water-soluble organic aerosols in Tokyo, *J. Geophys.*
662 *Res.*, *112*, D01203, doi:10.1029/2006JD007056, 2007.

663
664 [Lee, A.K.Y., K.L. Hayden, P. Herckes, W.R. Leitch, J. Liggio, A.M. Macdonald, and J.P.D.](#)
665 [Abbatt, Characterization of aerosol and cloud water at a mountain site during WACS](#)
666 [2010: Secondary organic aerosol formation through oxidative cloud processing, *Atmos.*](#)
667 [*Chem. Phys.*, *12*, 7103-7116, doi:10.5194/acp-12-7103-2012, 2012.](#)

668
669 [Lee, A.K.Y., R. Zhao, S.S. Gao, and J.P.D. Abbatt, Aqueous-phase OH Oxidation of Glyoxal:](#)
670 [Application of a Novel Analytical Approach Employing Aerosol Mass Spectrometry and](#)
671 [Complementary Off-Line Techniques, *Journal of Physical Chemistry A*, *115*, 10517-](#)
672 [10526, dx.doi.org/10.1021/jp204099g, 2011.](#)

673

674 Lim, Y.B., Y. Tan, M.J. Perri, S.P. Seitzinger, and B.J. Turpin, Aqueous Chemistry and its Role
675 in Secondary Organic Aerosol (SOA) Formation, *Atmos. Chem. Phys.*, *10*, 10521-10539,
676 doi:10.5194/acp-10-10521-2010, 2010.
677

678 Lambe, A.T., T.B. Onasch, P. Massoli, D.R. Croasdale, J.P. Wright, A.T. Ahern, L.R. Williams,
679 D.R. Worsnop, W.H. Brune, and P. Davidovits, Laboratory studies of the chemical
680 composition and cloud condensation nuclei (CCN) activity of secondary organic aerosol
681 (SOA) and oxidized primary organic aerosol (OPOA), *Atmos. Chem. Phys.*, *11*, 8913–
682 8928, 2011.
683

684 Miyazaki, Y., Y. Kondo, N. Takegawa, Y. Komazaki, K. Kawamura, M. Mochida, K. Okuzawa,
685 and R.J. Weber, Time-resolved measurements of water-soluble organic carbon in Tokyo,
686 *J. Geophys. Res.*, *111*, D23206, doi:10.1029/2006JD007125, 2006.
687

688 Monge, M.E., T. Rosenørn, O. Favez, M. Müller, G. Adler, A.A. Riziq, Y. Rudich, H. Herrmann,
689 C. George, and B. D’Anna, Alternative pathway for atmospheric particles growth, *PNAS*,
690 *109*, 6840-6844, doi:10.1073/pnas.1120593109, 2012.
691

692 Nguyen, T.B., P.B. Lee, K.M. Updyke, D.L. Bones, J. Laskin, A. Laskin, and S.A. Nizkorodov,
693 Formation of nitrogen- and sulfur-containing light-absorbing compounds accelerated by
694 evaporation of water from secondary organic aerosols, *J. Geophys. Res.*, *117*, D01207,
695 doi:10.1029/2011JD016944, 2012.
696

697 Nozière, B., P. Dziedzic, and A. Córdoba, Products and Kinetics of the Liquid-Phase Reaction of
698 Glyoxal Catalyzed by Ammonium Ions (NH₄⁺), *J. Phys. Chem. A*, *113*, 231-237, 2009.
699

700 Orsini, D.A., Y. Ma, A. Sullivan, B. Sierau, K. Baumann, and R.J. Weber, Refinements to the
701 particle-into-liquid sampler (PILS) for ground and airborne measurements of water-
702 soluble aerosol composition, *Atmos. Environ.*, *37*, 1243-1259, 2003.
703

704 Ortiz-Montalvo, D.L., S.A.K. Häkkinen, A.N. Schwier, Y.B. Lim, V.F. McNeill, and B.J.
705 Turpin, Ammonium Addition (and Aerosol pH) Has a Dramatic Impact on the Volatility
706 and Yield of Glyoxal Secondary Organic Aerosol, *Environ. Sci. Technol.*, *48*, 255-262,
707 2014.
708

709 Paatero, P., The multilinear engine – A table-driven, least squares program for solving
710 multilinear problems, including the n-way parallel factor analysis model, *J. Comput.*
711 *Graph. Stat.*, *8*, 854-888, 1999.
712

713 Perri, M.J., Y.B. Lim, S.P. Seitzinger, and B.J. Turpin, Organosulfates from glycolaldehyde in
714 aqueous aerosols and clouds: Laboratory studies, *Atmos. Environ.*, *44*, 2658-2664, 2010.
715

716 Rolph, G.D., Real-time Environmental Applications and Display sYstem (READY) Website,
717 available at: <http://www.arl.noaa.gov/ready/hysplit4.html> (last access: 5 August 2013),
718 NOAA Air Resources Laboratory, Silver Spring, MD, 2013.

719
720 Seinfeld, J.H. and S.N. Pandis, *Atmospheric Chemistry and Physics: From Air Pollution to*
721 *Climate Change*, John Wiley, Hoboken, NJ, 2006.
722
723 Seinfeld, J.H. and J.F. Pankow, Organic atmospheric particulate material, *Annu. Rev. Phys.*
724 *Chem.*, *54*, 121-140, 2003.
725
726 Sorooshian, A., S.M. Murphy, S. Hersey, R. Bahreini, H. Jonsson, R.C. Flagan, and J.H.
727 Seinfeld, Constraining the contribution of organic acids and AMS m/z 44 to the organic
728 aerosol budget: On the importance of meteorology, aerosol hygroscopicity, and region,
729 *Geophys. Res. Lett.*, *37*, L21807, doi:10.1029/2010GL044951, 2010.
730
731 Sullivan, A.P., R.E. Peltier, C.A. Brock, J.A. de Gouw, J.S. Holloway, C. Warneke, A.G.
732 Wollny, and R.J. Weber, Airborne measurements of carbonaceous aerosol soluble in
733 water over northeastern United States: Method development and an investigation into
734 water-soluble organic carbon sources, *J. Geophys. Res.*, *111*, D23S46,
735 doi:10.1029/2006JD007072, 2006.
736
737 Sullivan, A.P., R.J. Weber, A.L. Clements, J.R. Turner, M.S. Bae, and J.J. Schauer, A method
738 for on-line measurement of water-soluble organic carbon in ambient aerosol particles:
739 Recent results from an urban site, *Geophys. Res. Lett.*, *31*, L13105,
740 doi:10.1029/2004GL019681, 2004.
741
742 Sun, Y.L., Q. Zhang, C. Anastasio, and J. Sun, Insights into secondary organic aerosol formed
743 via aqueous-phase reactions of phenolic compounds based on high resolution mass
744 spectrometry, *Atmos. Chem. Phys.*, *10*, 4809-4822, doi:10.5194/acp-10-4809-2010, 2010.
745
746 Tan, Y., A.G. Carlton, S.P. Seitzinger, and B.J. Turpin, SOA from Methylglyoxal in Clouds and
747 Wet Aerosols: Measurement and Prediction of Key Products, *Atmos. Environ.*, *44*, 5218-
748 5226, 2010.
749
750 Tan, Y., Y.B. Lim, K.E. Altieri, S. Seitzinger, and B.J. Turpin, Mechanisms leading to oligomers
751 and SOA through aqueous photooxidation: Insights from OH radical oxidation of acetic
752 acid and methylglyoxal, *Atmos. Chem. Phys.*, *12*, 801-813, doi:10.5194/acp-12-801-2012,
753 2012.
754
755 Tan, Y., M.J. Perri, S.P. Seitzinger, and B.J. Turpin, Effects of Precursor Concentration and
756 Acidic Sulfate in Aqueous Glyoxal-OH Radical Oxidation and Implications for
757 Secondary Organic Aerosol, *Environ. Sci. Technol.*, *43*, 8105-8112, 2009.
758
759 ten Brink, H., R. Otjes, P. Jongejan, and S. Slanina, An instrument for semi-continuous
760 monitoring of the size-distribution of nitrate, ammonium, sulphate and chloride in
761 aerosol, *Atmos. Environ.*, *41*, 2768-2779, 2007.
762
763 Timonen, H., S. Carbone, M. Aurela, K. Saarnio, S. Saarikoski, N.L. Ng, M.R. Canagaratna, M.

764 Kulmala, V.-M. Kerminen, D.R. Worsnop, and R. Hillamo, Characteristics, sources and
765 water-solubility of ambient submicron organic aerosol in springtime in Helsinki, Finland,
766 *J. Aerosol Sci.*, *56*, 61-77, 2013.
767
768 Wexler, A.S. and S.L. Clegg, Atmospheric aerosol models for systems including the ions H^+ ,
769 NH_4^+ , Na^+ , SO_4^{2-} , NO_3^- , Cl^- , Br^- , and H_2O , *J. Geophys. Res.*, *107*, D14, 4207,
770 doi:10.1029/2001JD000451, 2002.
771
772 Yu, G., A.R. Bayer, M.M. Galloway, K.J. Korshavn, C.G. Fry, and F.N. Keutsch, Glyoxal in
773 Aqueous Ammonium Sulfate Solutions: Products, Kinetics, and Hydration Effects,
774 *Environ. Sci. Technol.*, *45*, 6336-6342, 2011.
775
776 [Yu, J.Z., X.H.H. Huang, J. Xu, and M. Hu, When aerosol sulfate goes up, so does oxalate:
777 Implications for the formation mechanisms of oxalate, *Environ. Sci. Technol.*, *39*, 128-
778 133, 2005.](#)
779
780 Zhang, X., J. Liu, E.T. Parker, P.L. Hayes, J.L. Jimenez, J.A. de Gouw, J.H. Flynn, N.
781 Grossberg, B.L. Lefer, and R.J. Weber, On the gas-particle partitioning of soluble organic
782 aerosol in two urban atmospheres with contrasting emissions: 1. Bulk water-soluble
783 organic carbon, *J. Geophys. Res.*, *117*, D00V16, doi:10.1029/2012JD017908, 2012.
784
785 Zhou, Y., H. Zhang, H.M. Parikh, E.H. Chen, W. Rattanavaraha, E.P. Rosen, W. Wang, and
786 R.M. Kamens, Secondary organic aerosol formation from xylenes and mixtures of
787 toluene and xylenes in an atmospheric urban hydrocarbon mixture: Water and particle
788 seed effects (II), *Atmos. Environ.*, *45*, 3882-3890, 2011.
789
790
791
792
793
794
795
796
797
798
799
800
801
802
803
804
805
806
807
808

809
810
811
812
813
814
815
816
817
818
819
820
821
822
823
824
825
826
827
828
829
830
831
832
833
834
835
836
837
838
839
840
841
842
843
844
845
846
847
848
849
850
851
852
853

Figure Captions

Figure 1. Left panel: characteristic 72 h air mass back trajectories for (a) Period A and (b) Period B at the PEGASOS ground sites of Bologna and SPC. All back trajectories are based on the NOAA ARL HYSPLIT trajectory model. Right panel: maps Maps created using Google Earth (version 7.1.5.1557) to show the areas surrounding the (ae) Bologna and (be) SPC sampling sites.

Figure 2. Characteristic 72 h air mass back trajectories for (a) Period A, (b) Period B, (c) Period C, and (d) Period D at the PEGASOS ground sites of Bologna and SPC. All back trajectories are based on the NOAA ARL HYSPLIT trajectory model.

Figure 23. Times series of hourly averaged measured (a) WSOC, ~~and~~ (b) calculated ALW, (c) RH, and (d) Temperature at SPC. Any gaps in ALW are due to missing PILS-IC data. The dashed vertical lines indicate midnight local time (UTC+2). Periods A, ~~and~~ B, C, and D are also indicated.

Figure 34. Hourly averaged WSOC as a function of RH for (a) Periods A and CB and (b) Periods B and D during the times of RH (a) increasing and (cb) Periods A and C and (d) Periods B and D during the times of RH decreasing at SPC. The WSOC was binned into 10% RH bands starting at 40% RH. The error bars represent the standard deviation at each bin. Numbers above or below points represent the number of data points in each bin.

Figure 45. Correlation of hourly averaged WSOC vs. OA for (a) Period A and (b) Period BC, ALW for (c) Period A and (d) Period BC, and RH for (e) Period A and (f) Period B-C at SPC. All plots are for during the times of RH increasing.

Figure 56. Correlation of hourly averaged WSOC vs. nitrate for (a) Period A and (b) Period BC, oxalate for (c) Period A and (d) Period BC, and sulfate for (e) Period A and (f) Period B-C at SPC. All plots are for during the times of RH increasing.

Figure 67. Times series of hourly averaged AMS nitrate observed at (a) SPC and (b) Bologna. The dashed vertical lines indicate midnight local time (UTC+2). Periods A, ~~and~~ B, C, and D are also indicated.

854
855 | **Figure 78.** Correlation of hourly averaged oxalate vs. sulfate for Periods A and ~~B~~-C during the
856 | times of RH (a) increasing and (b) decreasing, gas-phase glyoxal for Periods A and ~~B~~-C during
857 | the times of RH (c) increasing and (d) decreasing, and ALW for Periods A and ~~B~~-C during the
858 | times of RH (e) increasing and (f) decreasing at SPC.

859
860 | **Figure 89.** Times series of hourly averaged WSOC with AMS ME-2 factors (a) OOA-1, (b)
861 | OOA-2, (c) OOA-3, and (d) OOA-4 at SPC. The units for each factor have been converted from
862 | $\mu\text{g}/\text{m}^3$ to $\mu\text{g C}/\text{m}^3$ using their calculated OM/OC ratio (OOA-1 = 1.81, OOA-2 = 2.15, OOA-3 =
863 | 2.13, and OOA-4 = 1.62). The dashed vertical lines indicate midnight local time (UTC+2).
864 | Periods A, ~~and~~ B, C, and D are also indicated.

865
866 | **Figure 910.** Correlation of hourly averaged WSOC vs. AMS ME-2 factors OOA-1 for (a)
867 | Period A and (b) Period ~~B~~-C, OOA-2 for (c) Period A and (d) Period ~~B~~-C, OOA-3 for (e) Period A
868 | and (f) Period ~~B~~-C, and OOA-4 for (g) Period A and (h) Period ~~B~~-C at SPC. All plots are for
869 | during the times of RH increasing.

870
871 | **Figure 1011.** Time series of hourly averaged AMS ME-2 OOA factors, WSOC measured, and
872 | WSOC reconstructed for the whole measurement period (top), Period A (bottom left), and Period
873 | ~~B~~-C (bottom right) at SPC. The units for each OOA factor have been converted from $\mu\text{g}/\text{m}^3$ to
874 | $\mu\text{g C}/\text{m}^3$ using their calculated OM/OC ratio.

875
876 | **Figure 12.** Diurnal profile of WSOC, OOA-1, OOA-2, RH, temperature, ALW, and nitrate for
877 | (a) Period A and (b) Period C at SPC.

878
879 | **Figure 1113.** Times series of hourly averaged ammonia observed at (a) SPC and (b) Bologna.
880 | The dashed lines indicate midnight local time (UTC+2). Periods A, ~~and~~ B, C, and D are also
881 | indicated.

882
883

Table 1. Average concentrations of aerosol and gas-phase species along with various meteorological parameters observed during the times of RH increasing and decreasing during Periods A, and Period B, C, and D at SPC.

	OA ($\mu\text{g}/\text{m}^3$)	WSOC ($\mu\text{g}/\text{C}/\text{m}^3$)	Glycolate ($\mu\text{g}/\text{m}^3$)	Acetate ($\mu\text{g}/\text{m}^3$)	Formate ($\mu\text{g}/\text{m}^3$)	Chloride ($\mu\text{g}/\text{m}^3$)	Sulfate ($\mu\text{g}/\text{m}^3$)	Oxalate ($\mu\text{g}/\text{m}^3$)	Nitrate ($\mu\text{g}/\text{m}^3$)	Ozone ($\mu\text{g}/\text{m}^3$)	NO _x ($\mu\text{g}/\text{m}^3$)	SO ₂ (ppb)	Benzene ($\mu\text{g}/\text{m}^3$)	Toluene ($\mu\text{g}/\text{m}^3$)	Xylene ($\mu\text{g}/\text{m}^3$)	Glyoxal (ppb)	T (°C)	RH (%)
Period A RH Increasing	8.93	4.73	0.28	0.40	0.43	0.13	3.49	0.24	2.91	47.42	28.90	0.65	0.21	1.21	0.26	0.05	24.47	64.49
Period A RH Decreasing	9.63	5.09	0.30	0.33	0.47	0.17	3.23	0.23	5.61	63.70	17.75	1.14	0.27	1.78	0.34	0.09	26.09	57.66
Period B RH Increasing	2.05	1.55	0.24	0.28	0.23	0.11	2.80	0.13	1.18	61.29	9.72	0.40	0.17	1.18	0.40	0.05	23.31	60.60
Period B RH Decreasing	2.01	1.54	0.22	0.32	0.23	0.10	2.75	0.12	1.28	75.40	8.08	0.51	0.17	1.11	0.44	0.07	25.02	53.88
	OA ($\mu\text{g}/\text{m}^3$)	WSOC ($\mu\text{g}/\text{C}/\text{m}^3$)	Glycolate ($\mu\text{g}/\text{m}^3$)	Acetate ($\mu\text{g}/\text{m}^3$)	Formate ($\mu\text{g}/\text{m}^3$)	Chloride ($\mu\text{g}/\text{m}^3$)	Sulfate ($\mu\text{g}/\text{m}^3$)	Oxalate ($\mu\text{g}/\text{m}^3$)	Nitrate ($\mu\text{g}/\text{m}^3$)	Sodium ($\mu\text{g}/\text{m}^3$)	Ammonium ($\mu\text{g}/\text{m}^3$)	Potassium ($\mu\text{g}/\text{m}^3$)	Magnesium ($\mu\text{g}/\text{m}^3$)	Calcium ($\mu\text{g}/\text{m}^3$)	ALW ($\mu\text{g}/\text{m}^3$)			
Period A RH Increasing	8.93	4.73	0.28	0.40	0.43	0.13	3.49	0.24	2.91	NA	NA	NA	NA	NA	6.81			
Period A RH Decreasing	9.63	5.09	0.30	0.33	0.47	0.17	3.23	0.23	5.61	NA	NA	NA	NA	NA	7.29			
Period B RH Increasing	4.06	2.87	0.22	0.24	0.24	0.09	3.22	0.12	1.67	0.01	1.04	0.43	0.10	0.37	4.21			
Period B RH Decreasing	3.78	2.89	0.22	0.24	0.23	0.09	2.69	0.11	1.56	0.01	1.04	0.48	0.09	0.13	4.34			
Period C RH Increasing	2.05	1.55	0.24	0.28	0.23	0.11	2.80	0.13	1.18	0.04	0.92	0.51	0.11	0.26	2.89			
Period C RH Decreasing	2.01	1.54	0.22	0.32	0.23	0.10	2.75	0.12	1.28	0.04	0.94	0.54	0.09	0.06	2.64			
Period D RH Increasing	2.89	1.92	0.17	0.18	0.21	0.11	3.38	0.12	1.31	0.02	1.07	0.48	0.10	0.32	4.10			
Period D RH Decreasing	3.02	1.99	0.19	0.19	0.24	0.14	4.89	0.13	3.56	0.03	2.00	0.55	0.10	0.20	7.90			

	Ozone ($\mu\text{g}/\text{m}^3$)	NO _x ($\mu\text{g}/\text{m}^3$)	SO ₂ (ppb)	Benzene ($\mu\text{g}/\text{m}^3$)	Toluene ($\mu\text{g}/\text{m}^3$)	Xylene ($\mu\text{g}/\text{m}^3$)	Glyoxal (ppb)	T (°C)	RH (%)
--	---------------------------------------	---	--------------------------	---	---	--	------------------	--------	--------

Period A RH Increasing	<u>47.42</u>	<u>28.90</u>	<u>0.65</u>	<u>0.21</u>	<u>1.21</u>	<u>0.26</u>	<u>0.05</u>	<u>24.47</u>	<u>64.49</u>
Period A RH Decreasing	<u>63.70</u>	<u>17.75</u>	<u>1.14</u>	<u>0.27</u>	<u>1.78</u>	<u>0.34</u>	<u>0.09</u>	<u>26.09</u>	<u>57.66</u>
Period B RH Increasing	<u>76.6</u>	<u>10.94</u>	<u>0.68</u>	<u>0.19</u>	<u>0.83</u>	<u>0.53</u>	<u>0.06</u>	<u>26.74</u>	<u>60.87</u>
Period B RH Decreasing	<u>51.6</u>	<u>9.30</u>	<u>0.69</u>	<u>0.29</u>	<u>1.43</u>	<u>0.66</u>	<u>0.07</u>	<u>26.2</u>	<u>61.20</u>
Period C RH Increasing	<u>61.29</u>	<u>9.72</u>	<u>0.40</u>	<u>0.17</u>	<u>1.18</u>	<u>0.40</u>	<u>0.05</u>	<u>23.31</u>	<u>60.60</u>
Period C RH Decreasing	<u>75.40</u>	<u>8.08</u>	<u>0.51</u>	<u>0.17</u>	<u>1.11</u>	<u>0.44</u>	<u>0.07</u>	<u>25.02</u>	<u>53.88</u>
Period D RH Increasing	<u>87.21</u>	<u>8.93</u>	<u>0.30</u>	<u>0.12</u>	<u>0.52</u>	<u>0.23</u>	<u>0.05</u>	<u>25.63</u>	<u>63.45</u>
Period D RH Decreasing	<u>93.73</u>	<u>5.12</u>	<u>0.38</u>	<u>0.15</u>	<u>0.85</u>	<u>0.28</u>	<u>0.07</u>	<u>27.32</u>	<u>54.92</u>

Table 2. Equations for each of the linear regression plots shown in Figs. 4, 5, 7, and 9. Uncertainties with the least square regressions are one standard deviation.

Figure	Linear Regression Equation
4a	$y = 0.476x \pm 0.039 - 0.345 \pm 0.357$
4b	$y = 0.614x \pm 0.084 + 0.300 \pm 0.177$
4c	$y = 0.167x \pm 0.023 + 2.825 \pm 0.174$
4d	$y = 0.183x \pm 0.108 + 0.962 \pm 0.321$
4e	$y = 0.047x \pm 0.010 + 0.898 \pm 0.687$
4f	$y = -0.003x \pm 0.010 + 1.711 \pm 0.595$
5a	$y = 0.469x \pm 0.060 + 2.574 \pm 0.192$
5b	$y = 0.824x \pm 0.441 + 0.512 \pm 0.527$
5c	$y = 9.024x \pm 3.560 + 1.753 \pm 0.872$
5d	$y = 22.095x \pm 2.990 - 1.354 \pm 0.387$
5e	$y = 0.297x \pm 0.187 + 2.902 \pm 0.667$
5f	$y = 0.276x \pm 0.124 + 0.718 \pm 0.354$
7a	Period A $y = 0.040x \pm 0.007 + 0.097 \pm 0.025$ Period B $y = 0.014x \pm 0.004 + 0.090 \pm 0.012$
7b	Period A $y = 0.078x \pm 0.020 - 0.021 \pm 0.068$ Period B $y = 0.043x \pm 0.007 + 0.006 \pm 0.020$
7c	Period A $y = 0.904x \pm 0.538 + 0.186 \pm 0.030$ Period B $y = 0.388x \pm 0.410 + 0.106 \pm 0.024$
7d	Period A $y = -0.053x \pm 0.365 + 0.241 \pm 0.029$ Period B $y = 0.918x \pm 0.252 + 0.062 \pm 0.018$
7e	Period A $y = 0.001x \pm 0.003 + 0.229 \pm 0.019$ Period B $y = 0.005x \pm 0.004 + 0.114 \pm 0.013$
7f	Period A $y = 0.006x \pm 0.003 + 0.193 \pm 0.029$ Period B $y = -0.004x \pm 0.005 + 0.136 \pm 0.013$
9a	$y = 4.351x \pm 0.874 + 2.648 \pm 0.281$
9b	$y = 0.418x \pm 0.535 + 1.432 \pm 0.173$
9c	$y = 1.245x \pm 0.103 + 1.526 \pm 0.209$
9d	$y = 9.168x \pm 10.900 + 1.499 \pm 0.138$
9e	$y = 0.248x \pm 0.236 + 3.572 \pm 0.378$
9f	$y = 0.399x \pm 0.328 + 1.373 \pm 0.166$

9g	$y = -0.256x \pm 0.312 + 4.138 \pm 0.292$
9h	$y = 1.165x \pm 0.166 + 0.625 \pm 0.140$

Table 3. Parameters of the multilinear regression analysis of WSOC. Slope coefficients are reported for the individual AMS ME-2 factors, while y-intercepts are presented in the right column. Numbers in parenthesis refer to the percent contributions of each AMS factors (and of intercepts) to the measured WSOC. See the main text for further explanation.

		OOA-1	OOA-2	OOA-3	OOA-4	Intercept
Whole campaign	intercept forced to 0	0.56 (7%)	0.87 (12%)	0.83 (32%)	1.00 (49%)	-
	unforced	0.40 (5%)	0.94 (12%)	0.63 (24%)	0.92 (44%)	0.31 $\mu\text{gC}/\text{m}^3$ (15%)
Period A	intercept forced to 0	1.00 (7%)	0.88 (37%)	0.77 (32%)	1.00 (24%)	-
	unforced	0.88 (6%)	0.92 (38%)	0.48 (19%)	0.59 (14%)	0.72 $\mu\text{gC}/\text{m}^3$ (22%)
Period B	intercept forced to 0	0.83 (11%)	1.00 (1%)	0.93 (32%)	1.00 (56%)	-
	unforced	0.27 (4%)	1.00 (1%)	0.46 (15%)	1.00 (53%)	0.47 $\mu\text{gC}/\text{m}^3$ (28%)

Figure 2

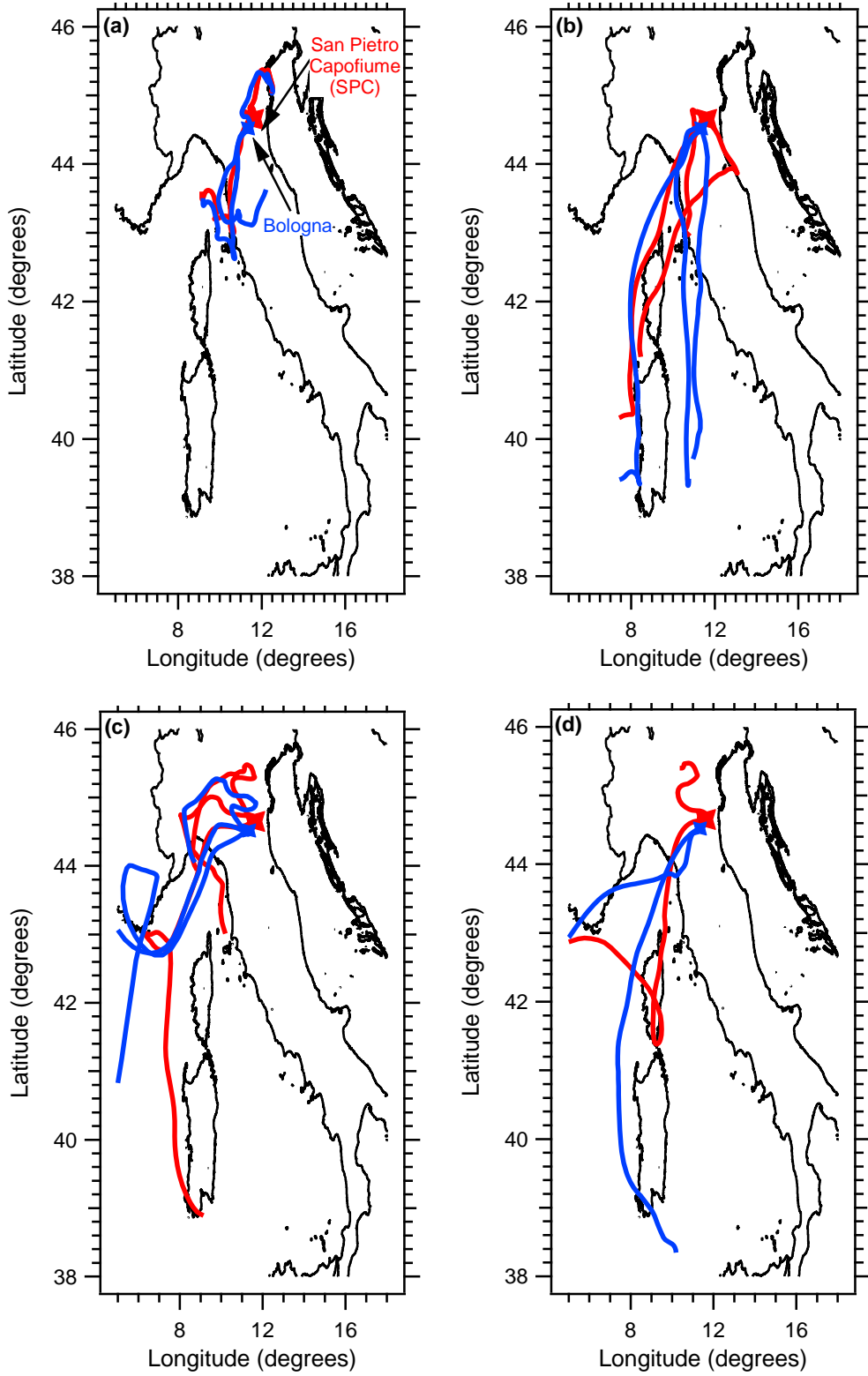


Figure 3

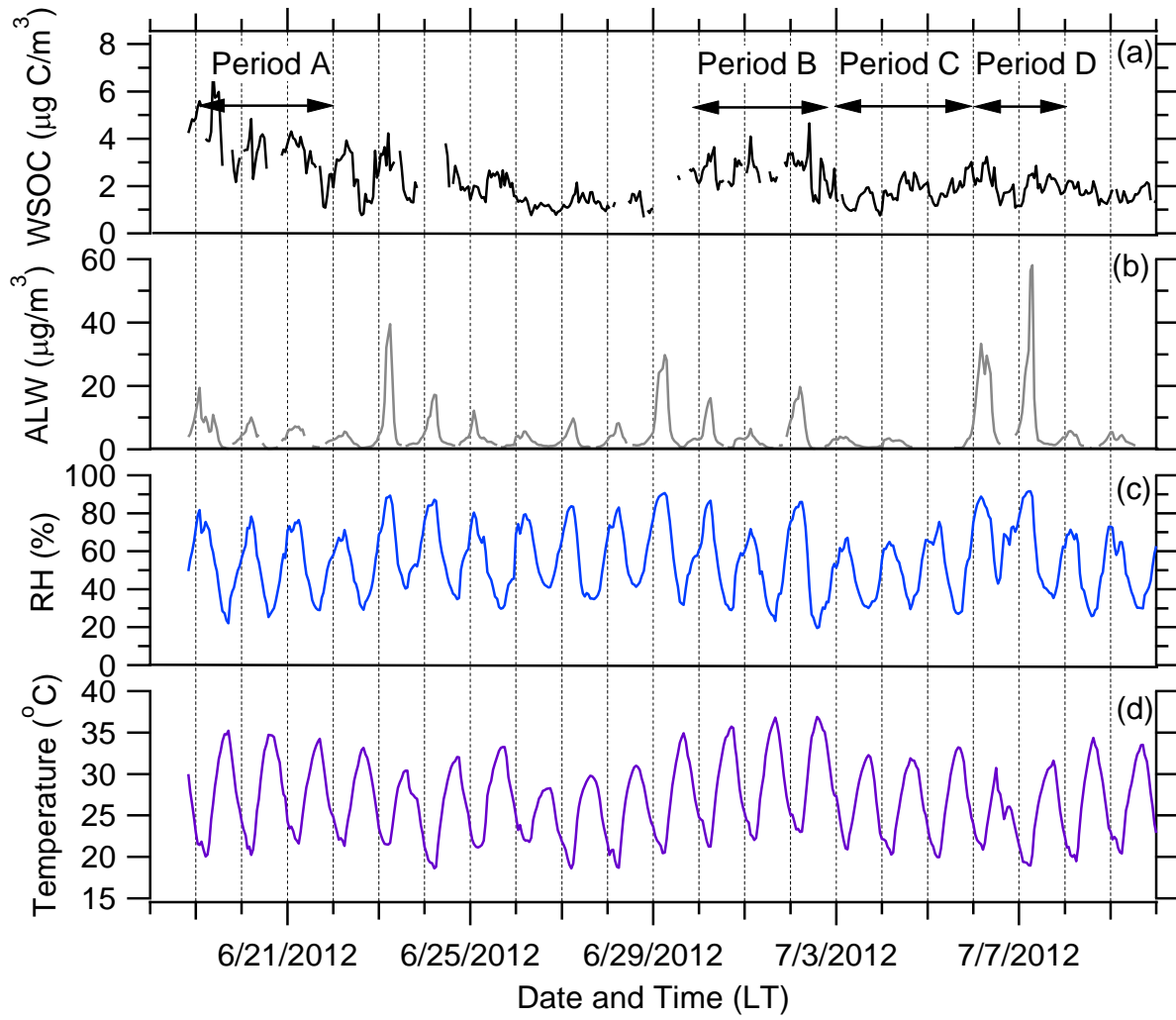
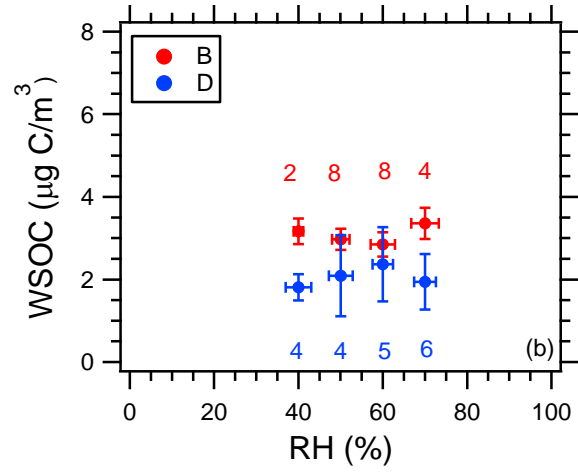
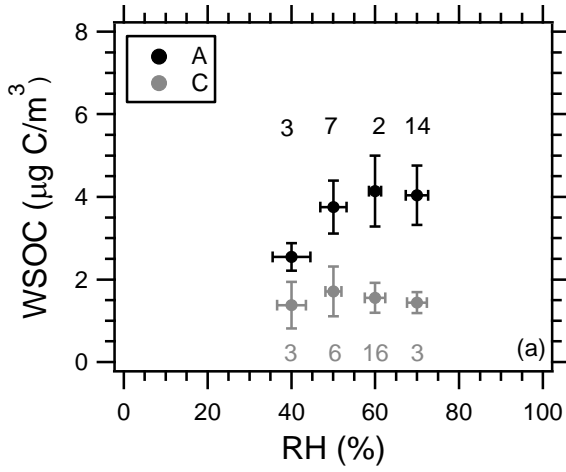


Figure 4

RH Increasing



RH Decreasing

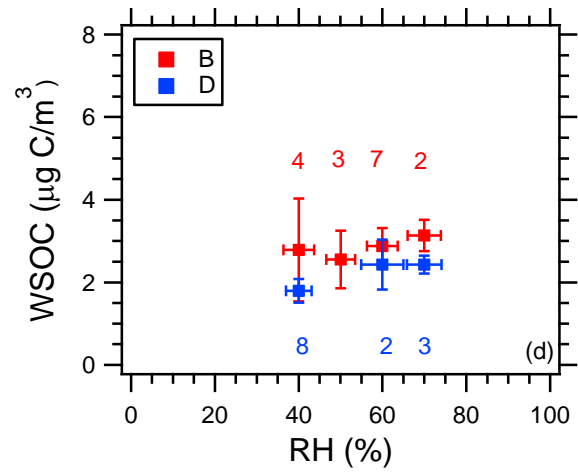
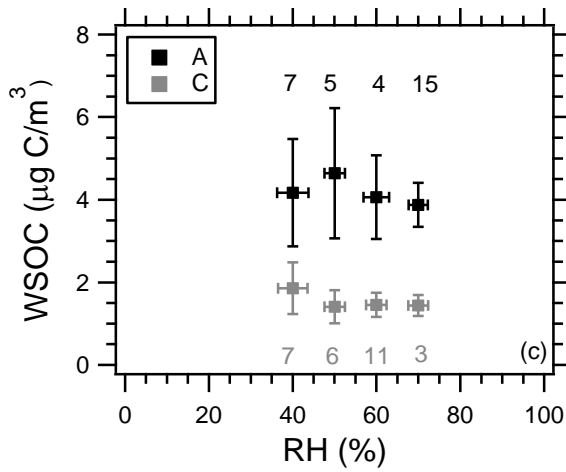


Figure 5

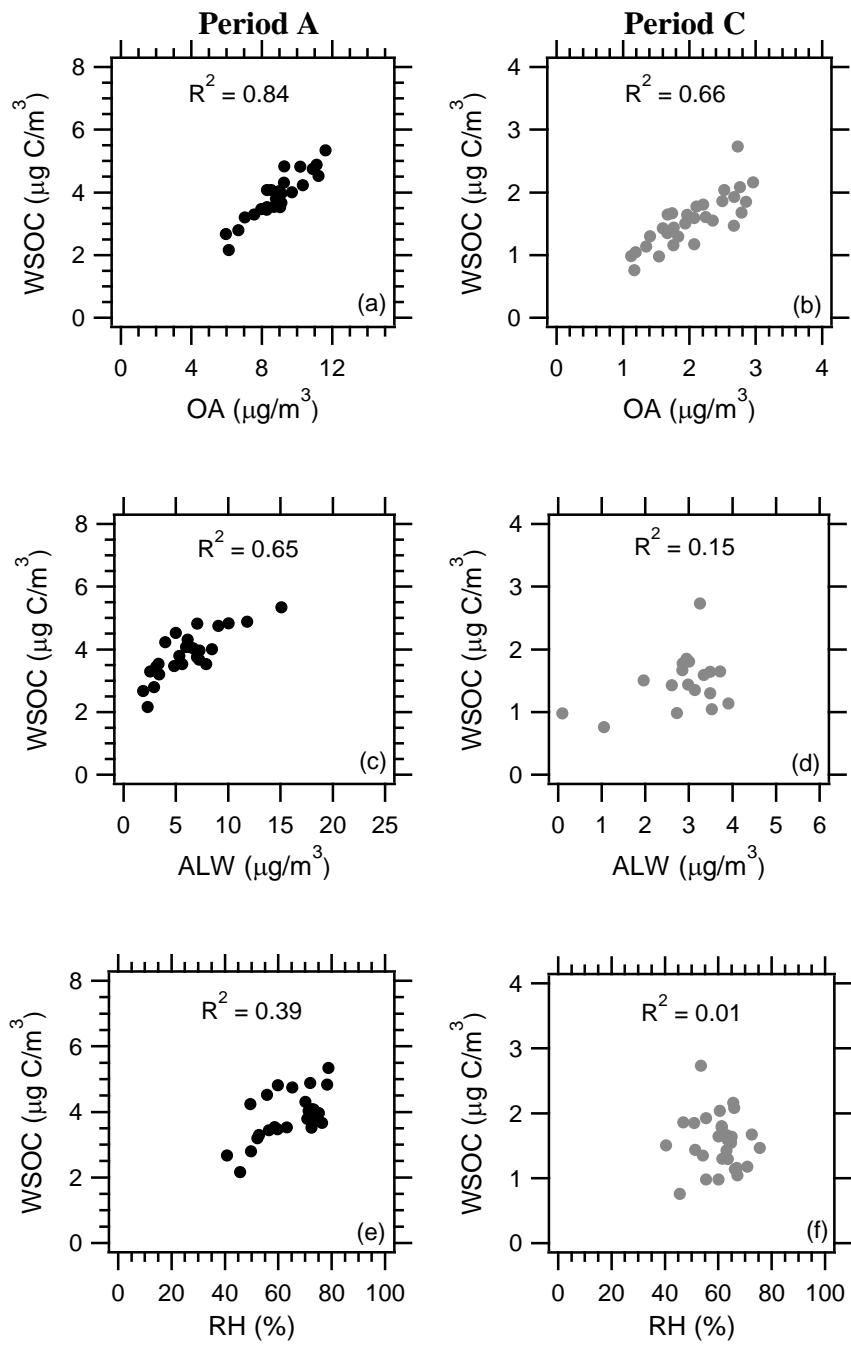


Figure 6

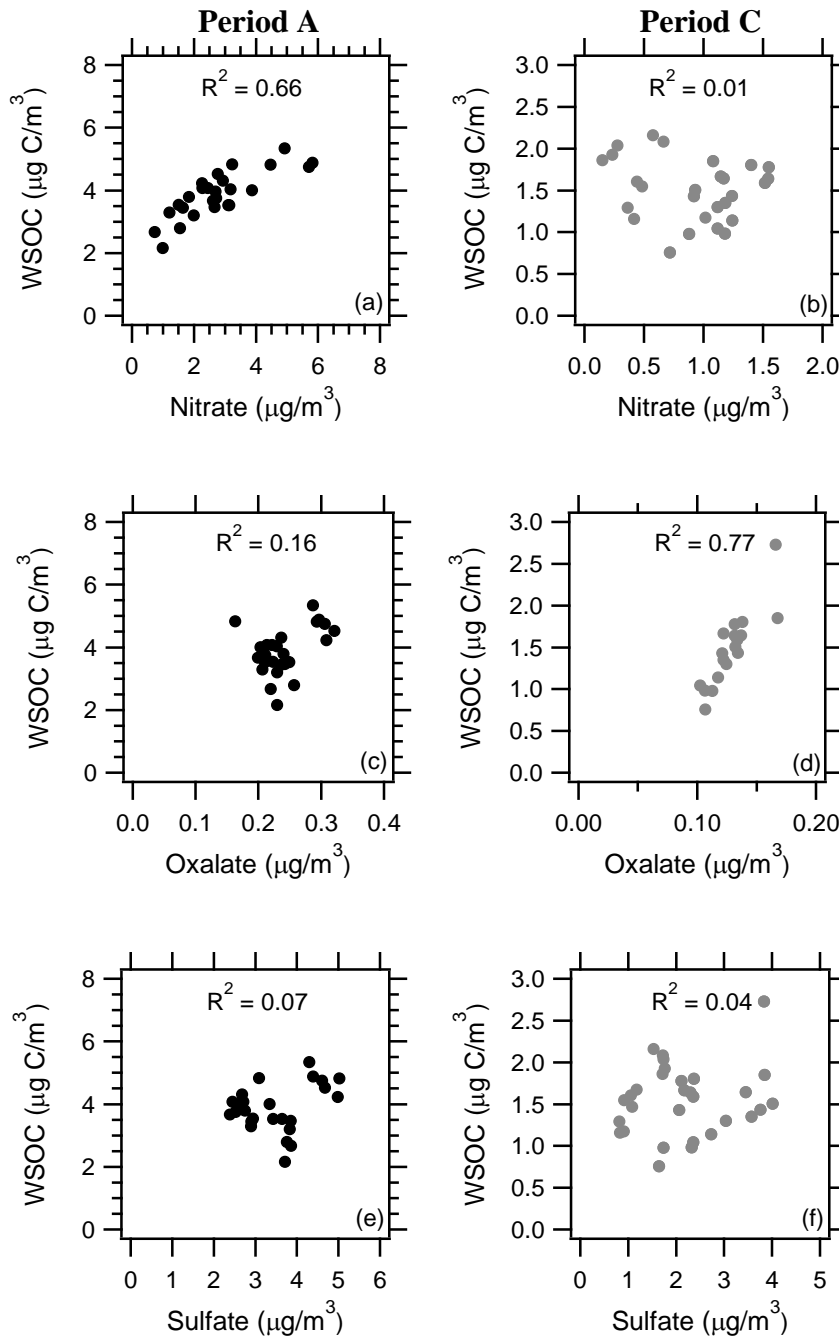


Figure 7

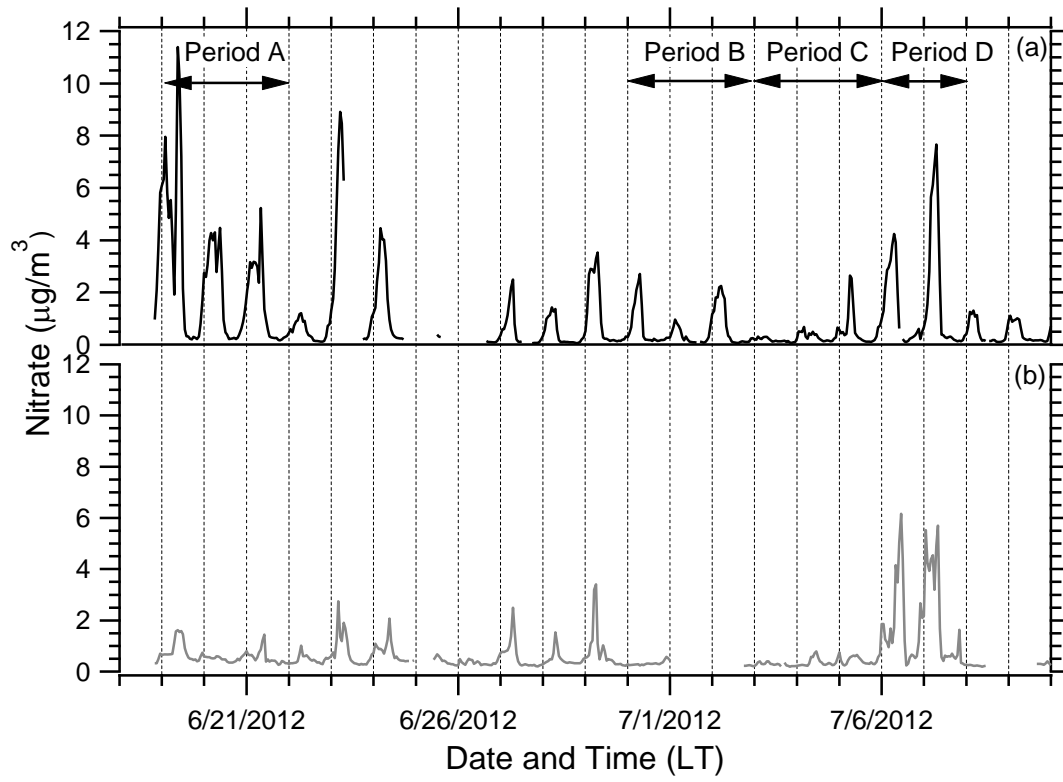


Figure 8

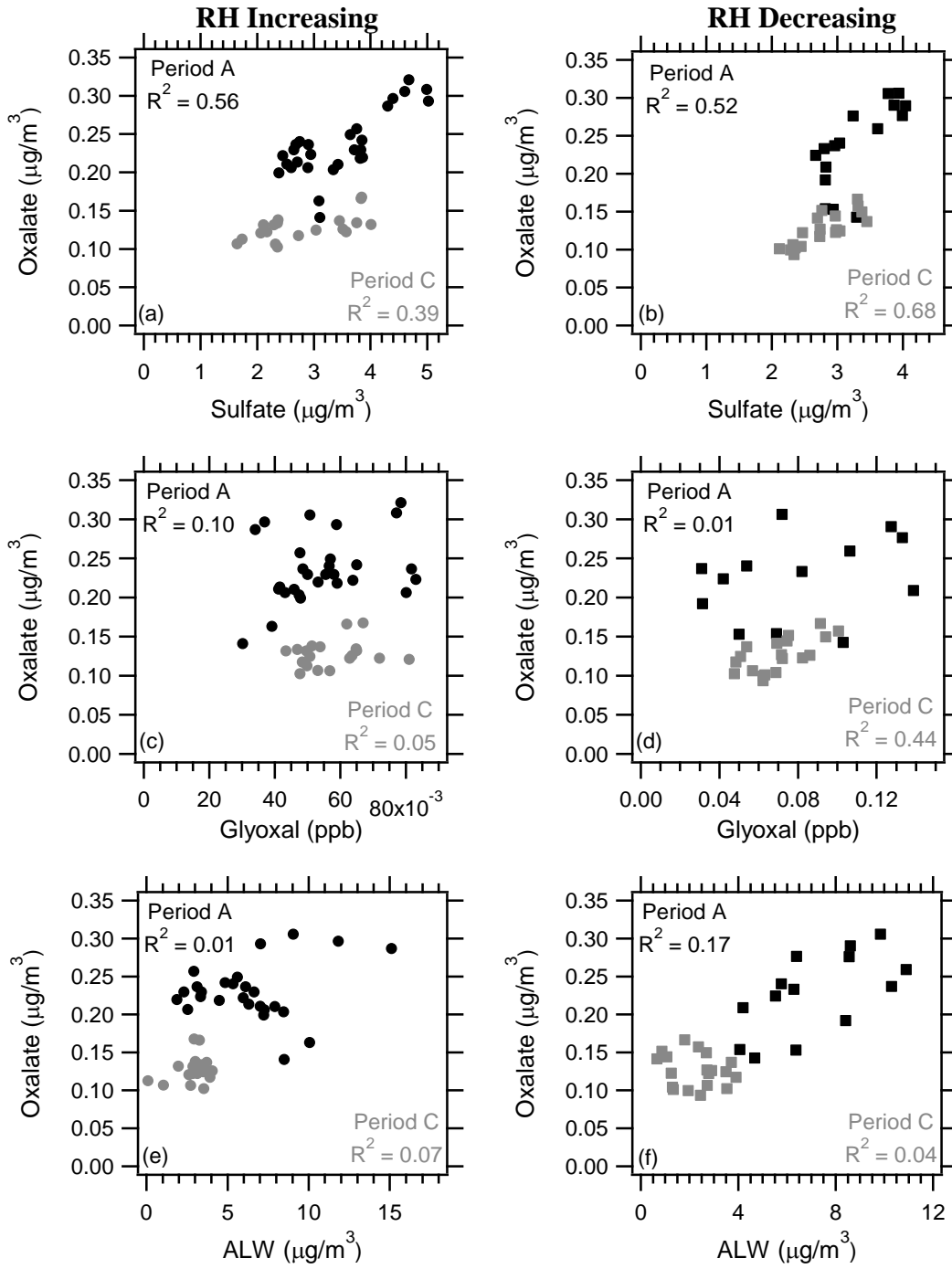


Figure 9

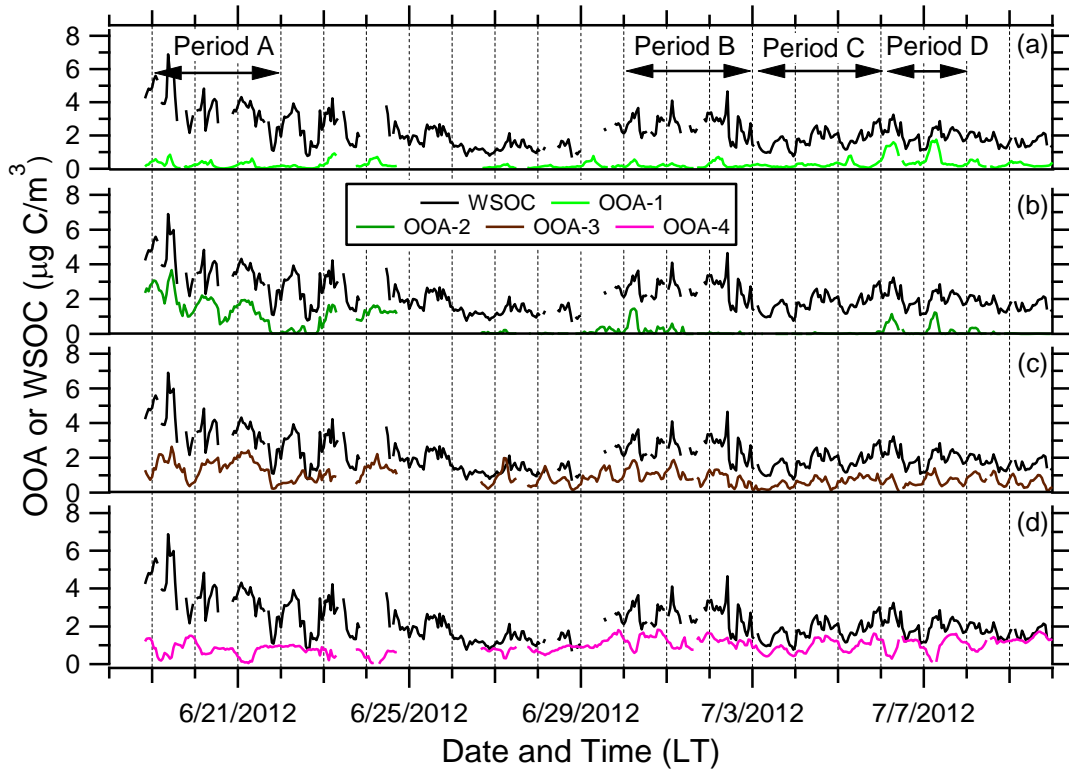


Figure 10

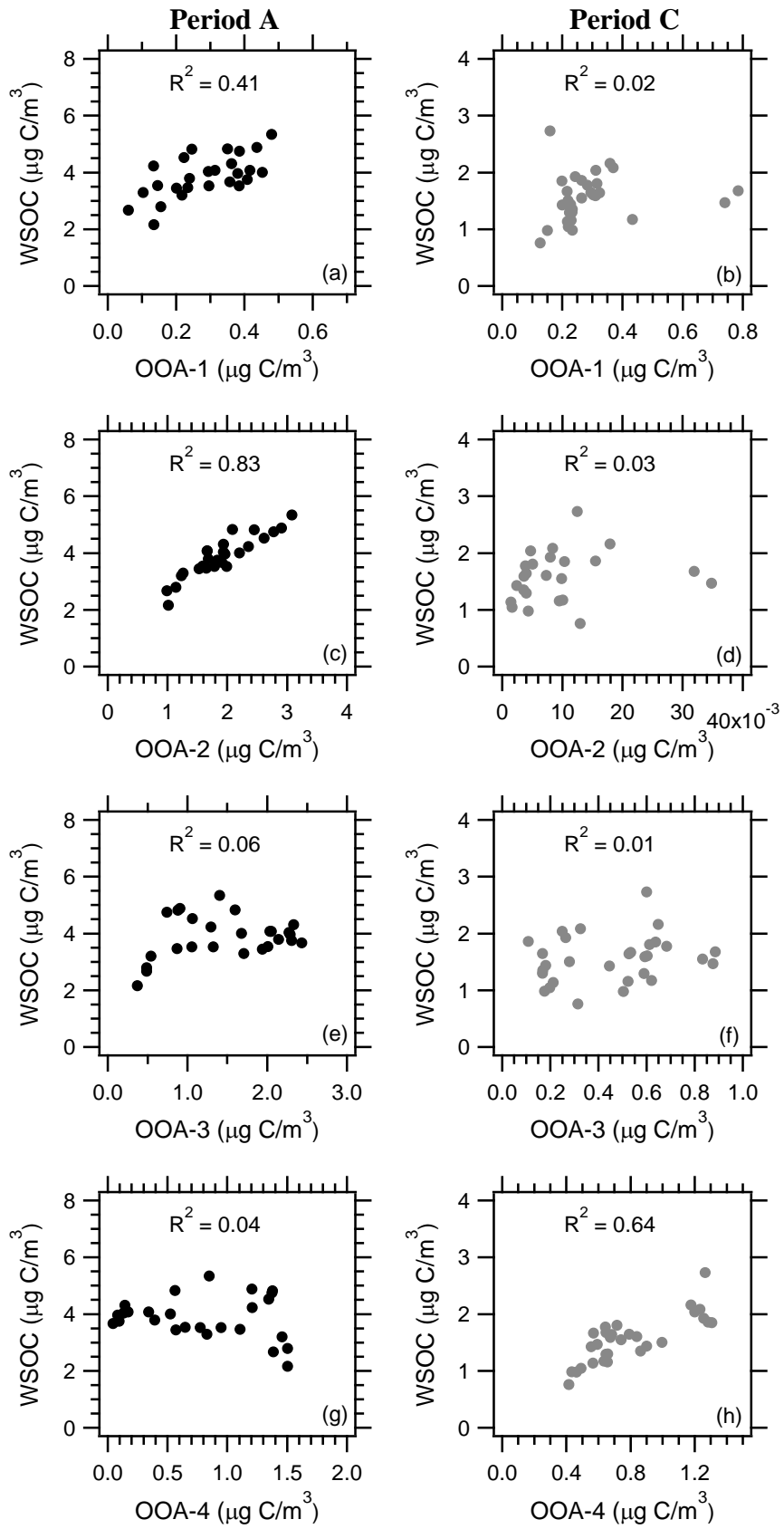


Figure 11

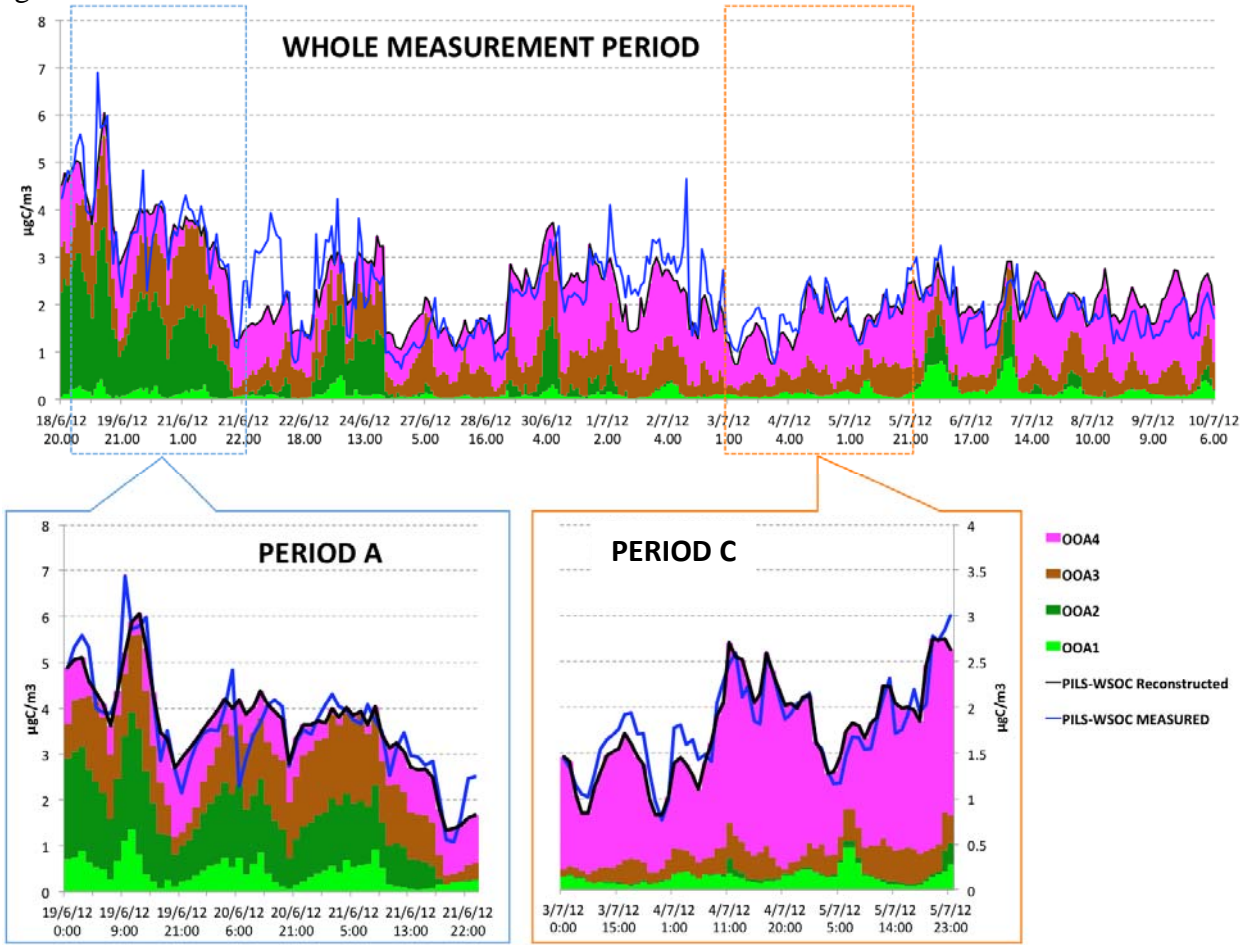


Figure 12

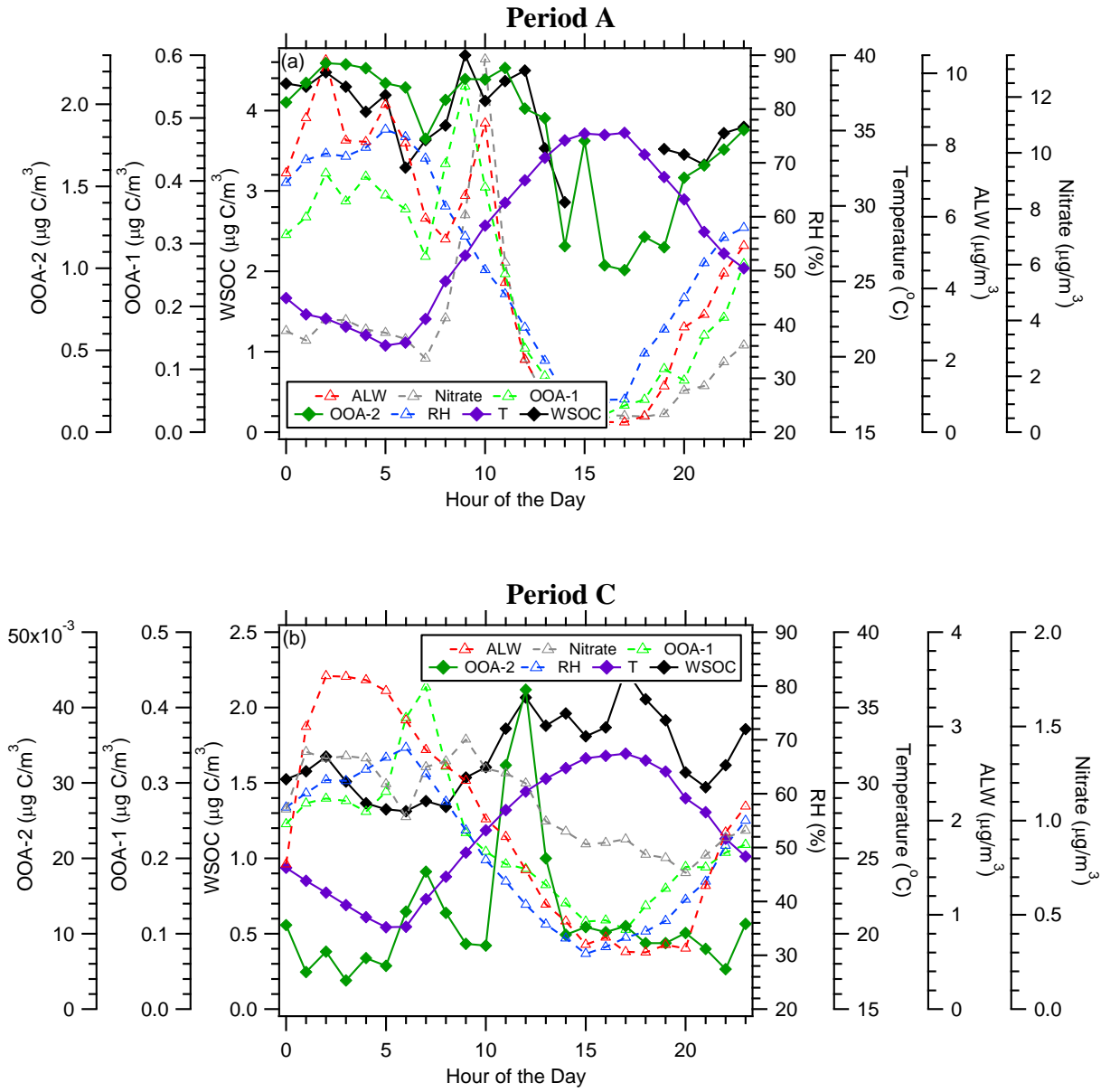
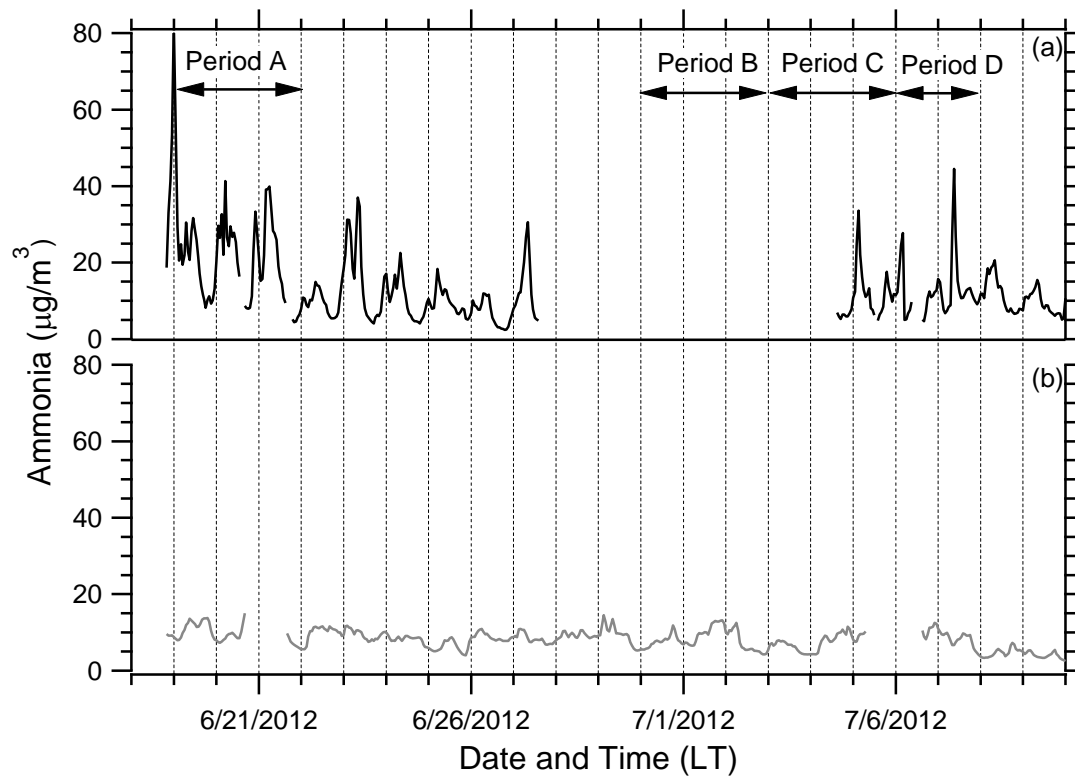


Figure 13



Supporting Information for

Evidence for Ambient Dark Aqueous SOA Formation in the Po Valley, Italy

A.P. Sullivan¹, N. Hodas², B.J. Turpin³, K Skog⁴, F.N. Keutsch^{4,5}, S. Gilardoni⁶, M. Paglione⁶,
M. Rinaldi⁶, S. Decesari⁶, M.C. Facchini⁶, L. Poulain⁷, H. Herrmann⁷, A. Wiedensohler⁷, E.
Nemitz⁸, M.M. Twigg⁸, and J.L. Collett, Jr.¹

AMS Organic Aerosol Source Apportionment

Source apportionment analysis on the high resolution organic aerosol (OA) mass spectra provided by the AMS was made using the Multilinear Engine algorithm (ME-2) developed by *Paatero* [1999] and the interface Solution Finder (SoFi 4.9) [*Canonaco et al.*, 2013]. Prior to analysis, the organic matrix was prepared according to the recommendations of *Ulbrich et al.* [2009]. First, isotope ions were removed and a minimum counting error was applied. Fragments with a signal-to-noise ratio (SNR) below 0.2 were down-weighted by a factor of 10 and fragments with a SNR between 0.2 and 2 were down-weighted by a factor of 2. Finally, the fragments related to ion CO_2^+ were also down-weighted since they are calculated as a constant fraction of the ion CO_2^+ [*Allan et al.*, 2004]. Elemental analysis on the mass spectra of the identified factors was performed using the Analytic Procedure for Elemental Separation (APES vers. 1.06) based on *Aiken et al.* [2007, 2008] and including the improved estimation from *Canagaratna et al.* [2015].

For the first attempt, a non-constrained approach was investigated using a factor number ranging from 1 to 6 and applying 10 seeds (Figure S1). The best solution was obtained for the 4-factors solution (Figure S2) including 3 different oxygenated OA (OOA-a, OOA-b and OOA-c) and a mixed-sources factor (mix-OA). The mix-OA factor contributes to 16% of the total OA and it has a mass spectrum with ions typically associated with hydrocarbon-like OA and shows the lowest O/C (oxygen/carbon) ratio (0.28) compared to the other factors. Although, it indicates that this factor can be related to primary OA, its elemental ratios are higher than reported Hydrocarbon-like OA (HOA) factors [*Canagaratna et al.*, 2015]. This factor also has a large contribution of oxygenated fragments at m/z 43 (CHO^+) and 44 (CO_2^+) compared to previously reported HOA factors. Regarding its time variation, this factor correlates relatively well with gas-phase primary emissions tracers (e.g., benzene ($r=0.35$), toluene ($r=0.48$)) and particulate black carbon (BC, $r=0.49$) as well as with semi-volatile inorganic compounds (e.g., nitrate ($r=0.57$)). Therefore, considering the mass spectrum and time series particularities, this factor was identified to represent a mixture of Hydrocarbon-like OA (HOA) and semi-volatile OA (SV-OOA). The three OOA factors have quite similar mass spectra, but they present clear distinct time trends. Therefore, they are considered as separate factors and identified as follows:

- OOA-a (10% of total OA) appears to be specific to a certain time period of the campaign characterized by high temperature, a high pressure system, and stagnant air masses. Therefore, this OOA-a factor can be related to an accumulation of aged particles on the regional background. The OOA-a mass spectrum is dominated by oxygenated ions and shows the highest O/C ratio (1.02) in agreement with aged OA.
- OOA-b (30% of total OA) is the least oxygenated OOA factors (O/C = 0.55). It also correlates well with sulfate ($r=0.58$), but also with methanesulfonic acid (MSA, $r=0.60$). Therefore, this suggested that OOA-b might be related to marine OA rather than continental OA. This is in agreement with previous measurements made at the same location by *Saarikoski et al.* [2012], who reported a factor with a source originating from the Mediterranean Sea.
- OOA-c (44% of total OA) correlates with particulate sulfate ($r=0.55$) but not with MSA, opposite to OOA-b, and therefore can be linked to more “continental” SOA formation.

Increasing the number of factors did not provide a significant change on the mix-OA factor as illustrated in Figure S3 but rather a change in the split of the different OOA factors. Therefore, as a second attempt, the source apportionment was performed in a semi-constrained mode in order to dissociate primary OA from semi-volatile OA more clearly. The principal primary OA source expected is the HOA factor. In contrary to *Saarikoski et al.* [2012] who reported the contribution of a Biomass Burning OA (BBOA) factor in the spring season, here no BBOA is expected since the contribution of the fragment m/z 60 (a tracer for BBOA) to total OA was systematically below the background level of 0.3% defined by *Cubison et al.* [2011]. Consequently, a reference HOA mass spectrum corresponding to an average of 2 HOA factors previously identified in this area (M. Rinaldi, personal communication) was used as a priori information to partially constrain the model.

For this approach, the number of factors was varied from 5 to 7 since at least 5 factors are expected based on previous AMS measurements in the Po Valley (HOA and 4 types of OOA). In order to test the sensitivity of the results, the difference in the degree of variation for the various fragments for the output HOA factor to the input reference mass spectra (the so-called a-value) was investigated for a-values ranging from 0.05 (i.e., extremely constrained run where fragments of the resulting HOA factor can only vary from 5% compared to the reference HOA) to 0.5 (50% variation). The contribution of the HOA to the total OA was extremely stable over the investigated a-value range indicating that identification of the HOA factor is quite robust (Figure S4). The 5-factors solution (with an a-value of 0.1) was considered as the final solution (Figure S5). This solution corresponds to better discrimination between HOA and the semi-volatile OA (referred in the following as OOA-1), while the 3 others OOA factors correspond to the previously identified ones in the non-constrained model and here are referred to as OOA-2 (12% of OA), OOA-3 (28% of OA), and OOA-4 (45% of OA) in order to avoid confusion when referring to the first (unconstrained) analysis (Figures S6 and S7). Increasing the number of factors to 6 or 7 solely leads to a further splitting of the OOA factors without a clear identification.

The HOA factor (4% of OA) now better follows the time trend of benzene ($r=0.58$), while no real improvement of the correlation with BC ($r=0.50$) and toluene ($r=0.49$) can be reported. However, the semi-volatile OOA-1 is now better correlated with nitrate ($r=0.74$) than HOA ($r=0.36$) confirming the presence of these two factors in the previously identified mix-OA.

Although the OOA-1 factor (12% of total OA) is related to semi-volatile OA, its mass spectrum appears to be more oxygenated (higher contribution of the CO_2^+ fragment compared to the CHO^+) than classical SV-OOA ($\text{CHO}^+ > \text{CO}_2^+$). However, this is quite similar to the previously reported semi-volatile OOA measured at SPC by *Saarikoski et al.* [2012].

Although contributions of the 3 others OOA factors (OOA-2, OOA-3, and OOA-4) to the total OA are quite similar to the contribution of their corresponding factors in the non-constrained mode (12%, 28% and 45%, respectively), some small differences can be reported either in terms of their mass spectra (and consequently their elemental ratios) or their time trends. These differences can be explained by a small contribution of the non-constrained OOA factors (i.e., OOA-a, OOA-b, and OOA-c) to OOA-1. The most stable factor is OOA-2 which correlates quite well with the previously identified OOA-a, even if the final factor has a lower oxidation state. Although OOA-2 contributed to 12% over the entire time period, during its prevalent period it accounted for up to more than half of the OA.

References

- Aiken, A. C., P.F. DeCarlo, and J.L. Jimenez, Elemental analysis of organic species with electron ionization high-resolution mass spectrometry, *Anal. Chem.*, **79**, 8350-8358, doi:10.1021/ac071150w, 2007.
- Aiken, A. C., P.F. Decarlo, J.H. Kroll, D.R. Worsnop, J.A. Huffman, K.S. Docherty, I.M. Ulbrich, C. Mohr, J.R. Kimmel, D. Sueper, Y. Sun, Q. Zhang, A. Trimborn, M. Northway, P.J. Ziemann, M.R. Canagaratna, T.B. Onasch, M.R. Alfarra, A.S.H. Prévôt, J. Dommen, J. Duplissy, A. Metzger, U. Baltensperger, and J.L. Jimenez, O/C and OM/OC ratios of primary, secondary, and ambient organic aerosols with high-resolution time-of-flight aerosol mass spectrometry, *Environ. Sci. Technol.*, **42**, 4478-4485, doi:10.1021/es703009q, 2008.
- Allan, J., A.E. Delia, H. Coe, K.N. Bower, R.M. Alfarra, J.L. Jimenez, A.M. Middlebrook, F. Drewnick, T.B. Onasch, M.R. Canagaratna, J.T. Jayne, and D.R. Worsnop, A generalised method for the extraction of chemically resolved mass spectra from Aerodyne aerosol mass spectrometer data, *J. Aerosol Sci.*, **35**, 909 - 922, doi:10.1016/j.jaerosci.2004.02.007, 2004.
- Canagaratna, M. R., J.L. Jimenez, J.H. Kroll, Q. Chen, S.H. Kessler, P. Massoli, L.H. Ruiz, E. Fortner, L.R. Williams, K.R. Wilson, J.D. Surratt, N.M. Donahue, J.T. Jayne, and D.R. Worsnop, Elemental ratio measurements of organic compounds using aerosol mass spectrometry: characterization, improved calibration, and implications, *Atmos. Chem. Phys.*, **15**, 253-272, doi:10.5194/acp-15-253-2015, 2015.
- Canonaco, F., M. Crippa, J.G. Slowik, A.S.H. Prévôt, and U. Baltensperger, SoFi, an IGOR-based interface for the efficient use of the generalized multilinear engine (ME-2) for the source apportionment: ME-2 application to aerosol mass spectrometer data, *Atmos. Meas. Tech.*, **6**, 3649-3661, doi:10.5194/amt-6-3649-2013, 2013.
- Cubison, M. J., A.M. Ortega, P.L. Hayes, D.K. Farmer, D.E. Day, M.J. Lechner, W.H. Brune, E.C. Apel, G.S. Diskin, J.A. Fisher, H.E. Fuelberg, A. Hecobian, D.J. Knapp, T. Mikoviny, D.D. Riemer, G. Sachse, W. Session, R.J. Weber, A.J. Weinheimer, A. Wisthaler, and J.L. Jimenez, Effects of aging on organic aerosol from open biomass burning smoke in aircraft and laboratory studies, *Atmos. Chem. Phys.*, **11**, 12049-12064, 2011.
- Paatero, P., The multilinear engine - A table-driven, least squares program for solving multilinear problems, including the n-way parallel factor analysis model, *Journal of Computational and Graphical Statistics*, **8**, 854-888, doi:10.2307/1390831, 1999.
- Saarikoski, S., S. Carbone, S. Decesari, L. Giulianelli, F. Angelini, M. Canagaratna, N.L. Ng, A. Trimborn, M.C. Facchini, S. Fuzzi, R. Hillamo, and D. Worsnop, Chemical characterization of springtime submicrometer aerosol in Po Valley, Italy, *Atmos. Chem. Phys.*, **12**, 8401-8421, doi:10.5194/acp-12-8401-2012, 2012.

Ulbrich, I. M., M.R. Canagaratna, Q. Zhang, D.R. Worsnop, and J.L. Jimenez, Interpretation of organic components from Positive Matrix Factorization of aerosol mass spectrometric data, *Atmos. Chem. Phys.*, 9, 2891-2918, doi:10.5194/acp-9-2891-2009, 2009.

Figure Captions

Figure S1. Evolution of the Q/Q_{exp} ratio (top) and factor contribution (bottom) over the investigated factor range for the non-constrained model.

Figure S2. Time series (top) and mass spectra colored by fragments family (bottom) for the non-constrained 4-factors solution.

Figure S3. Evolution of the mix-OA factor time series (top) and mass spectra (bottom) for different factor solutions (from 3 to 6). Numbers in parentheses on the bottom plots (following the number of the factor solution) correspond to the slope of the regression line compare to the selected 4-factors solution.

Figure S4. Evolution of the Q/Q_{exp} ratio (top) and factor contribution (bottom) over the investigated factor range for the partially-constrained model.

Figure S5. Overview of the partially-constrained factor solution including (a) time series of the factors and corresponding tracers, (b) mass fraction of the different factors to the total OA, and (c) mass spectra of the factors colored by fragment family.

Figure S6. Comparison between the time trends of the factors identified for the non-constrained (y-axis) and the ones identified for the partially-constrained (x-axis) analysis.

Figure S7. Comparison between the mass spectra of the factors identified for the non-constrained (y-axis) and the ones identified for the partially-constrained (x-axis) analysis.

Figure S8. Correlation of hourly averaged WSOC vs. OA for (a) Period B and (b) Period D, ALW for (c) Period B and (d) Period D, and RH for (e) Period B and (f) Period D at SPC. All plots are for during the times of RH increasing.

Figure S9. Correlation of hourly averaged WSOC vs. nitrate for (a) Period B and (b) Period D, oxalate for (c) Period B and (d) Period D, and sulfate for (e) Period B and (f) Period D at SPC. All plots are for during the times of RH increasing.

Figure S10. Diurnal profile of WSOC, OOA-1, OOA-2, RH, Temperature, ALW, and Nitrate for (a) Period B and (b) Period D at SPC.

Table S1. Dates and times for the times of RH increasing and decreasing during Periods A, B, C, and D.

Period	RH Increasing	RH Decreasing
<u>A</u>	<u>18 June at 20:00 – 19 June at 01:00,</u> <u>19 June at 20:00 – 20 June at 06:00,</u> <u>20 June at 21:00 – 21 June at 07:00</u>	<u>19 June at 02:00 – 19 June at 12:00,</u> <u>20 June at 03:00 – 20 June at 11:00,</u> <u>21 June at 00:00 – 21 June at 12:00</u>
<u>B</u>	<u>29 June at 19:00 – 30 June at 06:00,</u> <u>30 June at 19:00 – 1 July at 06:00,</u> <u>1 July at 21:00 – 2 July at 07:00</u>	<u>30 June at 04:00 – 1 July at 12:00,</u> <u>1 July at 01:00 – 1 July at 08:00,</u> <u>2 July at 02:00 – 2 July at 10:00</u>
<u>C</u>	<u>2 July at 21:00 – 3 July at 07:00,</u> <u>3 July at 23:00 – 4 July at 06:00,</u> <u>4 July at 20:00 – 5 July at 07:00</u>	<u>3 July at 03:00 – 3 July at 11:00,</u> <u>4 July at 01:00 – 4 July at 12:00,</u> <u>5 July at 05:00 – 5 July at 11:00</u>
<u>D</u>	<u>5 July at 19:00 – 6 July at 07:00,</u> <u>6 July at 16:00 – 7 July at 03:00</u>	<u>6 July at 01:00 – 6 July at 15:00,</u> <u>7 July at 07:00 – 7 July at 14:00</u>

Table S2. Parameters of the multilinear regression analysis of WSOC. Slope coefficients are reported for the individual AMS ME-2 factors, while y-intercepts are presented in the right column. Numbers in parenthesis refer to the percent contributions of each AMS factors (and of intercepts) to the measured WSOC. See the main text for further explanation.

		<u>OOA-1</u>	<u>OOA-2</u>	<u>OOA-3</u>	<u>OOA-4</u>	<u>Intercept</u>
Whole campaign	<u>intercept forced to 0</u>	<u>0.56</u> <u>(7%)</u>	<u>0.87</u> <u>(12%)</u>	<u>0.83</u> <u>(32%)</u>	<u>1.00</u> <u>(49%)</u>	-
	<u>unforced</u>	<u>0.40</u> <u>(5%)</u>	<u>0.94</u> <u>(12%)</u>	<u>0.63</u> <u>(24%)</u>	<u>0.92</u> <u>(44%)</u>	<u>0.31 $\mu\text{gC}/\text{m}^3$</u> <u>(15%)</u>
Period A	<u>intercept forced to 0</u>	<u>1.00</u> <u>(7%)</u>	<u>0.88</u> <u>(37%)</u>	<u>0.77</u> <u>(32%)</u>	<u>1.00</u> <u>(24%)</u>	-
	<u>unforced</u>	<u>0.88</u> <u>(6%)</u>	<u>0.92</u> <u>(38%)</u>	<u>0.48</u> <u>(19%)</u>	<u>0.59</u> <u>(14%)</u>	<u>0.72 $\mu\text{gC}/\text{m}^3$</u> <u>(22%)</u>
Period B	<u>intercept forced to 0</u>	<u>0.83</u> <u>(11%)</u>	<u>1.00</u> <u>(1%)</u>	<u>0.93</u> <u>(32%)</u>	<u>1.00</u> <u>(56%)</u>	-
	<u>unforced</u>	<u>0.27</u> <u>(4%)</u>	<u>1.00</u> <u>(1%)</u>	<u>0.46</u> <u>(15%)</u>	<u>1.00</u> <u>(53%)</u>	<u>0.47 $\mu\text{gC}/\text{m}^3$</u> <u>(28%)</u>

Figure S1

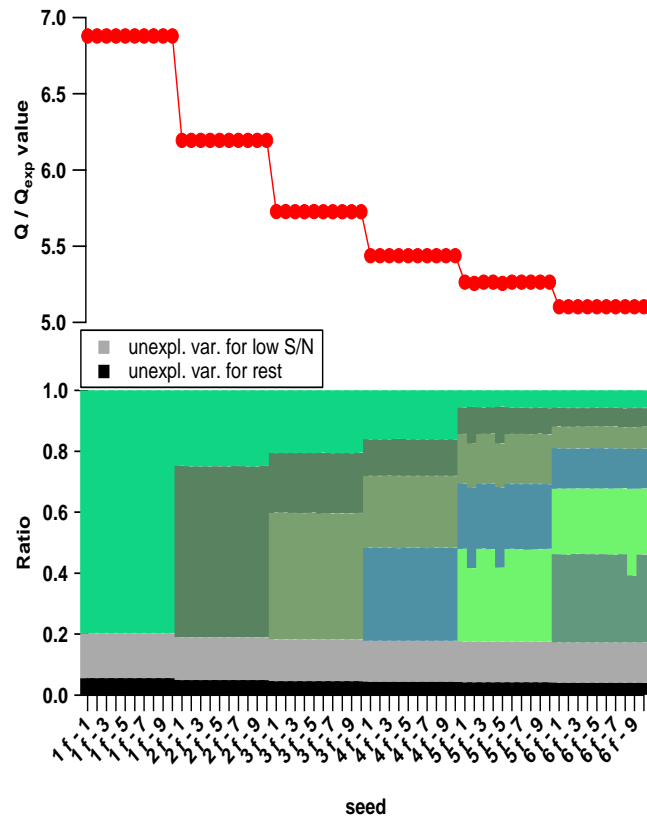


Figure S2

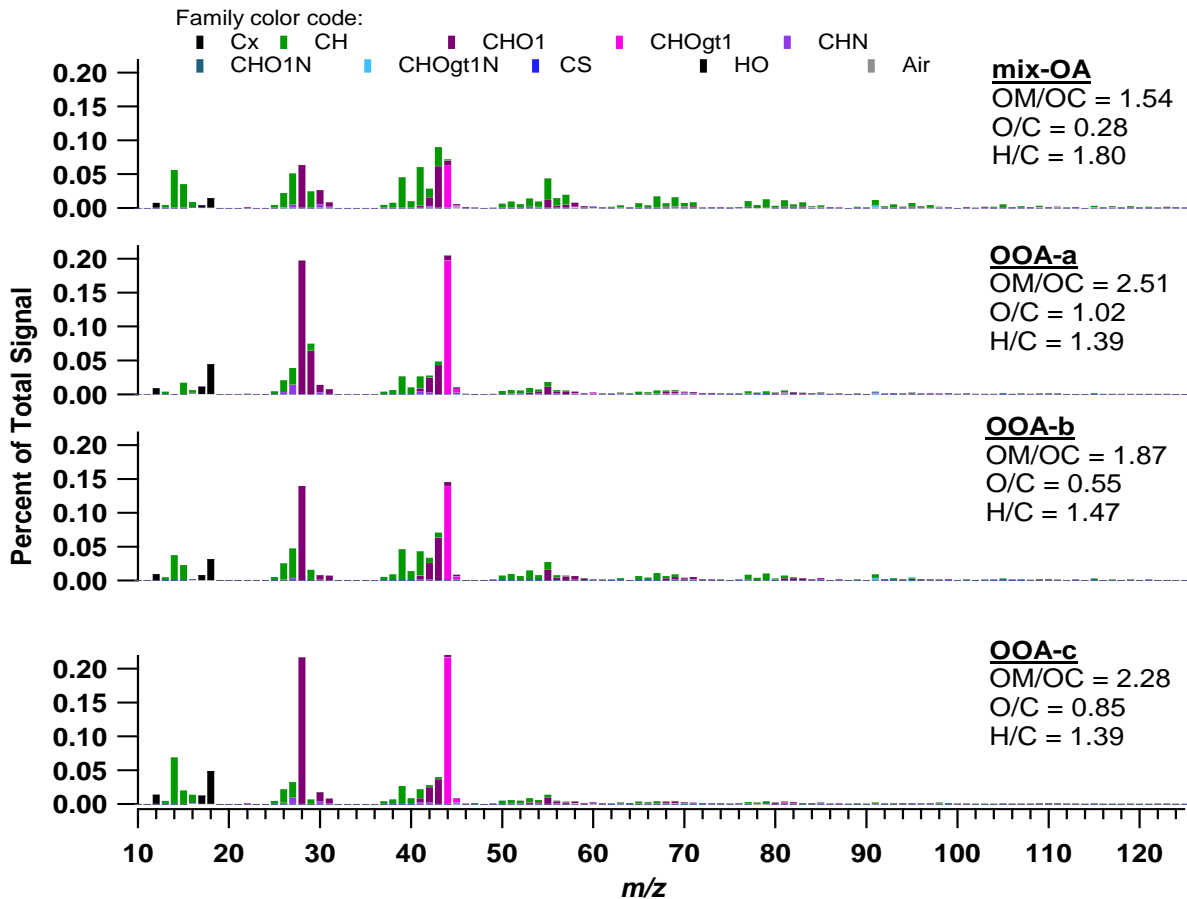
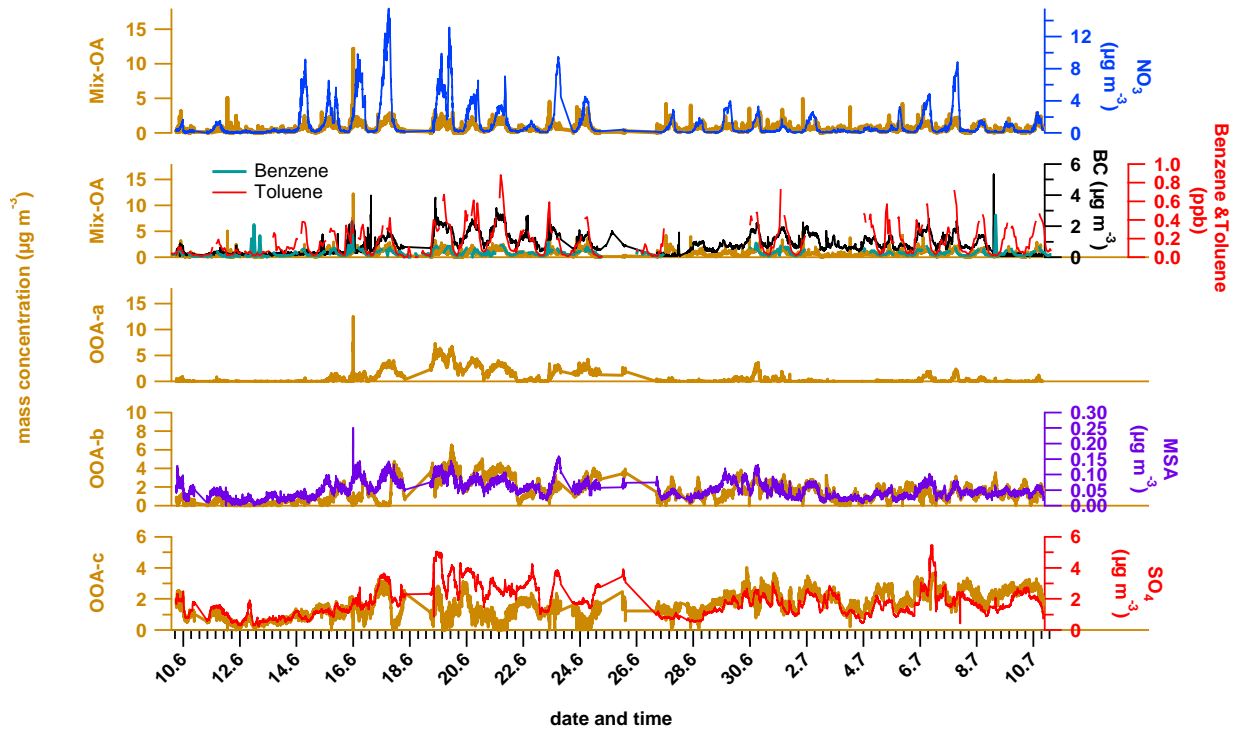


Figure S3

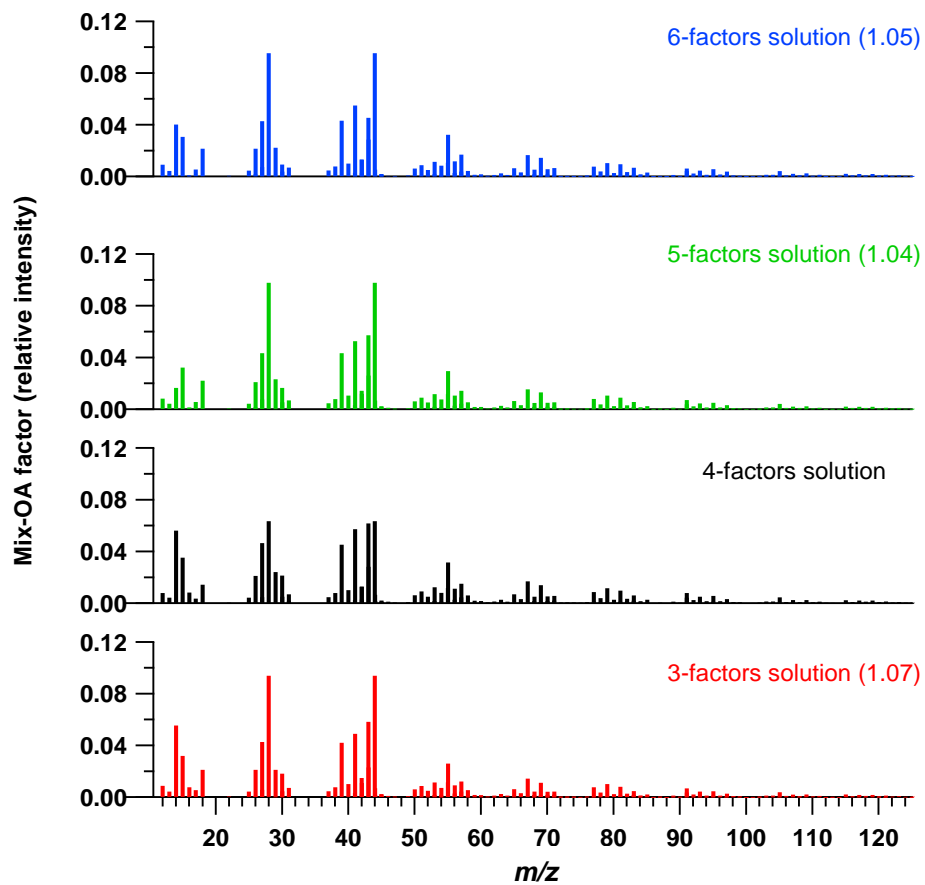
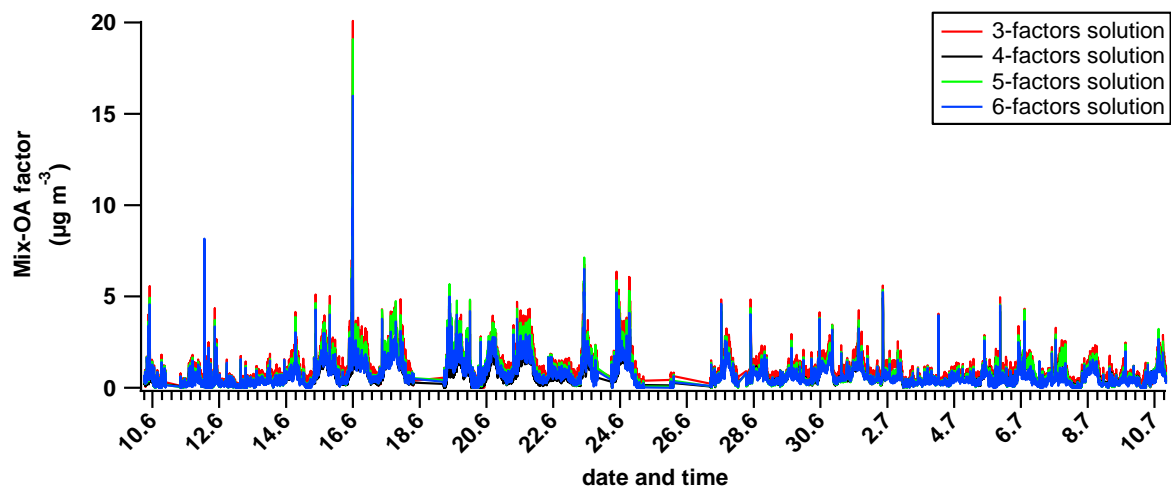


Figure S4

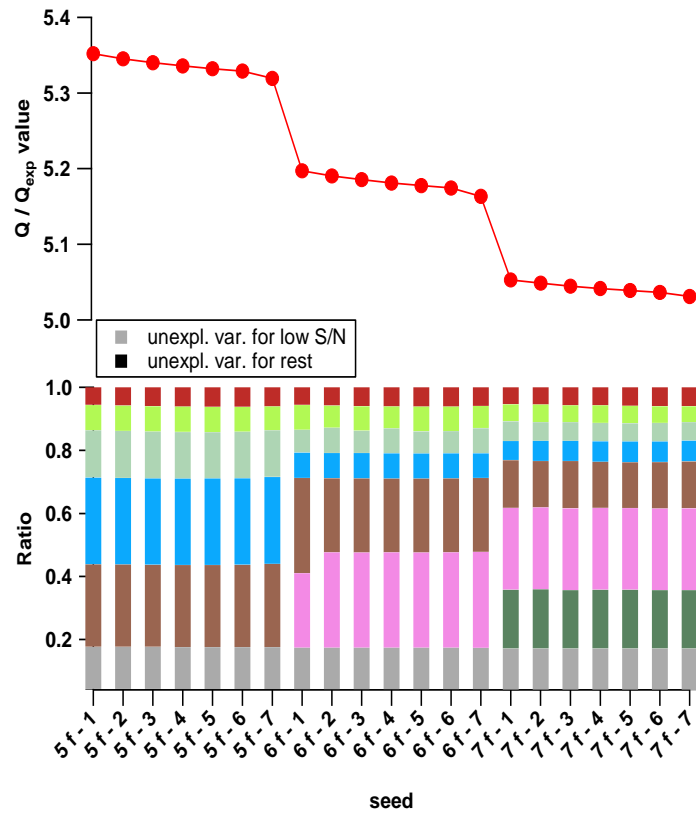
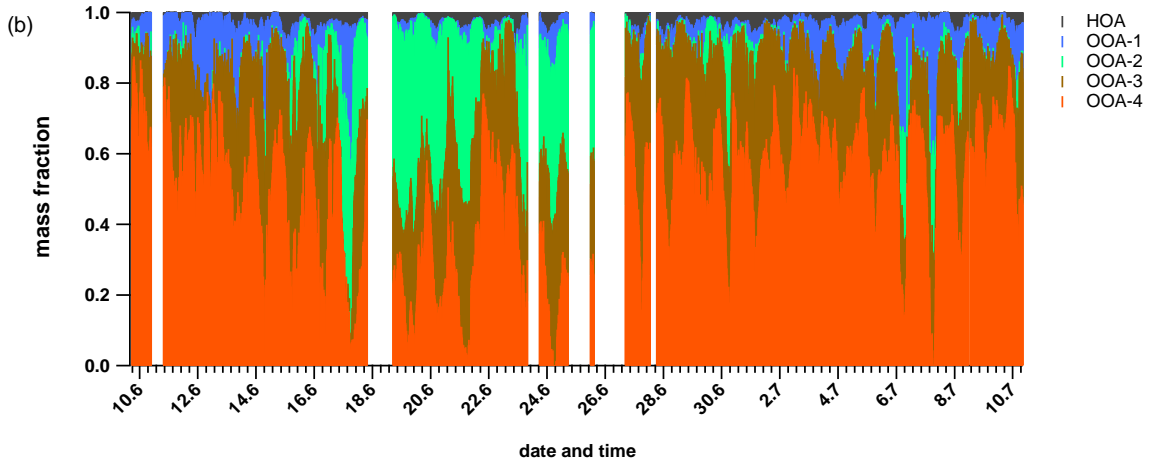
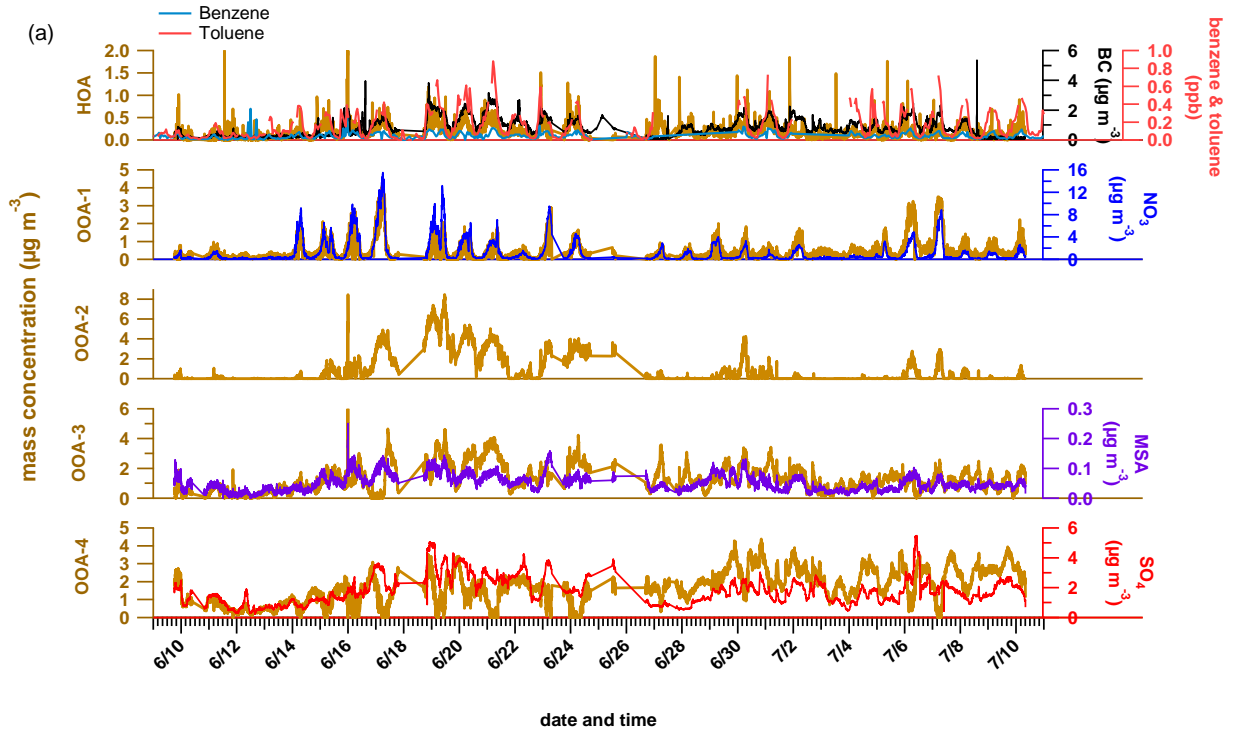


Figure S5



(c)

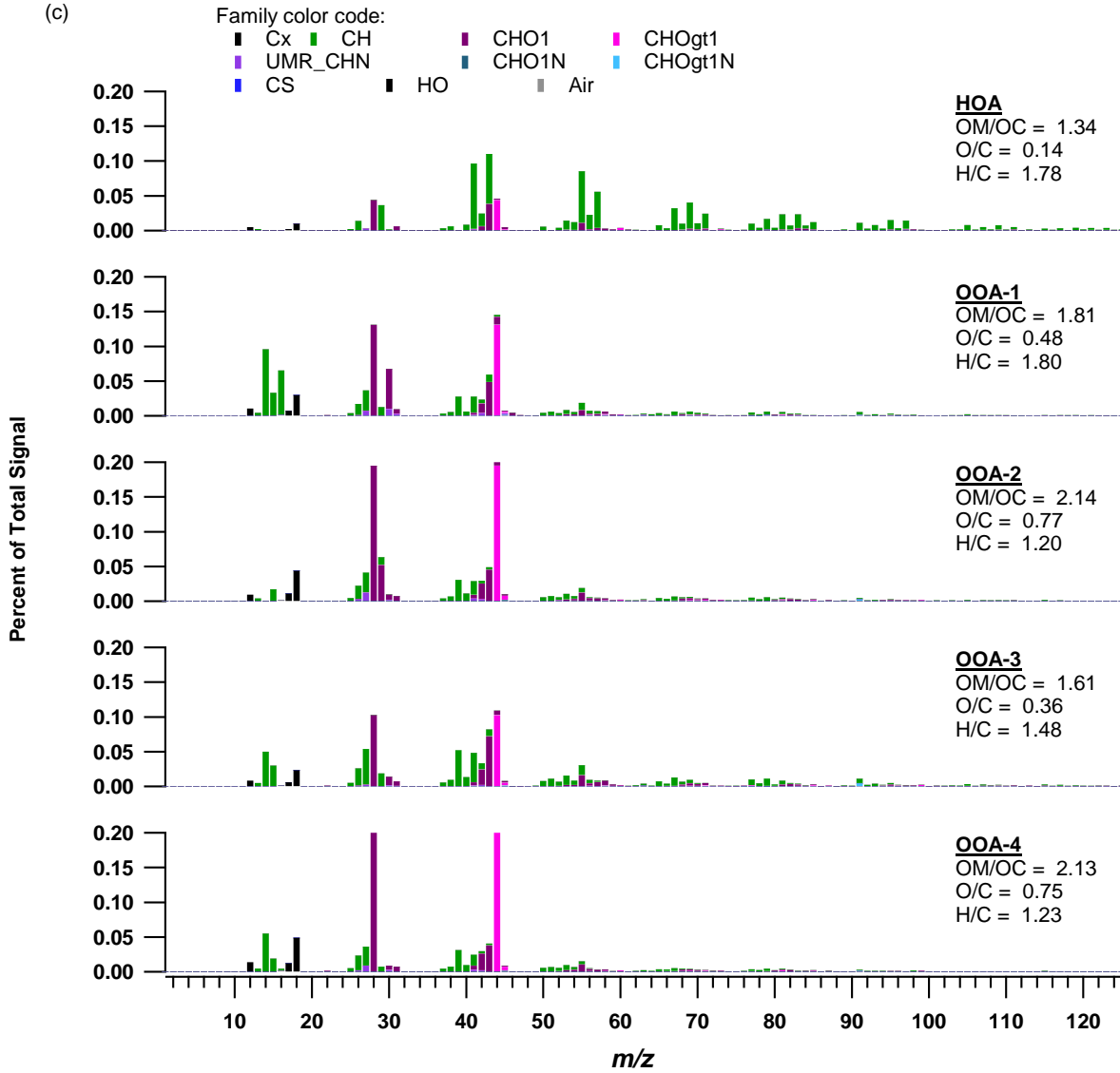


Figure S6

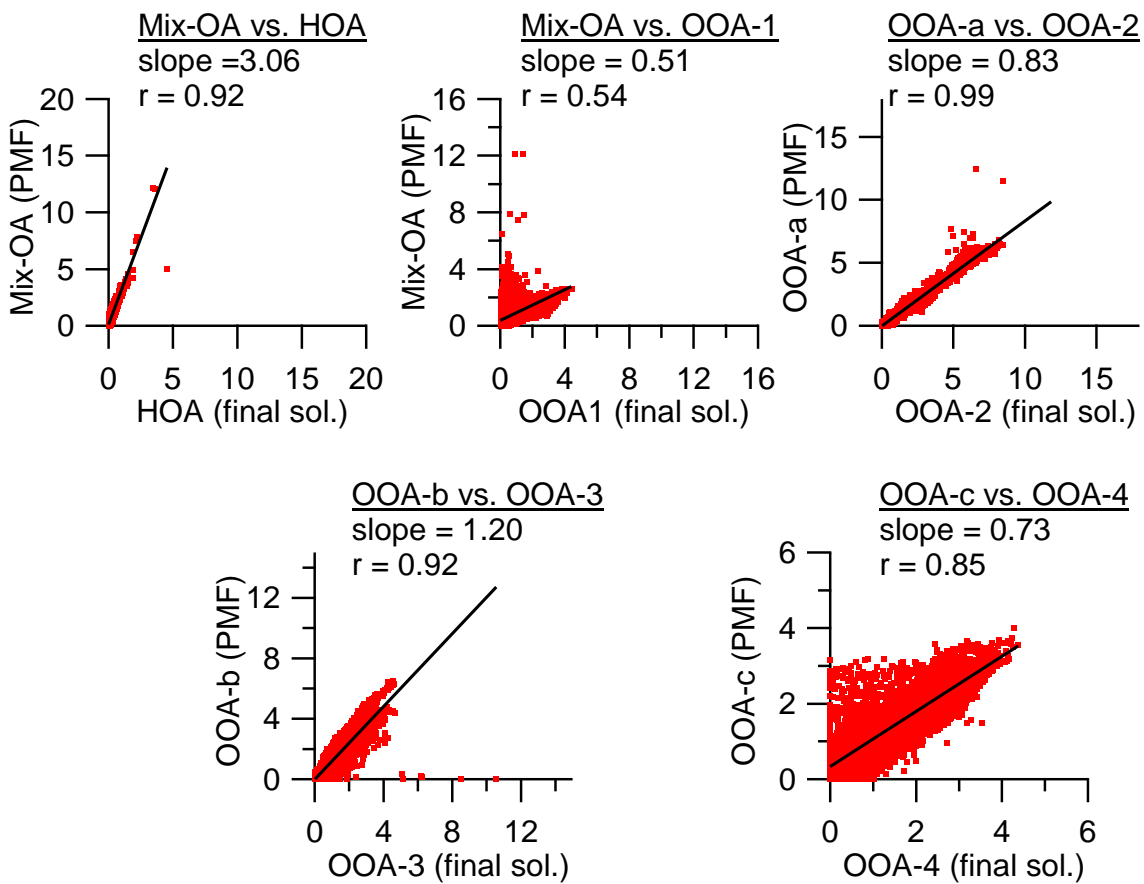


Figure S7

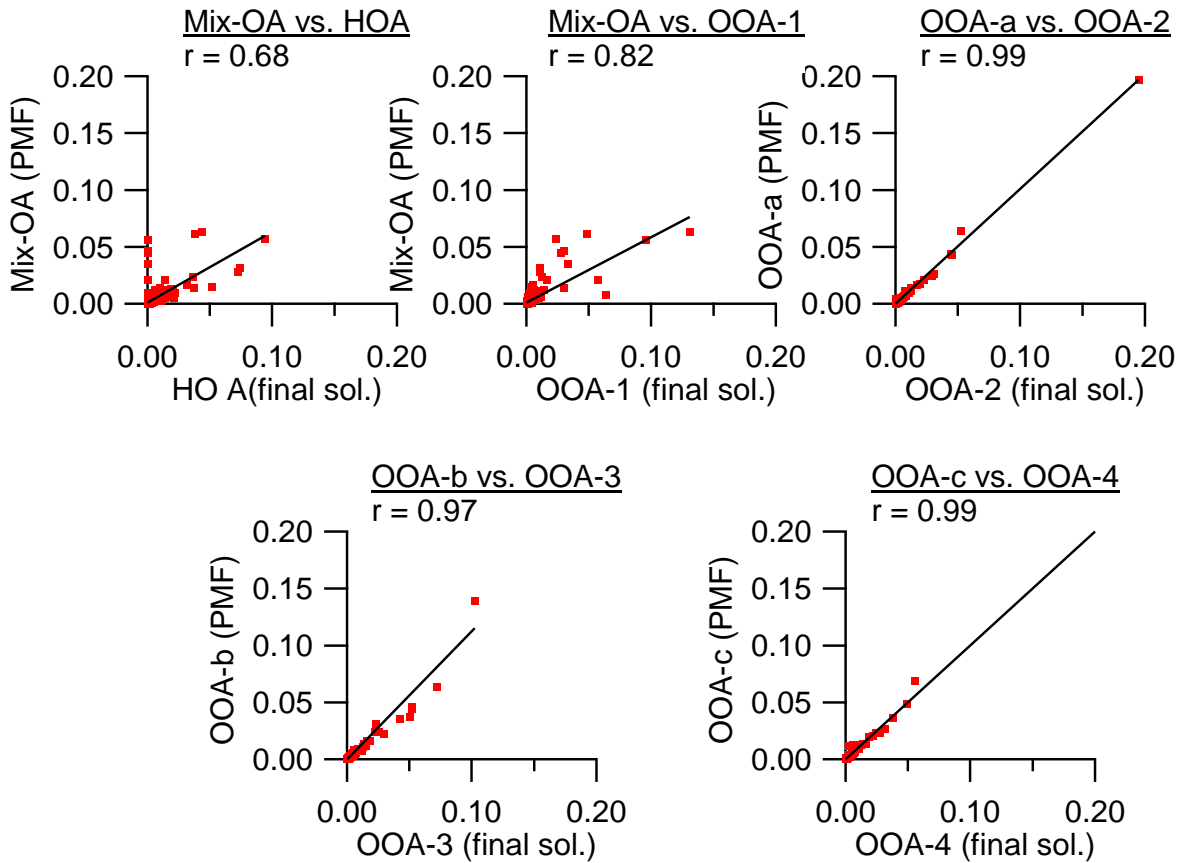


Figure S8

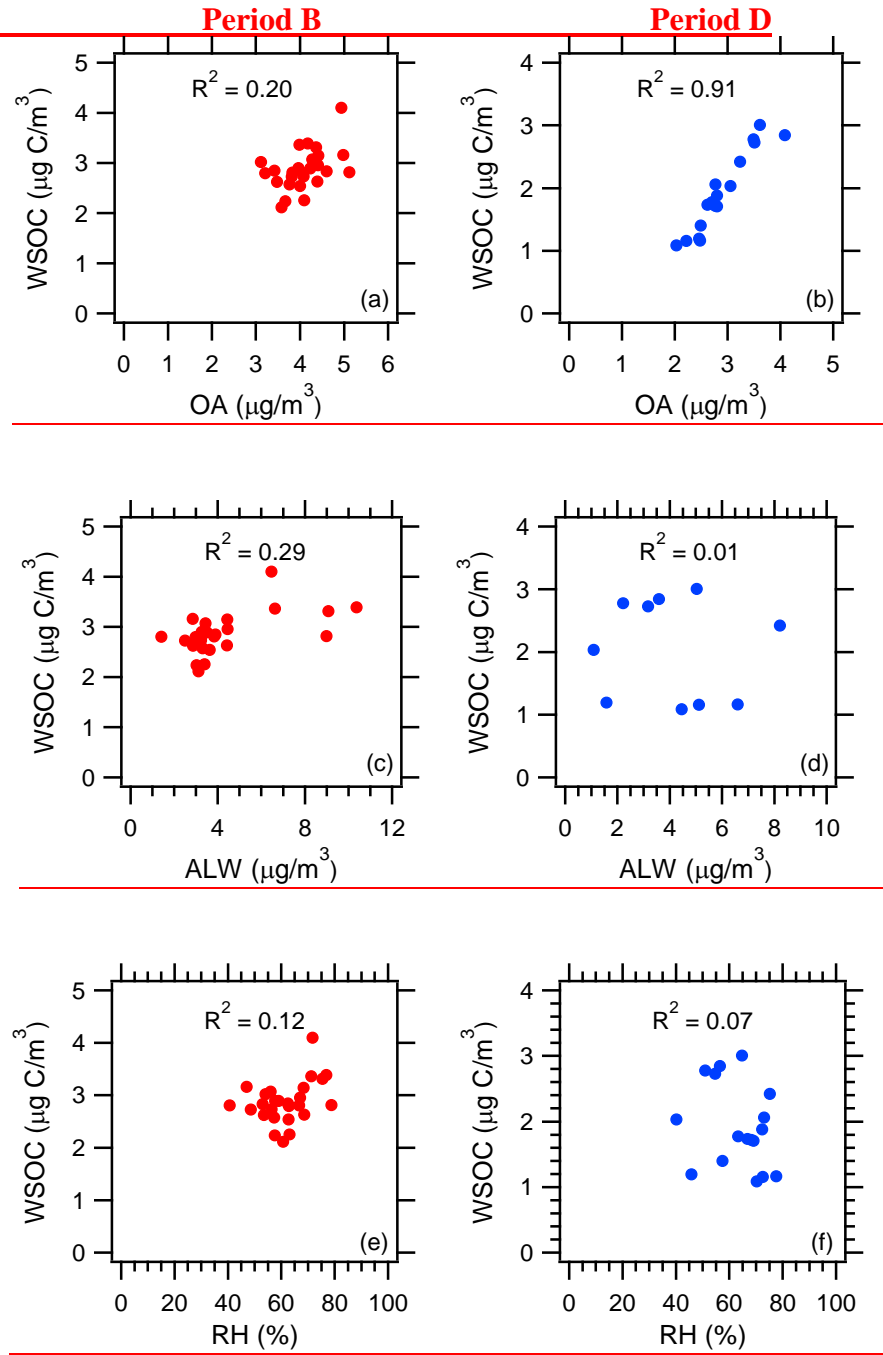


Figure S9

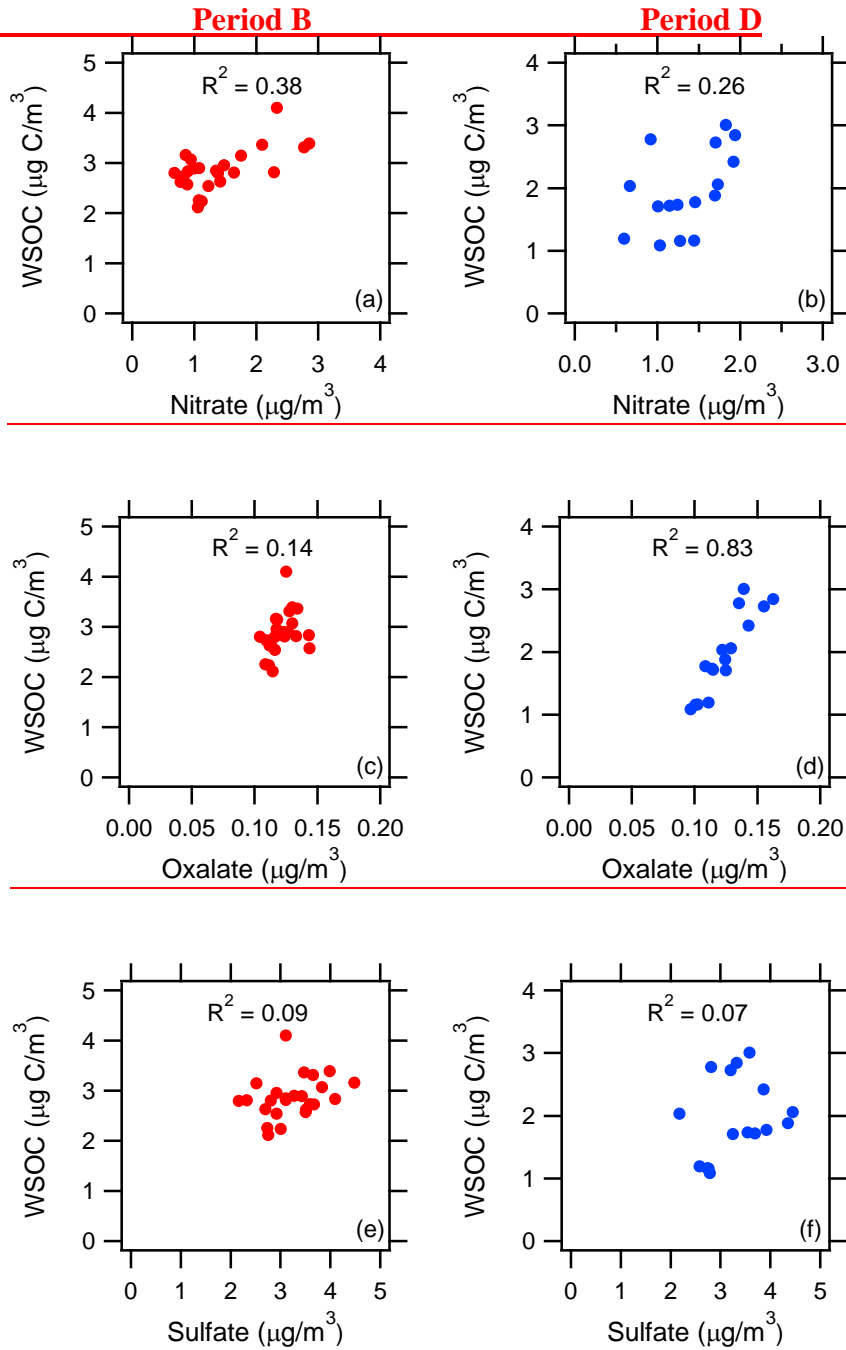


Figure S10

